

MODELS FOR THERMO-MECHANICAL RELIABILITY TRADE-OFFS FOR
BALL GRID ARRAY AND FLIP CHIP PACKAGES
IN EXTREME ENVIRONMENTS

Except where reference is made to the work of others, the work described in this thesis is my own or was done in collaboration with my advisory committee. This thesis does not include proprietary or classified information.

Ganesh Hariharan

Certificate of Approval:

Jeffrey C. Suhling
Quina Distinguished Professor
Mechanical Engineering

Pradeep Lall, Chair
Thomas Walter Professor
Mechanical Engineering

Roy W. Knight
Assistant Professor
Mechanical Engineering

Joe F. Pittman
Interim Dean
Graduate School

MODELS FOR THERMO-MECHANICAL RELIABILITY TRADE-OFFS FOR
BALL GRID ARRAY AND FLIP CHIP PACKAGES
IN EXTREME ENVIRONMENTS

Ganesh Hariharan

A Thesis

Submitted to

the Graduate Faculty of

Auburn University

in Partial Fulfillment of the

Requirement for the

Degree of

Master of Science

Auburn, Alabama

May 10, 2007

MODELS FOR THERMO-MECHANICAL RELIABILITY TRADE-OFFS FOR
BALL GRID ARRAY AND FLIP CHIP PACKAGES
IN EXTREME ENVIRONMENTS

Ganesh Hariharan

Permission is granted to Auburn University to make copies of this thesis at its discretion, upon the request of individuals or institutions at their expense. The author reserves all publication rights.

Signature of Author

Date of Graduation

VITA

Ganesh Hariharan, son of Mr.Hariharan Mahadevan and Smt. Lakshmi. Hariharan, was born on September 05, 1982, in Mumbai, Maharashtra, India. He graduated in 2004 with a Bachelor of Engineering degree in Mechanical Engineering from University Of Madras, Chennai, India. In the pursuit of enhancing his academic qualification he joined the M.S. Program at Auburn University in the Department of Mechanical Engineering in fall, 2004. Ever since he enrolled for the M.S. program at Auburn University, he has worked for Center for Advanced Vehicle Electronics (CAVE) as a Graduate Research Assistant in the area of harsh environment electronic packaging reliability.

THESIS ABSTRACT

MODELS FOR THERMO-MECHANICAL RELIABILITY TRADE-OFFS FOR

BALL GRID ARRAY AND FLIP CHIP PACKAGES

IN EXTREME ENVIRONMENTS

Ganesh Hariharan

Master of Science, May 10, 2007
(B.E. Mechanical Engineering, University Of Madras, India, 2004)

Typed Pages 202

Directed by Pradeep Lall

In the current work, decision-support models for deployment of various ball grid array devices and flip chip electronics under various harsh thermal environments have been presented. The current work is targeted towards government contractors, OEMs, and 3rd party contract manufacturers who intend to select part architectures and board designs based on specified mission requirements. In addition, the mathematical models presented in this paper provide decision guidance for smart selection of BGA and Flip Chip packaging technologies and for perturbing presently-deployed product designs for minimal risk insertion of new materials and architectures. The models serve as an aid for understanding the sensitivity of component reliability to geometry, package architecture, material properties and board attributes to enable educated selection of appropriate device formats.

Modeling tools and techniques for assessment of component reliability in extreme environments are scarce. Previous studies have focused on development of modeling tools at sub-scale level. The tools are often available only in an offline manner for decision support and risk assessment of advanced technology programs. There is need for a turn key approach, for making trade-offs between geometry and materials and quantitatively evaluating the impact on reliability. Application of BGA and Flip Chip assemblies in benign office environments and wireless applications is not new, however their reliability in extreme environments is still not very well understood.

Multiple linear regression, principal components regression and power law based modeling methodologies have been used for developing prediction models that enables higher-accuracy prediction of characteristic life by perturbing known accelerated-test data-sets using models, using factors which quantify the sensitivity of reliability to various design material, architecture and environmental parameters. The multiple linear regression approach uses the potentially important variables from stepwise regression methods, and the principal components regression uses the principal components obtained from the eigen values and eigen vectors of correlation matrix for model building. The power law modeling is a non regression based approach that uses the method of maximum likelihood for developing power law relationship between characteristic life and the package parameters. Convergence between statistical model sensitivities and failure mechanics based model sensitivities has been demonstrated. Predictions of sensitivities have also been validated against the experimental test data.

ACKNOWLEDGEMENTS

The author would like to thank his advisor Dr. Pradeep Lall, Dr. Jeffrey .C. Suhling and other committee members for their invaluable guidance and help during the course of this study. The author acknowledges and extends gratitude for financial support received from the NSF Center for Advanced Vehicle Electronics (CAVE).

Author would like to express his deep gratitude and gratefulness to his father Mr. Hariharan for being a constant source of inspiration and motivation, mother Mrs. Lakshmi for her enduring love and immense moral support and family members Mahadevan, Sirisha and Samhita. The author wishes to acknowledge his colleagues for their friendship, help and all the stimulating discussions.

Style manual or journal used: Guide to Preparation and Submission of Theses and
Dissertations

Computer software used: Microsoft Office 2003, Minitab 13.1, Ansys 7.0,
Matlab 7.0.1, SAS 9.1

TABLE OF CONTENTS

LIST OF FIGURES.....	xiv
LIST OF TABLES.....	xvii
CHAPTER 1 INTRODUCTION.....	1
CHAPTER 2 LITERATURE REVIEW.....	11
2.1 Physics of failure Based Models.....	11
2.2 Statistical Prediction Models.....	13
2.3 Finite Element Models.....	16
2.4 Solder Joint Constitutive Equations.....	19
2.5 Solder Joint Fatigue Modeling.....	21
2.6 Experimental Methods.....	23
CHAPTER 3 STATISTICS BASED CLOSED FORM MODELS FOR FLEX-BGA PACKAGES.....	26
3.1 Overview.....	26
3.2 Flex-BGA Package Architecture.....	27
3.3 Data Set.....	27
3.4 Model Input Selection.....	29
3.5 Multiple Linear Regression.....	33
3.6 Hypothesis Testing.....	37
3.7 Model Adequacy Checking.....	38

3.8	Model Correlation With Experimental Data.....	42
3.9	Model Validation.....	44
3.9.1	Die To Body Ratio.....	44
3.9.2	Ball Count.....	46
3.9.3	Ball Diameter.....	46
3.9.4	PCB Thickness.....	48
3.9.5	Encapsulant Mold Compound Filler Content.....	51
3.9.6	Solder Mask Definition.....	49
3.9.7	Board Finish.....	51
3.9.8	Delta T.....	56
3.10	Design Guidelines.....	56
CHAPTER 4 STATISTICS BASED CLOSED FORM MODELS FOR FLIP CHIP PACKAGES.....		59
4.1	Flip Chip package Architecture.....	60
4.2	Data Set.....	62
4.3	Model Input Selection.....	62
4.4	Multiple Linear Regression.....	67
4.5	Hypothesis Testing.....	68
4.6	Model Adequacy Checking.....	71
4.7	Principal Components Regression.....	74
4.8	Hypothesis Testing.....	80
4.9	Model Adequacy Checking.....	81
4.11	Model Correlation With Experimental Data.....	81

4.10	Model Validation.....	82
4.11.1	Die Length.....	86
4.11.2	Solder Joint Diameter.....	87
4.11.3	Solder Joint Height.....	87
4.11.4	Solder Modulus.....	90
4.11.5	Ball Pitch.....	90
4.11.6	Underfill Modulus.....	92
4.11.7	Delta T.....	95
4.11.8	Undercover Area.....	95
4.11	Design Guidelines.....	98
CHAPTER 5 STATISTICS BASED CLOSED FORM MODELS FOR CBGA PACKAGES.....		101
5.1	CBGA Package Architecture.....	102
5.2	Data Set.....	102
5.3	Model Input Selection.....	105
5.4	Multiple Linear Regression Models.....	106
5.5	Hypothesis Testing.....	107
5.6	Model Adequacy Checking.....	109
5.7	Model Correlation With Experimental Data.....	112
	Model Validation.....	114
5.7.1	Diagonal Length.....	114
5.7.2	Substrate Thickness.....	115
5.7.3	Ball Count.....	118

5.7.4	Ceramic CTE.....	118
5.7.5	Solder CTE.....	120
5.7.6	Solder Joint Diameter.....	123
5.7.7	Underfill Modulus.....	123
5.7.8	Underfill CTE.....	126
5.7.9	PCB Thickness.....	126
5.7.10	Delta T.....	129
5.8	Design Guidelines.....	129
CHAPTER 6 STATISTICS BASED CLOSED FORM MODELS FOR CCGA PACKAGES.....		132
6.1	Data Set.....	134
6.2	Model Input Selection.....	134
6.3	Multiple Linear Regression.....	136
6.4	Hypothesis Testing.....	137
6.5	Model Adequacy Checking.....	139
6.6	Model Correlation With Experimental Data.....	142
6.7	Model Validation.....	144
6.7.1	Substrate Area.....	144
6.7.2	Substrate Thickness.....	145
6.7.3	Ball Height.....	148
6.7.4	Solder Volume.....	148
6.7.5	Delta T.....	151
6.8	Design Guidelines.....	153

CHAPTER 7 POWER DEPENDENCY OF PREDICTOR VARIABLES.....	154
7.1 Box Tidwell Power Law Modelling.....	154
7.2 Power Law Dependency Of Flip Chip Predictor Variables.....	156
7.3 Power Law Dependency Of CBGA Predictor Variables.....	159
7.4 Power Law Dependency Of CCGA Predictor Variables.....	160
7.5 Power Law Dependency Of Flex-BGA Predictor Variables.....	160
CHAPTER 8 SUMMARY AND CONCLUSION.....	165
BIBLIOGRAPHY.....	168
APPENDIX LIST OF SYMBOLS.....	179

LIST OF FIGURES

1.1: Cross-sectional view of PBGA package.....	3
1.2: Cross-Sectional View of Flex-BGA Package.....	5
1.3: Cross- Sectional view of CBGA Package.....	7
1.4: Cross Sectional View of Flip-Chip BGA.....	8
1.5: Solder joint fatigue failure due to thermal cycling.....	10
3.1: Cross-Section of Flex BGA Package.....	28
3.2: Layered View Of Flex-BGA Package.....	28
3.3: Residual plot of Flex-BGA multiple linear regression model.....	40
3.4 Effect of die to body ratio on thermal fatigue reliability of Flex-BGA package.....	45
3.5: Effect of ball count on thermal fatigue reliability of CBGA packages.....	47
3.6: Effect of ball diameter on thermal fatigue reliability of Flex-BGA packages.....	49
3.7 Effect of PCB thickness on thermal fatigue reliability of Flex-BGA packages.....	50
3.8: Effect of EMC filler content on thermal fatigue reliability of Flex-BGA package...	52
3.9 : Effect of solder mask definition on thermal fatigue reliability of Flex-BGA Packages.....	54
3.10 : Effect of board finish on thermal fatigue reliability of Flex-BGA packages.....	55
3.11: Effect of Delta T on thermal fatigue reliability of Flex-BGA packages.....	57
4.1: Cross Section of Flip Chip BGA Package.....	61
4.2: Residual plots of log transformed flip chip prediction model.....	72

4.3: Scree plot for selecting the number of principal components.....	76
4.4 : Residual plot of principal components regression model.....	83
4.5 : Chi Square plot of principal components regression model.....	84
4.6: Q-Q plot of principal components regression model.....	84
4.7: Effect of die length on thermal fatigue reliability of encapsulated flip-chip with Sn37Pb solder joints.....	88
4.8 Effect of solder joint diameter on thermal fatigue reliability of flip-chip packages subjected to thermal cycling of -550C to 1250C.....	89
4.9: Effect of ball height on thermal fatigue reliability of flip-chip packages.....	91
4.10: Effect of solder modulus on thermal fatigue reliability of flip-chip packages.....	93
4.11: Effect of ball pitch on thermal fatigue reliability of flip-chip packages.....	94
4.12: Effect of underfill modulus on thermal fatigue reliability of flip-chip packages....	96
4.13: Effect of Delta T on thermal fatigue reliability of flip-chip packages.....	97
4.14 : Effect of under cover area on thermal fatigue reliability of flip-chip packages.....	99
5.1: Motorola CBGA Cross-Section View.....	103
5.2: Residual plot of CBGA multiple linear regression model.....	110
5.3 :Effect of diagonal length on thermal fatigue reliability of CBGA packages.....	116
5.4: Effect of substrate thickness on thermal fatigue reliability of CBGA packages.....	117
5.5: Effect of ball count on thermal fatigue reliability of CBGA packages.....	119
5.6: Effect of ceramic CTE on thermal fatigue reliability of CBGA packages.....	121
5.7: Effect of solder CTE on thermal fatigue reliability of CBGA packages.....	122
5.8: Effect of ball diameter on thermal fatigue reliability of CBGA packages.....	124
5.9: Effect of underfill modulus on thermal fatigue reliability of CBGA packages.....	125

5.10: Effect of underfill CTE on thermal fatigue reliability of CBGA packages.....	127
5.11: Effect of PCB thickness on thermal fatigue reliability of CBGA packages.....	128
5.12: Effect of Delta T on thermal fatigue reliability of CBGA packages.....	130
6.1: Layered View of IBM CCGA Package.....	133
6.2: Column Grid Arrays of IBM CCGA Package.....	133
6.3: Residual plots of CCGA multiple linear regression model.....	140
6.4: Effect of substrate area on thermal fatigue reliability of CCGA packages.....	146
6.5 Effect of substrate thickness on thermal fatigue reliability of CCGA packages.....	147
6.6: Effect of ball height on thermal fatigue reliability of CCGA packages.....	149
6.7: Effect of solder volume on thermal fatigue reliability of CCGA package.....	150
6.8: Effect of DeltaT on thermal fatigue reliability of CCGA packages.....	152

LIST OF TABLES

3.1: Scope of accelerated test database.....	30
3.2: Stepwise regression of Flex-BGA predictor variables.....	32
3.3 Multiple linear regression model of Flex-BGA package.....	36
3.4: Analysis of variance of Flex-BGA multiple linear regression model.....	36
3.5: Pearson’s correlation matrix of Flex-BGA predictor variables.....	41
3.6: Single factor analysis of variance.....	43
3.7: Sensitivity of the package reliability to die to body ratio and comparison of model predictions with actual failure data.....	45
3.8: Sensitivity of the package reliability to ball count and comparison of model predictions with actual failure data.....	47
3.9: Sensitivity of the package reliability to ball count and comparison of model predictions with actual failure data.....	49
3.10: Sensitivity of the package reliability to PCB thickness and comparison of model predictions with actual failure data.....	50
3.11: Sensitivity of the package reliability to encapsulant mold compound filler content and comparison of model predictions with actual failure data.....	52
3.12: Sensitivity of the package reliability to pad configuration and comparison of model predictions with actual failure data.....	54

3.13: Sensitivity of the package reliability to board finish and comparison of model predictions with actual failure data.....	55
3.14: Sensitivity of the package reliability to Delta T and comparison of model predictions with actual failure data.....	57
4.1 Scope of accelerated test database.....	63
4.2: Stepwise Regression of Flip-Chip Predictor Variables.....	66
4.3 Pearson's correlation matrix of flip chip predictor variables.....	69
4.4: Multiple linear regression model of Flip-Chip package using natural log transformed flip chip predictor variables.....	70
4.5 : Analysis of variance of log transformed flip chip prediction model.....	70
4.6: Pearson's correlation matrix of log transformed flip chip predictor variables.....	73
4.7: Multiple linear regression model using principal components of flip chip predictor variables.....	78
4.9: Analysis of variance of multiple linear regression model with principal components as variables.....	78
4.9: Principal component regression model using original flip chip predictor variables.....	79
4.10: Single Factor Analysis of Variance.....	85
4.11 : Pair-wise T Test.....	85
4.12: Sensitivity of the package reliability to the die length and comparison of model predictions with actual failure data.....	88
4.14: Sensitivity of the package reliability to the solder joint diameter and comparison of model predictions with actual failure data.....	89

4.15: Sensitivity of the package reliability to the solder joint height and comparison of model predictions with actual failure data.....	91
4.16: Sensitivity of the package reliability to the solder modulus and comparison of model predictions with actual failure data.....	93
4.17: Sensitivity of the package reliability to ball pitch and comparison of model predictions with actual failure data.....	94
4.18 : Sensitivity of the package reliability to underfill modulus and comparison of model predictions with actual failure data.....	96
4.19 : Sensitivity of the package reliability to Delta T and comparison of model predictions with actual failure data.....	97
4.20: Sensitivity of the package reliability to undercover area and comparison of model predictions with actual failure data.....	99
5.1: Scope of accelerated test database.....	104
5.2: Multiple linear regression model of CBGA package.....	108
5.3: Analysis of variance of CBGA multiple linear regression model.....	111
5.4: Pearson’s correlation matrix of CBGA predictor variables.....	113
5.5: Single factor analysis of variance.....	116
5.6: Sensitivity of the package reliability to diagonal length and comparison of model predictions with actual failure data.....	116
5.7: Sensitivity of the package reliability to substrate thickness and comparison of model predictions with actual failure data.....	117
5.8: Sensitivity of the package reliability to ball count and comparison of model	

predictions with actual failure data.....	119
5.9: Sensitivity of the package reliability to ceramic CTE and comparison of model predictions with actual failure data.....	121
5.10: Sensitivity of the package reliability to Solder CTE and comparison of model predictions with actual failure data.....	122
5.11: Sensitivity of the package reliability to ball diameter and comparison of model predictions with actual failure data.....	124
5.12: Sensitivity of the package reliability to underfill modulus and comparison of model predictions with actual failure data.....	125
5.13: Sensitivity of the package reliability to underfill CTE and comparison of model predictions with actual failure data.....	127
5.14: Sensitivity of the package reliability to PCB thickness and comparison of model predictions with actual failure data.....	128
5.15: Sensitivity of the package reliability to Delta T and comparison of model predictions with actual failure data.....	130
6.1: Accelerated test database.....	135
6.2: Multiple linear regression model for characteristic life prediction of CCGA package	138
6.3: Analysis of variance of CCGA multiple linear regression model.....	138
6.4: Pearson's correlation matrix of CCGA predictor variables.....	141
6.5: Single factor analysis of variance.....	143
6.6: Sensitivity of the package reliability to Delta T and comparison of model predictions with actual failure data.....	146

6.7: Sensitivity of the package reliability to die length and comparison of model predictions with actual failure data.....	147
6.8: Sensitivity of the package reliability to ball height and comparison of model predictions with actual failure data.....	149
6.9: Sensitivity of the package reliability to solder volume and comparison of model predictions with actual failure data.....	150
6.10: Sensitivity of the package reliability to Delta T and comparison of model predictions with actual failure data.....	152
7.1: Power law dependency of flip chip predictor variables.....	158
7.2: Power law dependency of CBGA predictor variables.....	162
7.3: Power law dependency of CCGA predictor variables.....	163
7.4: Power law dependency of Flex-BGA predictor variables.....	164

CHAPTER 1

INTRODUCTION

The emergence of microelectronics industry [Suhir, 2000] has revolutionized telecommunication, information and engineering industries of the 20th century leaving a dramatic, pervasive and beneficial influence on our everyday living. Electronic packaging may be understood as the technology of packaging electronic equipments which includes the interconnection of electronic components into printed wiring board (PWB), and printed wiring boards into electronic assembly. The role of electronic packaging in a device includes, providing interconnections for signal and power distribution, structural integrity for protection from environment loads and stresses and heat dissipation.

The major trends in microelectronics industry are driven by constant need for smaller, faster, more reliable and less expensive IC's. The need for cramming more number of devices onto a silicon chip has given life for small scale integration (SSI), medium scale integration (MSI), large scale integration (LSI) and very large scale integration (VLSI). In today's VLSI era, when a typical chip contains 10 million devices, the perimeter of the device alone is not sufficient to accommodate all of the input- output interconnections (I/Os), driving the need for area array interconnection.

Ball-grid array (BGA) is an area array interconnection technology with an array of balls on the bottom of the package used for making interconnection with the printed wiring board. Since the BGA provides interconnection of an area instead of the perimeter, high interconnection densities are achievable [McKewon, 1999]. Also, with no leads to bend, and self centered solders, BGA's offer reduced co-planarity and minimized handling and placement problems. In addition BGA packages offer better electrical performance and can be extended to multi chip modules easily. BGA's are available in a variety of types, ranging from plastic over molded BGA's called PBGA's, flex tape BGA's called FlexBGA or FTBGA, ceramic substrate BGA's named CBGA and CCGA and flip chip BGA's with wire-bonds replaced with flip chip interconnects.

A plastic ball grid array consists of silicon chip die mounted on to a Bismaleimide Triazine (BT) substrate using a die attach adhesive. The BT substrate is used over standard FR4 laminate for its high glass transition temperature and heat resistance. Electrical signal from the chip are carried by gold wire bonds which is then bonded to the substrate. Traces from the wire-bond pads take the signals to the via's which then carry them to the bottom side of the substrate and then to the solder pads. An encapsulant is provided covering the chip, wires and the substrate wire-bond pads for protection from environment. PBGA packages are found in applications requiring improved portability, form factor and high performance such as cellular phones, laptop pc's, video cameras, wireless PCMCIA cards, automotive under-hood components and other similar products. A cross section of PBGA package is given by Figure 1.1

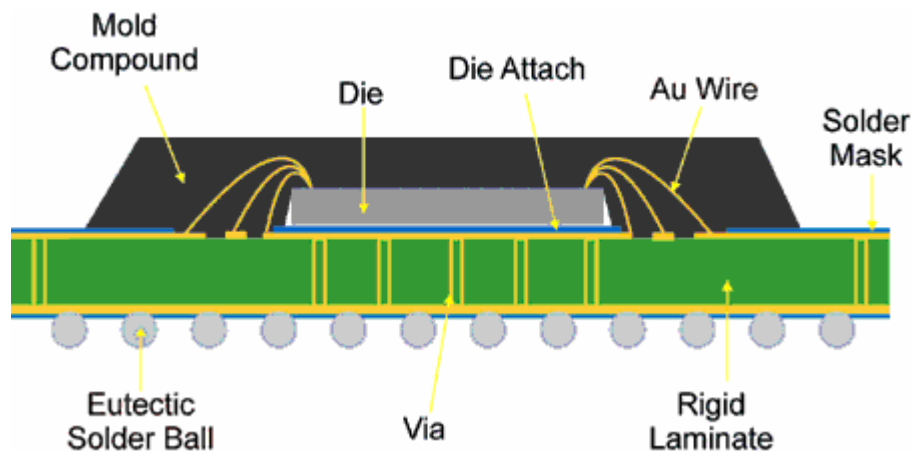


Figure 1.1: Cross-sectional view of PBGA package.

Flex tape ball grid array package is a cavity down package that uses a flex tape as a substrate. The presence of a nickel plated copper heat spreader in Flex BGA's improve the thermal and electrical performance and reliability making them a better choice for extreme conditions than their plastic counterparts [Karnezos 1996]. The die is attached beneath the stiff metal heat spreader with silver filled epoxy to provide thermal conductivity to the heat spreader and wire bonded to the tape traces with gold wire. Encapsulation is provided in the bottom to protect the die and the wire bonds from the environment. Flex BGA packages are used in hard drives, PDA's, global positioning systems, ASICs, controllers, Flash Memory, digital consumer electronics, wireless telecommunications, and various other portable products.

Ceramic ball grid array (CBGA) packages [Figure 1.3] are an extension of controlled collapsed chip connection (C4) and use a co-fired alumina ceramic substrate [Lau 1995]. The multilayered ceramic substrates are chosen for their superior electrical performance such as option for multiple power and ground planes and the ability to choose the signal, power and ground locations within the column array locations. Also, the low difference coefficients of thermal expansions of ceramic (6.7 ppm/C) and silicon (2.7ppm/C) increases the component level reliability [Burnette 2000], making ceramic substrates a good choice for flip chip applications. Ceramic column grid array packages are very similar to ceramic ball grid array but use a solder column instead of a solder ball for improved thermal fatigue resistance. The solder column consists of wires of high lead (90Pb/10Sn) solder attached to the substrate with eutectic (63Sn/37Pb) solder. CBGA and CCGA packages find a wide range of applications in high end microprocessors

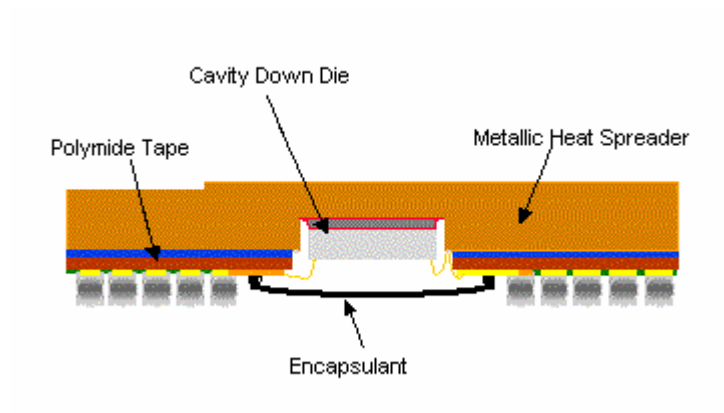


Figure 1.2: Cross-Sectional View of Flex-BGA Package

personnel computer microprocessors [Master 1998], telecommunication products [Lau 2003], workstations and avionic products.

Flip chip is not a specific package type like CBGA or PBGA, but a method of electrically connecting the die to the package carrier. In flip chip packaging the die is inverted face down directly onto a package or a printed wired board, by means of solder bumps typically deposited on the integrated circuit or wafer and bonded to the package or PWB. A typical flip chip on board (FCOB) is shown in Figure 1.4. Flip chip packages offer the advantages of high I/O, shortest electrical connection and hence improved electrical performance, low cost and high speed production. An underfill is used in flip chip packages for distributing the stresses in the solder thereby increasing the thermo-mechanical reliability of solder joints. Flip chip packaging has been implemented in wide variety of applications including portable consumer electronics like cellular phones [Sillanpaa et al. 2004], laptops [Pascariu et al. 2003], under-the-hood electronics [Jung et al. 1998], microwave applications [Bedinger 2000], system in package (SIP) [Van den Crommenacker, 2003], high-end workstations [Ray et al., 1997], and other high performance applications.

Thermo-mechanical failures are caused by stresses and strains generated within an electronic package due to significant difference in coefficients of thermal expansion of silicon chip and organic-laminate substrate. The coefficient of thermal expansion of organic PWB is significantly higher than that of the silicon. When the chip heats up through the electronic operation or environment, the PWB will heat up and expand a great deal more than the silicon. When the temperature decreases, due to cessation of the

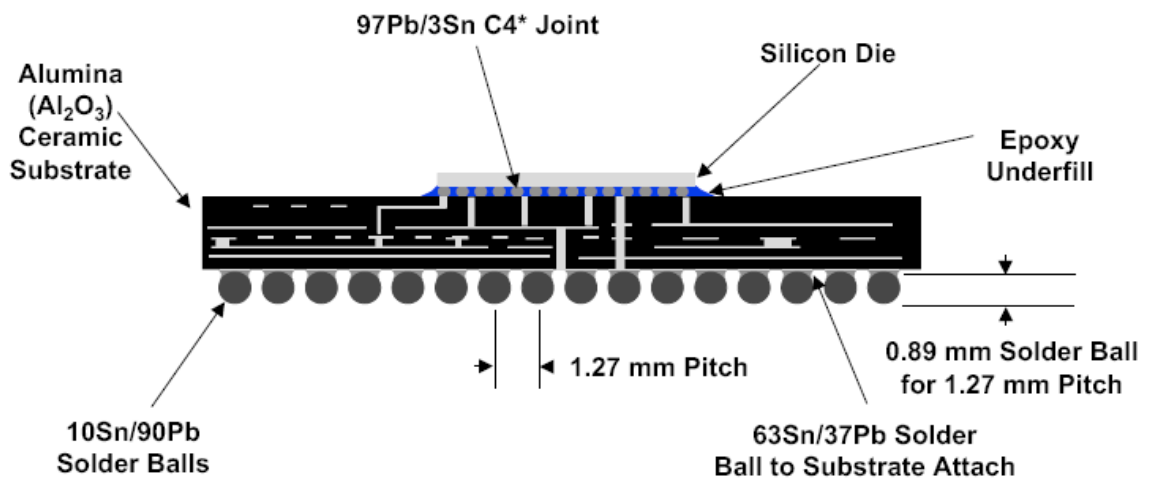


Figure 1.3: Cross- Sectional view of CBGA Package

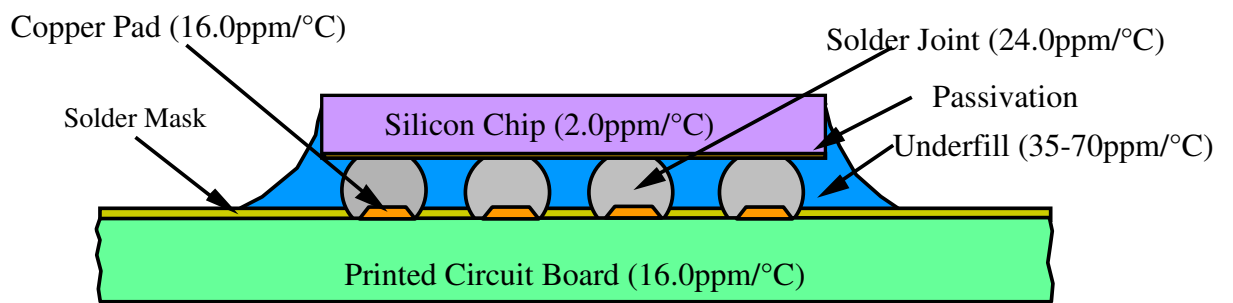
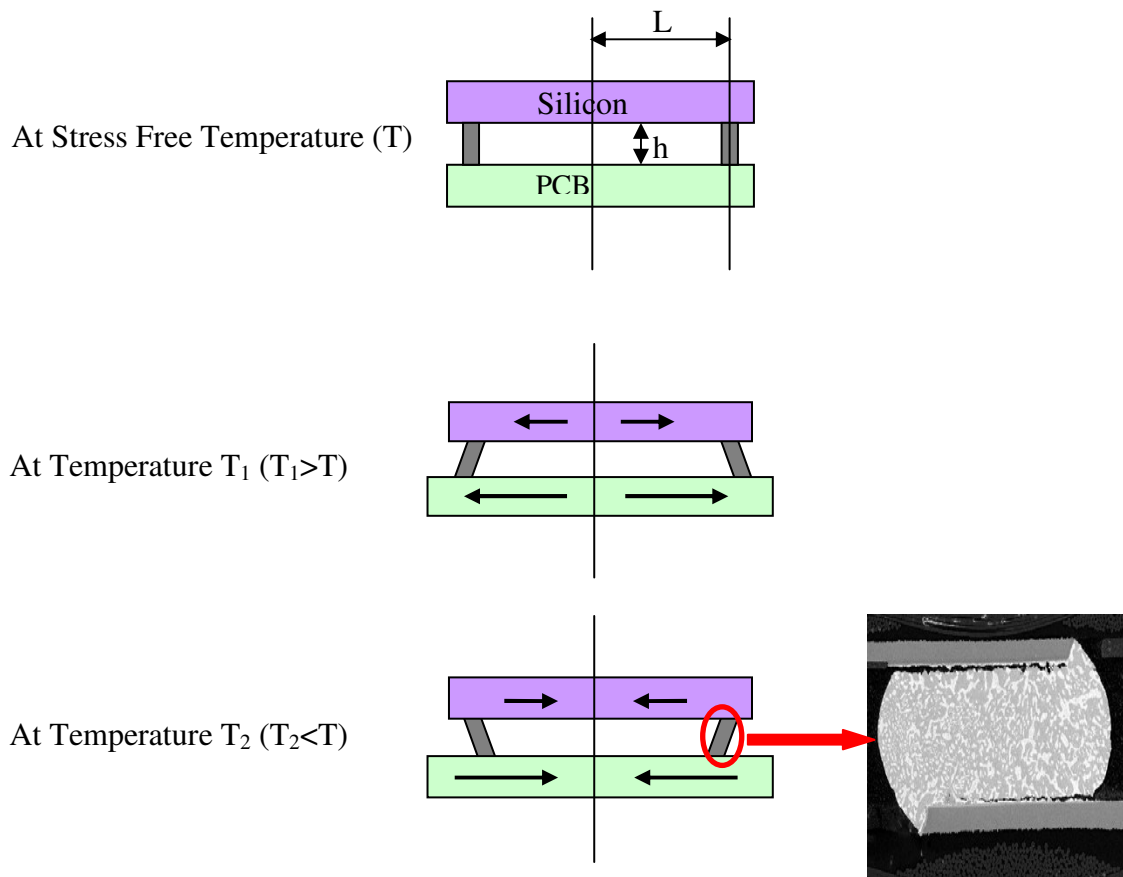


Figure 1.4: Cross Sectional View Of Flip-Chip BGA

operation or environment, the PWB will contract. The expansion and contraction introduces shear strains and shear stresses in the solder joint. High shear stress can cause delamination of various interfaces like UBM/intermetallic, solder/underfill etc. Apart from delamination, the repeated heating and cooling can eventually cause fatigue of the solder joints. The high shear stresses would enhance the fatigue initiation making solder interconnect more susceptible to such fatigue failures [Figure 1.5]. Hence evaluation of stresses at the joints has become critical to predict the reliability of the assembly.

Increasing the I/O distributes the shear stress among large number of solder interconnects, increasing the life of the joint. Also, increasing the ball height and ball diameter reduces the stress concentration and increases the crack propagation path leading to improved reliability of the joint. However, increasing the I/O leads to decreasing the bump diameter and height. Thus reliability is improved by increasing ball count, ball diameter and ball height, but how much it increases for an increase in ball count and a parallel decrease in ball height has to be explored. Also, there is a growing need for understanding the effect of various other parameters including die size, underfill properties, solder properties, solder properties, environmental conditions, etc, and their individual effects and coupled effects on thermo-mechanical reliability. This research aims at accomplishing the same.



CHAPTER 2

LITERATURE REVIEW

Demands on package miniaturization, high density and reliability are driving the need for predictive methodologies for maintaining high levels of reliability and performing thermo-mechanical trade-offs. A reliability assessment numerical model that could take into account the geometric details of the package, the material properties of the widely used material and the operating conditions could be of great help in obtaining the failure modes such as die cracking, solder joint fatigue failure, de-lamination etc. Solder joint fatigue failure being a dominant failure mode contributing 90% of all structural and electrical failures [Tummala 1997] demands greater focus for improving the mechanical reliability of the package. In this section, traditional approaches for solder joint reliability prediction, including physics of failure based models, statistical models, finite element models and experimental techniques have been discussed.

2.1 PHYSICS OF FAILURE BASED MODELS

Manson and Coffin [1965, 1954] developed an equation that related plastic strain $\Delta\varepsilon_p$, with number of cycles to failure N . Goldmann [1969] analyzed a controlled collapse joint with spherical dimensions for developing an equation that related the plastic strain of a joint with relative thermal expansion coefficients of chip to substrate, distance from chip neutral point to substrate, height of the solder, volume of solder, radius of the cross section under consideration and exponent from plastic shear stress strain relationship. The

plastic strain obtained from Goldmann formulation can be substituted in Coffin- Manson equation for predicting the number of cycles for fatigue failure. Norris and Landzberg [1969] studied the effect of cycling frequency and maximum temperature of cycling on fatigue failure of solder joints and added an empirical correction factor for time dependent and temperature dependent effects for the thermal fatigue model.

Solomon [1986] analyzed the fatigue failure of 60Sn/40Pb solder for various temperatures and developed an isothermal low cycle fatigue equation that correlated the number of cycles to failure with applied shear strain range. Solomon also studied the influence of frequency, and temperature changes and added corrections that account for temperature changes, cycling wave shape and joint geometries.

Engelmaier [1990] developed a surface mount solder joint reliability prediction model containing all the parameters influencing the shear fatigue life of a solder joint due to shear displacement caused by thermal expansion mismatch between component and substrate. Engelmaier developed separate equation for stiff solder joints and compliant solder joints. The parameters of the model include effective solder joint area, solder joint height, diagonal flexural stiffness, distance from neutral point and thermal coefficient mismatch thermal cycling conditions, degree of completeness of stress relaxation and slope of weibull distribution.

Knecht and Fox [1991] developed a strain based model using creep shear strain as damage metric to determine the number of cycles to failure. The creep shear strain included creep of component due to matrix creep alone ignoring the plastic work. The equation was applicable to both 60Sn40Pb and 63Sn37Pb solder joints.

Vandeveldel [1998] developed thermo-mechanical models for evaluating the solder joint forces and stresses. Barker et al [2002] synthesized the Vandeveldel models for calculating the solder joint shear forces in ceramic and plastic ball grid array packages. Clech [1996] developed a solder reliability solutions model for leadless and leaded eutectic solder assemblies and extended it to area array and CSP packages. Clech obtained the inelastic strain energy density from area of solder joint hysteresis loop and developed a prediction equation correlating inelastic strain energy density with number of cycles to failure.

Singh [2006] developed failure mechanics based models for solder joint life prediction of ball array and flip chip packages. He calculated the maximum shear strain using a simplified DNP formula which was then used for initiating a hysteresis loop iteration for both global and local thermal mismatch. Inelastic strain energy was then calculated from the area of the hysteresis loop for both the thermal mismatch cases. The number of cycles for failure was determined using Lall [2003] model.

2.2 STATISTICAL PREDICTION MODELS

Statistical prediction models developed include cumulative failure distribution functions for expressing the experimental failure data as a probability function of time to failure for any failure distribution. Weibull distribution and Log normal distribution have been most widely used failure distribution functions. Log normal distributions [Muncy 2004] have widely been used for modeling failure due to slow degradation such as chemical reactions and other corrosions and weibull distributions have been used for modeling failures due to weak link propagations such as solder joint failure.

Regression analysis and analysis of variance have been widely used by researchers for correlating the reliability of a package with its geometric attributes, material properties and operating conditions. Muncy [2004] conducted air to air thermal cycling and liquid to liquid to liquid thermal shock tests on a flip chip package for 1200 test boards with four different die sizes, eight board configurations, two underfill materials and two substrate metallizations. The predictor variables considered for model building include substrate metallization, substrate mask opening area versus the UBM area of the flip chip bump, die size, perimeter or full area array flip chip interconnect pattern, underfill material properties, location of the die on the test board, frequency of cycling, number of interconnects, and percent area voiding. Multiple linear regression modelling and regression with life data modeling methodologies were used for obtaining the parameters of regression.

Perkins [2004] developed a multiple linear regression based polynomial equation for correlating fatigue life of a ceramic package with its design parameters. A data matrix was formulated using a full factorial design of simulation study for the five design parameters including substrate size, substrate thickness, CTE mismatch between substrate and board, board thickness and solder ball pitch with two levels each. Simulations were run for each data point using a finite element analysis and the fatigue life was extracted. Interactions between the predictor variables were studied and a regression model with both main terms and interaction terms was built.

Singh [2006] developed multivariate regression based models for life prediction of BGA packages. The input data for model building was collected from published literature and accelerated test reliability database based on the harsh environment testing

of BGA packages by the researchers at the NSF Center for Advanced Vehicle Electronics (CAVE). The predictor variables considered for model building included die, die to body ratio, ball count, ball diameter, solder mask definition, printed circuit board surface finish, printed circuit board thickness, encapsulant mold compound filler content and ΔT . Dummy variables were used for categorical variables like board finish, encapsulant mold compound filler content and solder mask definition. Linear, modified linear and non-linear models were developed using regression analysis and analysis of variance and validated with experimental data.

Iyer [2005] correlated the reliability of a flip chip package with its properties of underfill and flux using a regression and back propagation neural networks based models. Data from accelerated life testing of flip chip package with 95 different underfill flux combinations was used for model building. The underfill parameters for model building included modulus of elasticity, coefficient of thermal expansion, glass transition temperature and filler content. The flux parameters studied include acid number and viscosity. The regression models and the neural network models were validated using a test data set and the neural networks model was found to outperform the regression model owing to minimum residual mean square errors.

Stoyanov [2002] used a design of experiments and response surface modeling methodology for building a quadratic equation that related underfill modulus, underfill CTE, stand off height and substrate thickness with number of cycles to failure for a flip chip package. The data for model building was collected from a finite element analysis of a flip chip package. Residual analysis, analysis of variance and statistical efficiency measure were used for validating the models. Taguchi optimization technique was used

by Lai [2005] for optimizing the thermo-mechanical reliability of a package on package for various design parameters. The package parameters considered for optimization included die thickness, package size, mold thickness, substrate thickness and solder joint stand off.

Jagarkal, et al. [2004] developed an optimization based solder joint reliability prediction model for a board level generic electronic package. Finite element analysis was conducted on the package and PWB in- plane young's modulus, PWB in- plane coefficient of thermal expansion, PWB core thickness and solder joint stand-off height were found to be the most important design parameters using built in optimization module of ANSYS. Optimization models using sub-approximation, design of experiment and central composite design based response surface methodology were developed for studying the sensitivity of design parameters on thermo-mechanical reliability.

2.3 FINITE ELEMENT ANALYSIS

Numerical techniques such as finite element analysis can be employed for assessing the fatigue failure of a solder joint. Finite element analysis techniques extract a damage parameter such as plastic work, creep strain, plastic strain etc and map them into an experimentally obtained data or empirical relationship between fatigue life and number of cycles to failure to predict the expected service life of a solder joint. Darveaux [1991] developed a linear-non linear analysis method in which he used a linear finite element analysis for calculating the assembly stiffness and the imposed strain's on the solder joints. A one dimensional non linear analysis was then performed for calculating

the strain energy density accumulated per cycle. Coffin- Manson relation was used for calculating the number of cycles to failure.

Corbin [1991] developed a micro-macro approach for solder joint reliability prediction. A coarse macro model with thin plate elements was used for modeling the ceramic module and the FR4 board and a group beam elements were used for modeling a coupling between card and the module. The beam element was used for determining the major thermal deformation modes which were then input to the more detailed micro level solder joint as boundary conditions. Linear elastic properties have been used for the macro model and visco-plastic properties for the micro model. Plastic strain was extracted from the micro model and the fatigue life was calculated using Coffin-Manson equation.

Darveaux [1996] developed a three dimensional non-linear slice model with accumulated strain energy density as the damage metric for solder joint reliability predictions. Solder joint was modeled as visco-plastic solid, printed circuit board as orthotropic linear elastic and rest of the material as linear elastic. The model was imposed with symmetric boundary conditions on the slice plane coinciding with true symmetry plane. The extracted plastic work accumulated per unit volume per thermal cycle was used for crack growth correlations. Volume averaging was applied to reduce the sensitivity of strain energy to meshing.

Riebling [1996] developed a global local modeling approach with plastic work as damage parameter for solder joint reliability predictions. An octant of the packaged device with linear material behavior was modeled as the global model and a single solder joint with PCB and all the package parameters and non linear material behavior was

modeled as the local model. The model was imposed with symmetric boundary conditions on the slice plane coinciding with true symmetry plane. The global model was subjected to a one degree temperature change, providing displacement fields on a per degree basis. The scaled displacement fields in accordance with the thermal cycling was used as the boundary conditions for the local model of the critical joint. Plastic work was extracted from the solder joint and Darveaux's crack growth correlations have been used for determining the number of cycles to failure.

Pang, et al. [2001] developed an elastic plastic creep analysis for solder joint reliability prediction of a ceramic ball grid array package. In this method the temperature was allowed to ramp from low temperature to high temperature and elastic plastic analysis was conducted for every 5⁰C increment. The model was then held at dwell high temperature and a creep analysis was performed. The temperature was again ramped down from high temperature to low temperature and elastic plastic analysis was conducted for every 5⁰C increment. The model was then held at dwell low temperature and a creep analysis was performed. The temperature cycling pattern was repeated thrice and the complete equivalent stress and strain were obtained which was then used for fatigue and creep life prediction.

Werner, et al [2004] integrated a finite element stress module within a CFD module to predict the solder joint life of a resistor package using finite element and finite volume codes. Hong [1998], Farooq, et al[2003] developed finite element models for studying the thermo-mechanical fatigue reliability of lead free CBGA packages. The lead free alloys for CBGA packages were found to perform better than the traditional dual alloy Sn/Pb alloys. Perkins, et al. [2004] conducted Coffin-Manson based non linear

finite element analysis on CBGA packages for various combinations of substrate size, substrate thickness, board thickness, CTE mismatch and ball pitch.

Braun, et al. [2005] conducted thermo-mechanical simulations for studying the solder joint reliability of SnAg solder bumps mounted on high T_g FR4 substrate with immersion Sn and Ni/Au finishes. Pang, et al. [2004] analyzed 96.5Sn-3.5Ag solder joints for flip chip application using elastic plastic creep finite element analysis. The flip chip packages were subjected to both thermal cycling and thermal shock conditions. Gonzalez, et al. [2005] studied the advantages, challenges and limitations of using finite element prediction model for lead free solder joint prediction of flip chip packages. Cheng [2004] studied the effect of underfill on flip-chip packages with different ball diameters and stand-off height's.

2.4 SOLDER JOINT CONSTITUTIVE EQUATIONS

Since the solder material has a high homologous temperatures of about 0.65 even at room temperature, creep process are expected to dominate its deformation kinetics giving rise to complex behavior. Constitutive models have used explicit creep equations or unified viscoplastic models for modeling the rate dependent behavior of the solder material. The creep models developed include power law creep models [Ju et al, 1994], Harper Dorn creep models and hyperbolic creep models [Garafalo, 1965]. Since the unified visco-plastic model combines the rate dependent plasticity and creep, they are highly desired as the use of explicit creep equation would require the addition of rate dependent plasticity in the material model.

A unified visco-plastic model for 60Sn/40Pb taking into account the measured stress-dependence of the activation energy and the strong Bauschinger effect exhibited by the solder was developed by Busso, et al. [1992]. Qian, et al. [1997] described the transient stage of a stress/strain curve through back stress for building a unified constitutive model for tin lead solder. Skioper, et al. [1996] developed constitutive models for 63Sn/37Pb eutectic solders using unified Bodner-Partom model. Yi et al [2002] developed a constitutive model based on a combination of grain boundary sliding and matrix dislocation deformation mechanisms. Most of the above mentioned models require user defined subroutine codes for representing the non linear rate dependent stress strain relations in a finite element package.

Anand [1985] and Brown [1989] developed a set of constitutive equations for large isotropic, visco-plastic deformation and small elastic deformation using a single scalar internal variable model. This model presented the advantage of easy implementation in commercially available finite element packages such as ANSYS. Daveaux and Banerji [1992] determined the material parameters of the Anand's model for 62Sn36Pb2Ag, 60Sn40Pb, 96.5Sn3.5Ag, 97Pb3Sn and 95Pb5Sn solder joints from experimental results. Wang, et al.[2001] determined the material parameters of the constitutive relations for 62Sn36Pb2Ag, 60Sn40Pb, 96.5Sn3.5Ag, and 97.5Pb2.5Sn solders from separate constitutive relations and experimental results and tested for constant strain rate testing, steady-state plastic flow and stress/strain responses under cyclic loading. Amagai, et al. [2002] conducted material characterization tests of Sn-Pb based and Sn-Ag based lead-free solders (63Sn37Pb, 62Sn36Pb2Ag, Sn3.5Ag0.75Cu, Sn2.0Ag0.5Cu), and fitted the data to the Anand's constitutive model which unifies both

rate-dependent creep and rate independent plasticity via viscoplastic flow equation and evolution equation.

2.5 **SOLDER JOINT FATIGUE MODELLING**

Solder joint fatigue models are used for determining the number of cycles that the package would survive before the solder joint fails. Several of the physics of failure models [Engelmeir, Knecht and Fox, Duan] can be used in conjunction with finite element analysis for predicting the fatigue failure of solder joints. Ostergren [1979] formulated an energy based method for fatigue life prediction of solder joints. A damage function that incorporated both stress and inelastic strain energy was used as a damage proxy for low cycle fatigue damage at elevated temperatures. The number of cycles to failure was then calculated by replacing the plastic strain of Coffin-manson relation with the damage function. Vayman [1989] studied the effect of strain range, ramp time, hold time and temperature on isothermal fatigue failure of tin lead solder joints and developed a strain range partitioning model that partitioned the inelastic strain energy into time dependent plasticity and time dependent creep to include the effects of ramp and hold time on fatigue failure of solder joints. Duan [1988] synthesized the strain range partitioning and the damage function and developed a strain energy partitioning method for low cycle fatigue life prediction of heat resistant alloys.

Darveaux [1997] developed an energy based model that used accumulated plastic strain energy as damage metric for finding the number of cycles to failure. Darveaux conducted extensive thermal cycling experiments on CBGA samples and measured the crack length in the solder ball during thermal cycling for developing a model that related

laboratory measurements of low cycle fatigue crack initiation and crack growth rates with inelastic work of the solder. Anand's constitutive model was used for modeling the solder material. The model used inelastic strain energy density extracted from finite element analysis, along with crack growth data, for determining the number of cycles for crack initiation and number of cycles for crack propagation along the solder joint.

Amagai [1998] developed a visco-plastic constitutive model for analyzing the thermally induced creep and plastic deformation for chip scale packages and multi layer ball grid array packages on printed circuit boards. Fusaro [1997] analyzed a copper base plate attachment to a power module using visco-plastic properties of eutectic solder joint. Dougherty [1997] developed solder joint reliability models for micro miniature electronic packages. Johnson [1999] studied Darveaux's model and identified key parameters affecting solder joint reliability. Pitarressi [2000] developed fatigue models for solder joint reliability prediction of multiple ball grid array packages. Zahn [2000] developed a comprehensive solder fatigue and thermal characterization model for a multi chip module package. Goetz et al [2000] developed a solder joint fatigue model for a silicon based system in package. Shi, et al. [2000] developed a strain based model that uses plastic strain range as a damage proxy for predicting the number of cycles to failure. The model considered the effect of both temperature and frequency on low cycle fatigue life of eutectic solder joint. Lall, et al. [2003] modified Darveaux's model for PBGA and CSP packages for harsh environments. Syed [2004] developed creep strain and strain energy density based thermal fatigue life prediction model for lead free solder joints.

2.6 EXPERIMENTAL METHODS

Temperature cycling is a widely method for solder joint reliability predictions. In this method the component is exposed to a series of low and high temperatures accelerating the failure modes caused by cyclic stresses. The thermal cycling uses a single air chamber in which the temperature ramp can be controlled carefully. Thermal shock tests like thermal cycling are used for accelerated life testing of solder joints. Thermal shock testing is a liquid-liquid test in which two liquid chambers at different temperatures are used. Thermal shock tests generate very high ramp rates.

Master, et al. [1998] conducted accelerated thermal cycling tests on CBGA packages for various body size and assembly parameters to study the effect of package thickness and card pad design on reliability of the package. Master, et al. [1995] studied the effect of column length on fatigue life of solder joint for two different thermal profiles using accelerated thermal cycling tests. Gerke, et al. [1995] studied the reliability of high I/O CBGA packages used in computer environment using accelerated thermal cycling tests for two different thermal profiles. Kang [2004] evaluated the thermal fatigue life and failure mechanism of Sn-Ag-Cu solder joints with reduced Ag contents for a CBGA package. Hong [1998] predicted the mean fatigue life of CBGA packages with lead free (Sb5-Sn95, Ag3.5-Sn96.5, Zn9-Sn91) solder fillets and found the lead free joints outperform the leaded ones. Ingallas [1998] conducted accelerated thermal cycling tests on CCGA packages for two different ball pitch, to study the effect of solder ball pitch on solder joint reliability of the package. He found the 1mm pitch to be providing significant improvement in solder joint reliability of CCGA package.

Zhang, et al. [2001] evaluated the reliability of SnCu0.7, SnAg3.8Cu0.7 and SnAg3.5 solder joints on both NiP and Cu under bump metallurgies for flip-chip application. Peng, et al. [2004] analyzed the sensitivity of reliability of flip chip package to solder joint geometric parameters such as stand-off height, lower and upper contact angles, and solder joint profile using accelerated thermal cycling tests. Wang, et al. [2001] assessed the reliability of flip chip packages with no flow underfills using liquid to liquid thermal shock tests. Hou, et al. [2001] conducted liquid to liquid thermal shock tests for reliability assessment of flip chip packages with SnAgAu joints. He found the leaded solder joints perform better than the lead free ones. Teo, et al. [2000] conducted accelerated thermal cycling tests for investigating the effect of under bump metallurgy solder joint reliability of flip chip packages. Braun, et al. [2005] studied the high temperature potential of flip chip assemblies for automotive applications. Darveaux, et al [2000] studied the impact of design and material choice on solder joint fatigue life of various BGA packages including PBGA, FlexBGA, tape array BGA and mBGA.

Moire interferometry is an optical method which provides whole field contour maps of in-plane displacements with sensitivity as low as $0.417\mu\text{m}$ [Tunga 2004]. Moire Interferometry technique has been increasingly employed in mapping thermally induced deformation of electronic packages. Meng [1997] applied this technique for solder joint reliability prediction of BGA, CSP and flip chip packages. He subjected the packages to a temperature cycling and extracted the accumulated thermal deformations for reliability predictions. Zhu [1997] studied the reliability of OMPAC BGA and a flip chip BGA using moiré interferometry technique. Zhu also studied the effect of bonding,

encapsulation, soldering and geometry on the reliability of both the packages and using the same technique.

CHAPTER 3

STATISTICS BASED CLOSED FORM MODELS FOR FLEX-BGA PACKAGES

Multiple linear regression is a method of developing a prediction equation that predicts the value of a response variable Y given the values of predictor variables X . Multiple linear regression has been used for developing models for characteristic life prediction of Flex-BGA packages given its geometric aspects, material properties and its operating conditions. The developed prediction models have been validated for underlying statistical assumptions of model building and correlated with physics of failure to develop more meaningful closed form statistical models for flex-BGA package reliability predictions. The prediction ability of the closed form models have been validated by correlating the prediction results of the closed form models with actual experimental failure data.

3.1 OVERVIEW

This section presents multiple linear regression based statistical models for life prediction of Flex-BGA packages in harsh environments. The models act as a tool for fast track reliability prediction for a given component architecture and serve as an aid for understanding the sensitivity of component reliability to geometry, package architecture, material properties and board attributes to enable educated selection of appropriate device

formats. In addition, categorical variables such as solder mask definition and board finish can be incorporated in this model.

3.2 FLEX-BGA PACKAGE ARCHITECTURE

Flex-BGA packages are a family of cavity down BGA's that have the die, the flex tape and the solder balls attached to the bottom side of a metallic heat spreader. The nickel plated copper heat spreader is the stiffest member and is used for handling the package during assembly, test and reflow on the mother board. The interconnect circuit is flexible copper/polyimide tape with one or two metal layers and has solder mask on the metal layer that carries the solder balls. It is laminated to the heat spreader using a pressure sensitive adhesive. The die is attached into the cavity with silver filled die attach epoxy to provide thermal conductivity to the heat spreader. The die is wire bonded to the tape traces and the heat spreader with gold wire. Encapsulation protects the die and wire bonds and fills the cavity.

3.3 DATASET

The dataset used for model building has been accumulated from an extensive Flex-BGA accelerated test reliability database based on the harsh environment testing by the researchers at the NSF Center for Advanced Vehicle Electronics (CAVE). This database has also been supplemented with the various datasets published in the literature. Each data point in the database is based on the characteristic life of a set of Flex-BGA devices of a given configuration tested under harsh thermal cycling or thermal shock conditions. The range of data collected in each case is given by Table 3.1.

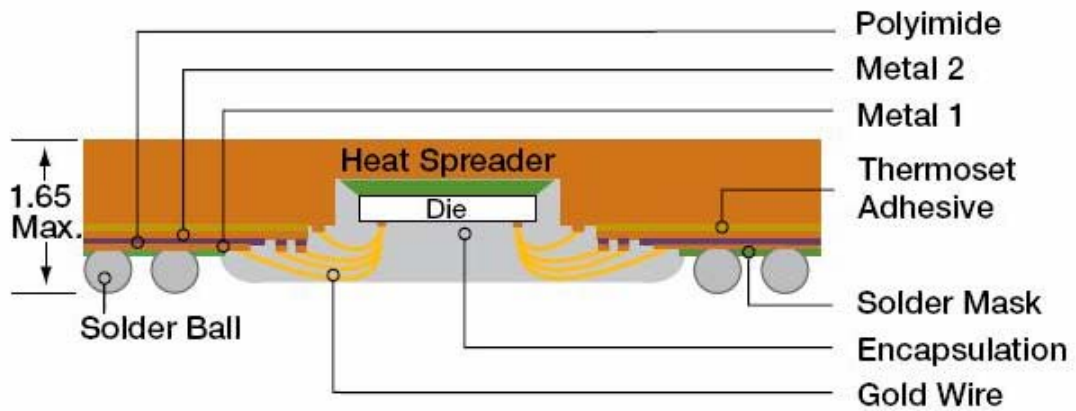


Figure 3.1: Cross-Section of Flex BGA Package

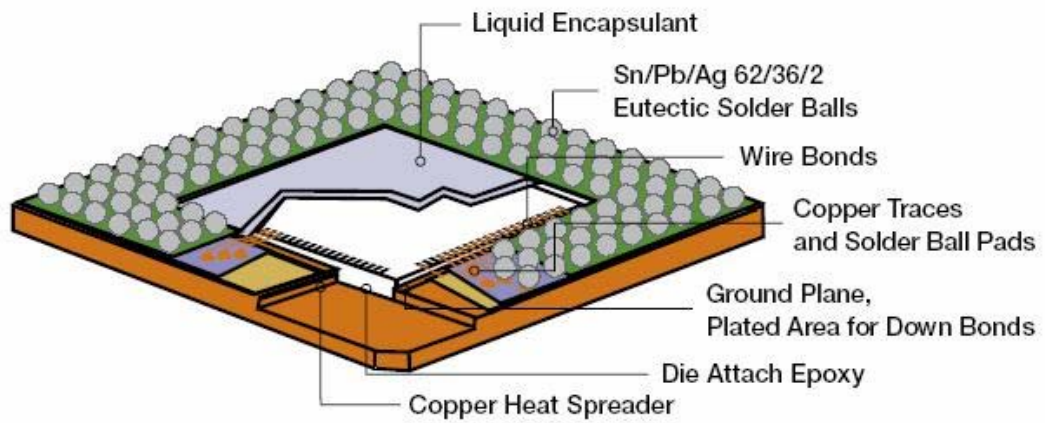


Figure 3.2: Layered View of Flex-BGA package

3.4 MODEL INPUT SELECTION

Model input variables have been chosen by defining all predictors that are known and then selecting a subset of predictors to optimize a predefined goodness-of-fit function. From a mathematical point of view, the featured selection problem can be formulated as a combinatorial optimization problem. Efforts have been made to trade-off accuracy and bias to find the “best” set of predictors for a model. Increasing the number of variables increases the model-information, at the expense of increased variance and model-complexity. Reduction in the number of variables reduces error-variance, but it biases the least square estimators and error variances. Let k denote the number of potential predictors for a model. If each variable either enters the model or is excluded from it, the total number of possible configurations is in the order $O(2^k)$, making it a complex combinatorial problem. Stepwise regression based on forward selection performance optimization and method of best subsets has been used for automatic search and identification of the best subset of predictor variables [Malthouse 2002, Dwinnell 1998, Cevenini 1996, McCray 2004, Mendes 2002, Kitchenham 2002]. Other methods studied include, Simulated Annealing (SA) [Brooks 2003], Principal Component Analysis (PCA) [King 1999] and Neural Network based Radial Basis Function (RBF) [Swanson 1995]. Stepwise Regression, which is a combination of forward selection and backward elimination process, has been selected because of availability in standard statistical packages. This search method develops a sequence of regression models, at each step adding or deleting a predictor variable. The criterion for adding or deleting a

Parameter	Data Range
Body Size	7.5 mm to 16 mm
Die to Body Ratio	0.3 to 0.81
Ball Count	40 to 280
Ball Pitch	0.5 mm to 1 mm
Ball Diameter	0.3 mm to 0.5 mm
Substrate Type	2L tape, 3L Tape
PCB Thickness	0.8 mm to 1.6 mm
PCB Surface Finish	OSP, HASL & Ni/Au
EMC Filler Content	Low, High
Solder Mask Definition	SMD, NSMD
T _{High} , Accelerated Test	100°C, 125°C, 150°C
T _{Low} , Accelerated Test	-55°C, -40°C, 0°C

Table 3.1: Scope of accelerated test database

predictor variable can be stated equivalently in terms of error sum of square reduction, coefficient of partial-correlation, t-statistic or f-statistic.

Forward search is initiated by trying all possible models that use a single input. The best single input is retained and a search begins on the remaining candidate inputs to become the second input. The input that most improves the model is kept and so on. This process ends either when the model ceases to improve or we run out of candidate inputs. A backward search works exactly like a forward search, except that it moves in the other direction. Backward searching begins with a model that uses all the inputs and then removes input variables one at a time.

The stepwise regression amounts to selecting of subset of $q \leq p$ candidate variable to be included in the model. Let set $\psi \subset \{1, 2, 3, \dots, p\}$ contains the indices of the variables selected. Each possible subset of variables is associated with one model. The scoring model associated with a particular subset ψ will be denoted by F_ψ . The objective function is based on method of least squares. For a linear functional form,

$$F_\psi = a + \sum_{k \in \psi} b_k x_k$$

where a and b_k ($k \in \psi$) are estimated using method of least squares. The stepwise regression initializes with $\psi = 0$, i.e. begins with no variables in the model and attempts to find the variable, which yields the maximum improvement.

Die to body ratio was identified as a potentially important and hence was selected as the first variable. A regression equation was fit with characteristic life as response variable and die to body ratio as predictor variable and the criteria's for model selection were studied. Die to body ratio was found to explain large proportion of variation at the cost of minimum mean square residual and bias values and hence was retained in the

Step	1	2	3	4	5	6	7	8	9	10
Constant	2964.7	2275.4	1372.1	606.9	1004.2	817.8	870.8	367.0	255.9	330.7
DieToBody	-2845	-3155	-2899	-2940	-2959	-2999	-3076	-2937	-2802	-2896
T- Statistic	-6.47	-7.91	-7.96	-9.07	-9.71	-10.9	-11.75	-11.19	-10.69	-11.54
P Value	0.000	0.000	0.000	0.000	0.000	0.000	0.000	0.000	0.000	0.000
MaskDefID		928	861	934	820	838	873	878	751	827
T- Statistic		3.63	3.75	4.55	4.14	4.69	5.15	5.37	4.42	5.23
P Value		0.001	0.001	0.000	0.000	0.000	0.000	0.000	0.000	0.000
Dwell Time			52	52	53	50	47	47	50	48
T- Statistic			3.43	3.91	4.20	4.36	4.40	4.52	4.94	4.79
P Value			0.001	0.000	0.000	0.000	0.000	0.000	0.000	0.000
BodySizeSqMM				57	60	67	67	46	-74	
T- Statistic				3.47	3.83	4.73	4.98	2.68	-1.17	
P Value				0.001	0.000	0.000	0.000	0.011	0.248	
PCBThicknessMM					-264	-379	-380	-412	-421	-415
T- Statistic					-2.54	-3.77	-4.01	-4.43	-4.70	-4.62
P Value					0.015	0.001	0.000	0.000	0.000	0.000
EMCFillID						332	359	334	387	363
T- Statistic						3.18	3.62	3.46	4.00	3.82
P Value						0.003	0.001	0.001	0.000	0.000
BoardFinishID							-225	-237	-210	-224
T- Statistic							-2.39	-2.60	-2.36	-2.53
P Value							0.022	0.013	0.024	0.016
BallDiaMM								1690	3719	2384
T- Statistic								1.96	2.80	3.47
P Value								0.058	0.008	0.001
BallCount									4.16	1.76
T- Statistic									1.97	3.18
P Value									0.057	0.003
S	390	346	309	275	258	233	220	212	205	206
R-Sq	48.73	60.75	69.34	76.31	79.61	83.82	85.93	87.25	88.04	88.49

Table 3.2: Stepwise regression of Flex-BGA predictor variables

model. Solder-mask definition was identified as the next potentially important variable and a regression equation with characteristic life as response variable and die to body ratio and solder mask definition as predictor variable was fit. Addition of solder mask definition yielded an increase in the coefficient of determination and reduction in residual mean square and hence was retained. DeltaT and body size were identified as next potentially important variables. With addition of dwell time there was substantial increase in coefficient of determination which was not the same with body size. Body size was thus dropped from the model.

Predictor variable were added in succession, regression equation was fit, criteria's of model selection were studied and decision for retention and drop of the variable was made. The best subset of variables from stepwise regression method includes die to body ratio, solder mask definition, DeltaT, PCB thickness, encapsulant mold compound filler content, board finish, solder ball diameter, substrate type and ball count. The results of stepwise regression method are given by Table 3.2

3.5 MULTIPLE LINEAR REGRESSION MODEL

Multiple linear regression attempts to model the relation between two or more predictor variables and a response variable. The relationship is expressed as an equation that predicts a response variable from a function of predictor variables and parameters. The parameters are adjusted so that a measure of fit is optimized. The prediction equations is given by Equation 3.1

$$t_{63.2\%} = a_0 + \sum_{k=1}^n b_k f_k \quad \text{Eq 3.1}$$

The response variable $t_{63.2\%}$ on the left hand side of the equation represents the characteristic life of three-parameter Weibull distribution for the flex-BGA package when subjected to accelerated thermo-mechanical stresses. The parameters on the right hand side of the equation are the predictor variables of the various parameters that influence the reliability of the package. The coefficient of each of the parameter is the indicator of the relative influence of that parameter on the characteristic life of the package.

Multiple linear regression estimates the coefficients of regression using the method of least squares. Because, the method of least squares assumes the errors to be normally, independently distributed with zero mean and constant variance, the developed models have to be validated for normality, heteroskedasticity and multi-collinearity. Residual analysis has been performed for validating normality and constant variance assumptions and Pearson's correlation analysis and variance inflation factor have been used for checking multi-collinearity.

Multiple linear regression models have been developed using commercially available statistical software, MINITABTM. The predictor variables for model building include the best subset of variables obtained from stepwise methods. Characteristic life of the package has been used as the response variable. Continuous variables such as ball count and ball diameter have been input in their original form. Categorical variables such as board finish, encapsulant mold compound filler content and solder mask definition have been input in binary form. Categorical variables with two and three levels have been modeled with one and two dummy variables respectively. Each level toggles between 0 and 1. In the case of a categorical variable with three levels, two dummy variables taking

the values 0-0, 1-0 and 0-1 for the levels 1, 2 and 3 respectively have been used. When both the dummy variables are input zero, both of the are knocked out from the prediction equation, modifying the equation for level one of the categorical variable. When 1 and 0 are input for first and second dummy variable the first dummy variable alone gets added to the equation, modifying the equation for level two of the categorical variable. When 0 and 1 are input for first and second dummy variable the first variable is knocked off and the second variable is added to the equation modifying the prediction equation for level 3 of the categorical variable.

The output of multiple linear regression is given by Table 3.3. The output of the multiple linear regression has been used in building a mathematical prediction equation that correlates the sensitivities of predictor variables with characteristic life of the package. The prediction equation has been used as a tool for prediction and comparison of characteristic life of Flex-BGA packages with different design and material attributes when subjected to different extreme environments. This prediction equation provides higher accuracy than any first order closed form model, and also allows the user to analyze the interaction effects of the various parameters on the package reliability, which are often ignored in the various first order closed form modeling methodologies and addressed only using finite element models or experimental accelerated test data. The prediction equation is given by Equation 3.2

$$\begin{aligned}
 N63\% = & 2968.9 - 2946.5 \times (\text{DieToBodyRatio}) + 1.8433 \times (\text{Ballcount}) \\
 & + 2216.4 \times (\text{BallDiaMM}) - 372.37 \times (\text{PCBThicknessMM}) + 341.30 \times \\
 & (\text{EMCFillID}) + 832.8 \times (\text{MaskDefID}) + 9.53 \times (\text{BoardFinishID1}) - \\
 & 656.7 \times (\text{BoardFinishID2}) - 11.318 \times (\text{DeltaT})
 \end{aligned}
 \tag{Eq 3.2}$$

Predictor	Coeff (bk)	SE Coeff	T	P-Value
Constant	2968.9	525	5.66	0.000
DieToBodyRatio	-2946.5	244	-12.06	0.000
BallCount	1.8433	0.5385	3.42	0.002
BallDiaMM	2216.4	673.4	3.29	0.002
PCBThicknessMM	-372.37	90.15	-4.72	0.000
EMCFillerID	341.30	95.34	3.81	0.001
MaskDefID	832.8	159.0	5.15	0.000
BoardFinishID1	9.53	152	2.49	0.952
BoardFinishID2	-656.7	208	-3.15	0.003
DeltaT	-11.318	2.370	4.93	0.000

Table 3.3 Multiple linear regression model of Flex-BGA package

Source	D.F	SS	MS	F	P
Regression	9	11642392	1293599	32.32	0.00
Residual Error	36	1440911	40025		
Total	45	13083303			

Table 3.4: Analysis of variance of Flex-BGA multiple linear regression model

3.6 HYPOTHESIS TESTING

Hypothesis testing aids in testing the overall adequacy of the multiple linear regression model and determining the significance of individual regression coefficients. The hypothesis tests assume normality, independence and constant variance of errors.

The test of overall adequacy of the model tests the linear dependence of characteristic life and any of the geometric, material properties and environmental conditions. The null hypothesis assumes changes in geometric, material properties and environmental condition do not affect the characteristic life of the Flex BGA package. Rejection of the null hypothesis implies there is at least one geometric, material property or environmental condition is contributing significant in predicting the characteristic life of the Flex-BGA package.

Analysis of variance (ANOVA), which provides information about levels of variability within a regression model, has been used for testing the overall adequacy of the model. The values of the ANOVA table, F statistic and P value are given by Table 3.4. The p-value in the ANOVA table indicates the statistical significance of the regression equation. A P value of less than 0.05 is a rejection of the null hypothesis signifying the presence of linear relationship between characteristic life and at least one of the geometric, material properties and environmental conditions. Thus the prediction equation was verified to be adequate.

Coefficient of determination, R^2 , which determine the percentage of variation of the response variable explained by the predictor variables, has been used for assessing the overall adequacy of the prediction model. A high R^2 value suggests the ability of the prediction equation in explaining most of the variations in characteristic life. The R^2

value of 0.90 suggests the developed prediction is adequate for prediction purposes. Since, R^2 increases for every additional predictor variable, adjusted R^2 , which is a modification of R^2 , that accounts of addition of new predictor variable has also been studied. An adjusted R^2 value of 87% of the prediction equation reconfirms the overall adequacy of the model.

Presence of unwanted predictor variable, which do not contribute significantly for prediction purpose, increases the residual mean square thereby, decreasing the prediction ability of the model. T tests on individual regression coefficients have been performed for determining the importance of each predictor variable for retaining in the model. The p-value of a parameter in Table 3.3 indicates the statistical significance of that parameter and the parameter with p-value less than 0.05 is considered to be statistically significant and expected to have a significant effect on the reliability of the package, with confidence level of more than 95.0%. All the predictor variables in Table 3.3 are statistically significant with p-values in the neighborhood of 0 to 5%.

3.7 MODEL ADEQUACY CHECKING

Model appropriateness for application has been checked using any one or combination of the several of the features of the model, such as linearity, normality, variance which may be violated. In this section, methods for determination of the appropriateness of the model have been discussed. Model residuals have been studied to measure the variability in the response variable not explained by the regression model. Residuals realized or observed values of the model errors any departures from the model errors show up in the residuals.

Residual plots studied include, the normal probability plot, histogram plot of residuals, plot of residuals against fitted values, plot of residual against regressor and plot of residual in time sequence. Departures from normality, and the resultant effect on t-statistic or f-statistic and confidence and prediction intervals have been studied using normal probability plots. A straight line variation for the multiple linear regression model (Figure 3.) indicates a cumulative normal distribution. The histogram plot of residuals has also been used to study non-normality. Plots of residuals against fitted values and plots of residuals against the regressors have been used to check for constant-variance. Existence of residuals within the normal band indicates constant variance for the multiple linear regression model. Violation of assumptions may have been indicated by inward and outward funneling. The plot of residual in time sequence is used to study correlation between model errors at different time periods. Patterns in the plot of residuals in time sequence have been studied to determine if the errors are auto-correlated. Random distribution of errors shows the absence of any auto-correlation problems.

Multi-collinearity is the near linear dependence of predictor variables. Multiple linear regression modeling assumes the predictor variables to be independent of each other. The presence of multi-collinearity can cause inflated variance and regression coefficients with wrong signs. Pearsons correlation matrix and variance inflation factor values have been used for studying multi-collinearity. The absence of high values in the Pearsons correlation matrix, given by Table 3.5, shows the absence of multi-collinearity problems.

Residual Model Diagnostics

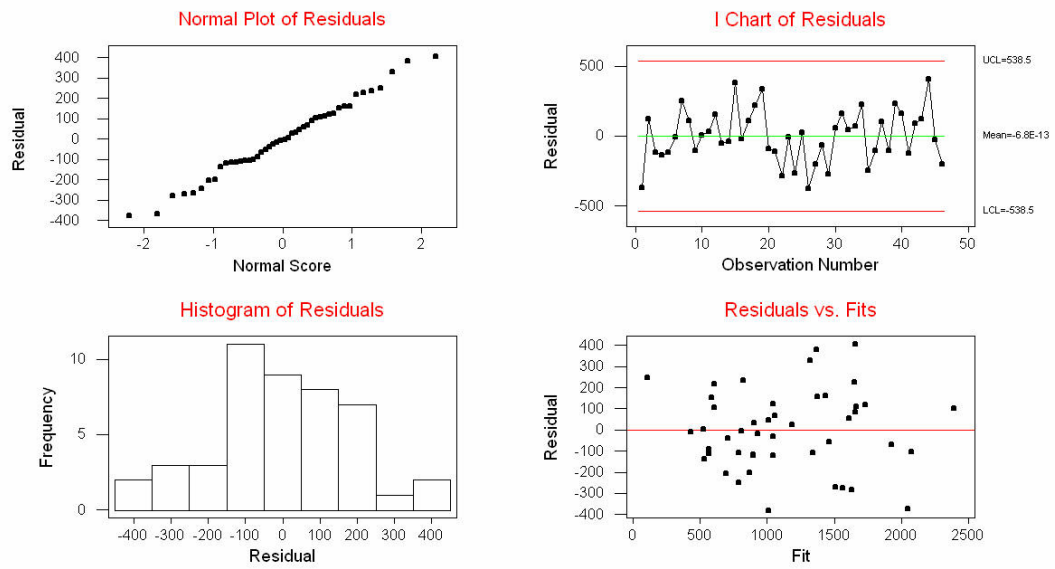


Figure 3.3: Residual plot of Flex-BGA multiple linear regression model.

	DieToBodyRatio	BallCount	BallDiaMM	PCBThickness	EMCFillerID	MaskDefID	BoardFinishID1	BoardFinishID2	DeltaT
DieToBodyRatio	1.000	0.073	-0.224	-0.077	-0.009	0.213	-0.092	-0.115	0.181
BallCount	0.073	1.000	0.302	-0.043	-0.268	0.035	-0.097	-0.058	0.083
BallDiaMM	-0.224	0.302	1.000	0.243	0.079	-0.156	0.059	0.035	-0.050
PCBThicknessMM	-0.077	-0.043	0.243	1.000	0.356	-0.242	0.020	0.169	-0.031
EMCFillerID	-0.009	-0.268	0.079	0.356	1.000	-0.090	0.105	0.063	-0.090
MaskDefID	0.213	0.035	-0.156	-0.242	-0.090	1.000	0.052	-0.031	-0.045
BoardFinishID1	-0.092	-0.097	0.059	0.0206	0.105	0.052	1.000	0.031	0.052
BoardFinishID2	-0.115	0.083	0.035	0.169	0.063	-0.031	0.031	1.000	0.031
DeltaT	0.181	0.083	-0.050	-0.031	-0.090	-0.045	0.052	0.031	1.000

Table 3.5: Pearson's correlation matrix of Flex-BGA predictor variables.

3.8 MODEL CORRELATION WITH EXPERIMENTAL DATA

Characteristic life predicted by statistical model have been validated against the actual values from the experimental database to assess the prediction ability of the statistical model. A single factor design of experiment study has been used for comparing the mean characteristic life predicted by both the methods at a 95% confidence interval. The objective of the design study is to determine the influence of the factor on the output response of the system. Prediction method with experiment and statistical model as its two levels has been investigated as the factor and the predicted characteristic life is considered as the response of the system. In other words the design of experiment study analyzes the influence of prediction method on predicted characteristic life.

Analysis of variance has been used for testing the equality of mean predicted life. The data set for analysis contains characteristic life as the response variable input in a continuous form and prediction method as the influencing factor, input in binary form. A value of zero is input for experimental method and one is input for statistical method. For every value of the characteristic life a zero or a one is input for the prediction method depending on the method by which the characteristic life has been obtained. Generalized linear model function of MINITAB™ has been used for testing the equality of means. The generalized linear model was used primarily because the data set was unbalanced.

The null hypothesis of the test assumes equality of mean predicted characteristic life. The generalized linear model uses an F statistic for testing the equality of means. The results of analysis of variance are given by Table 3.6. High P values of ANOVA Table 3.6 shows a clear acceptance of the null hypothesis. Thus it can be concluded as

Source	DF	SeqSS	Adj SS	Adj MS	F Statistic	P value
Prediction Method	1	44550	44550	44550	0.09	1.000
Error	90	24725672	24725672	274730		
Total	91	24725672				

Table 3.6: Single factor analysis of variance

no significant difference in the characteristic life predicted by the statistical models and experimental methods.

3.9 MODEL VALIDATION

The effect of various design parameters on the thermal reliability of package have been presented in this section. Multiple linear regression based sensitivity factors, quantifying the effect of design, material, architecture and environmental parameters on thermal fatigue reliability, have been used to compute life. The sensitivity study can be used in building confidence during trade-off studies by arriving at consistent results in terms of reliability impact of changes in material, configuration and geometry using different modeling approaches. The predictions from the statistical model have also been compared with the experimental data

3.9.1 DIE TO BODY RATIO

The Thermo-mechanical reliability of flex-BGA packages reduces with increase in diagonal length. Multiple linear regression models have been used for evaluating the sensitivity of solder joint reliability to diagonal length. The cycles for 63.2% failure from the experimental data and multiple linear regression models have been plotted against the die to body ratio of various devices. The predicted values from the prediction model follow the experimental values quite accurately and show the same trend (Figure 3.).

Flex BGA packages with die to body ratio of 0.34, 0.53 and 0.79 have been used for the comparison of multiple linear regression model predictions with the actual test failure data. All the three packages had different ball count, ball diameter and PCB thickness. Thus, the model is being tested for its ability to predict both single and coupled

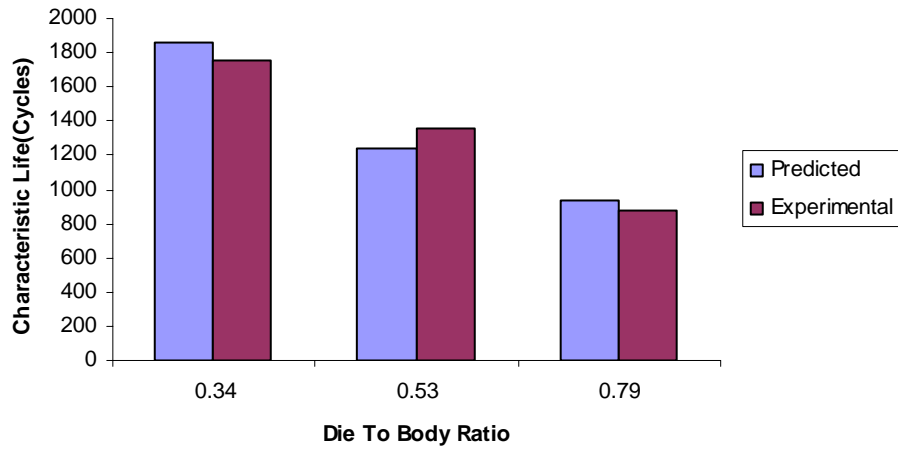


Figure 3.4 Effect of die to body ratio on thermal fatigue reliability of Flex-BGA packages.

Die To Body Ratio	Ball Count	Ball Diameter	Experiment	MLR	Sensitivity Factor For Die To Body Ratio
0.34	40	0.45	1855	1749	-2946.5
0.53	132	0.45	1238	1359	
0.79	132	0.45	940	872	

Table 3.7: Sensitivity of the package reliability to die to body ratio and comparison of model predictions with actual failure data

effects. A negative sensitivity has been computed for the effect of die to body ratio. A negative sensitivity factor indicates that the characteristic life of a Flex BGA package decreases when the die to body ratio increases.

3.9.2 BALL COUNT

The effect of ball count on thermo-mechanical reliability has been shown in Figure 3.. A trend of increase in the reliability with the increase in the ball count is visible, which is also supported by the failure mechanics theory. With the increase in the ball count the shear stress generated in the solder joints due to the thermal mismatch gets distributed, thus reducing the stress in the individual joint and increasing the life of the solder joint. Since this failure mechanics is only applicable in the case where the failure mode is solder joint cracking, so the trend might be different for other failure modes such as underfill delamination or copper trace cracking. Flex-BGAs packages with ball counts 96, 132 and 280 have been used to validate the effect of ball count on the thermo-mechanical reliability predicted by the model. The characteristic life predicted by the model lies in close proximity to the actual characteristic life from the experimental thermal cycling test. The sensitivity factor indicates an increase in characteristic life of FlexBGA package by 2 cycles for ever addition of a solder ball.

3.9.3 BALL DIAMETER

The solder joint diameter has a direct influence on thermo-mechanical reliability of Flex BGA packages. The thermo-mechanical reliability of the device increases with increase in the ball diameter. This trend is supported by failure mechanics theory as,

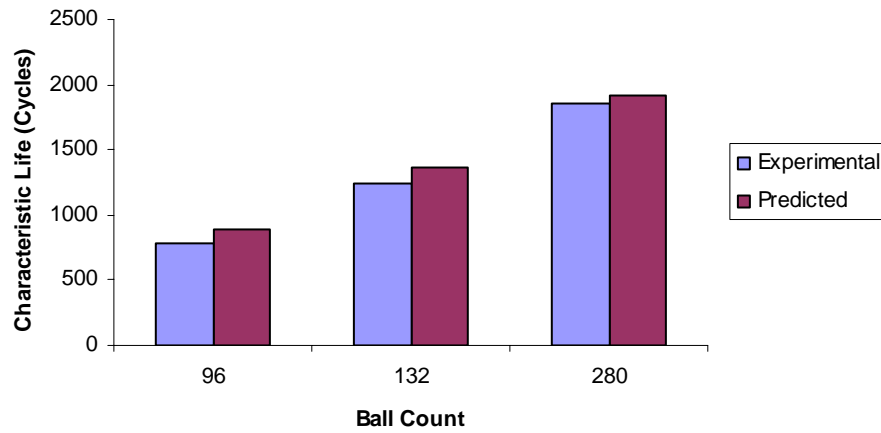


Figure 3.5: Effect of ball count on thermal fatigue reliability of CBGA packages.

Ball Count	Die To Body Ratio	Ball Diameter	PCB Thickness	Experiment	MLR	Sensitivity Factor For Ball Count
96	0.65	0.3	0.85	780	886	1.8433
132	0.53	0.45	0.85	1238	1359	
280	0.53	0.45	0.85	1862	1911.26	

Table 3.8: Sensitivity of the package reliability to ball count and comparison of model

predictions with actual failure data

solder joints with larger ball diameter have lower stress concentration and longer crack propagation path in the solder interconnects, thus adding to the thermo-mechanical reliability of the device. Since this failure mechanics is only applicable in the case where the failure mode is solder joint cracking, so the trend might be different for other failure modes such as underfill delamination or copper trace cracking. Flex BGA packages with solder joint diameter of 0.3 mm, 0.45 mm and 0.5 mm have been used for demonstrating this trend [Figure 3.]. A positive sensitivity factor indicates the characteristic life of flex BGA packages increases with increase in solder joint diameter. Model predictions show good correlation with experimental data.

3.9.4 PCB THICKNESS

The effect of PCB thickness on thermo-mechanical reliability of FlexBGA packages is given by Figure 3. . Thermo-mechanical reliability of FlexBGA packages decreases with increase in PCB thickness. This trend has been demonstrated for FlexBGA packages with PCB thickness of 0.85 mm and 1.6 mm. This trend is consistent from failure mechanics point of view as increased PCB thickness leads to higher assembly stiffness, which leads to increases stress levels in the interconnect. Sensitivity of thermo-mechanical reliability on PCB thickness has been determined using multiple linear regression method. The sensitivity factor indicates that for every unit increase of PCB thickness keeping all other parameters constant the characteristic life of the FlexBGA package decreases by 372 cycles. Model predictions show good correlation with experimental data.

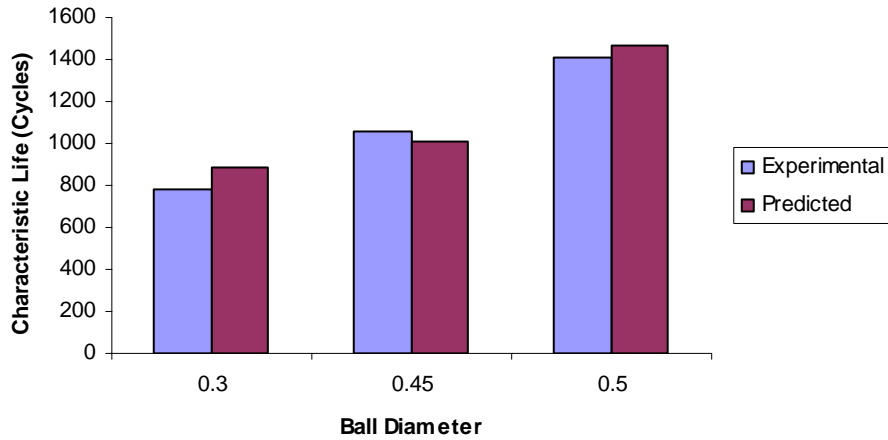


Figure 3.6: Effect of ball diameter on thermal fatigue reliability of Flex-BGA packages.

Ball Diameter	Die To Body Ratio	Ball Count	Delta T	Experiment	MLR	Sensitivity Factor For Ball Diameter
0.3	0.65	96	165	780	886	2216.4
0.45	0.72	280	165	1058	1009.72	
0.5	0.53	132	165	1408	1470	

Table 3.9 : Sensitivity of the package reliability to ball diameter and comparison of model predictions with actual failure data

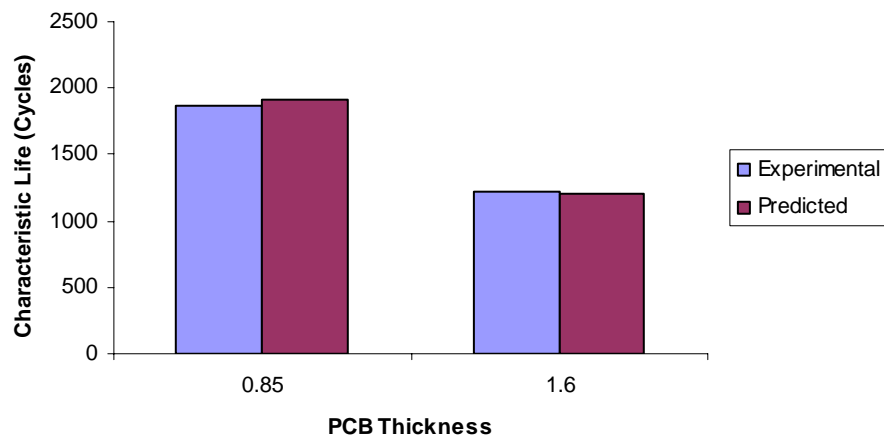


Figure 3.7 Effect of PCB thickness on thermal fatigue reliability of Flex-BGA packages

PCB Thickness	Die To Body Ratio	Ball Count	Ball Diameter	Experiment	MLR	Sensitivity Factor For PCB Thickness
0.85	0.53	280	0.45	1862	1911	-372.37
1.6	0.63	208	0.45	1215	1204	

Table 3.10: Sensitivity of the package reliability to PCB thickness and comparison of model predictions with actual failure data

3.9.5 ENCAPSULANT MOLD COMPOUND FILLER CONTENT

The silicon die of the FlexBGA is encapsulated in a mold compound to protect it from the external environment. Filler contents such as silica, with low CTE are added to reduce the CTE of the mold compound. The thermo-mechanical reliability of the device decreases with increase in the mold compound filler content. This is supported by failure mechanics as addition of filler content reduces the CTE of the material and increases the elastic modulus of the mold compound. Higher modulus of elasticity makes the package stiffer, therefore higher stresses are transmitted to the solder joint. Also, the lower CTE increases the local and global thermal mismatch. This trend has been demonstrated for two levels of mold compound filler content, high and low. A binary variable has been used for describing the two levels. A value of 1 has been assigned for low mold compound filler content and 0 for high mold compound filler content. This trend has been demonstrated in Figure 3. for die to body ratio of 0.63 and 0.72 respectively.

3.9.6 SOLDER MASK DEFINITION

The thermo-mechanical reliability of FlexBGA packages is higher for solder joints with NSMD pad configuration than SMD pad configuration. This trend has been demonstrated for Flex BGA package with a die to body ratio of 0.54, subjected to thermal cycling of -40°C to 125°C . This is supported by failure mechanics theory as SMD pad configuration can introduce stress concentrations near the solder mask overlap region that can result in solder joint cracking under extreme fatigue conditions. However, in a NSMD pad configuration the solder is allowed to wrap around the sides of the metal pads

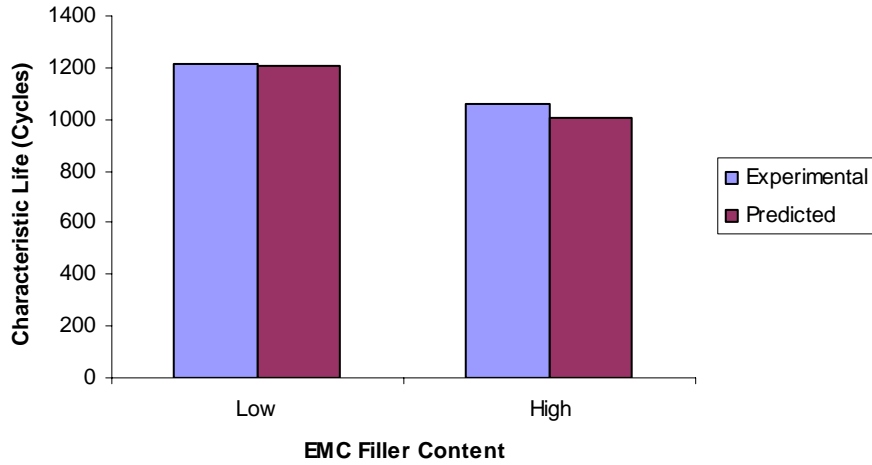


Figure 3.8: Effect of EMC filler content on thermal fatigue reliability of Flex-BGA packages.

EMC Filler ID	Die To Body Ratio	Ball Count	Ball Diameter	Experiment	MLR	Sensitivity Factor For EMC Filler ID
Low	0.63	208	0.45	1215	1204	341.30
High	0.72	280	0.45	1058	1009	

Table 3.11: Sensitivity of the package reliability to encapsulant mold compound filler content and comparison of model predictions with actual failure data

on the board that improves the reliability of solder joint. This trend is applicable only in the case where the failure mode is solder joint cracking. The package may show opposite trend in case the failure is due to the tearing out of the laminate under bending as shown by Mawer et. al.[1996]. In that case the solder mask on top of the SMD pad helps to anchor the pad to the laminate core which leads to better thermal fatigue reliability. A binary variable toggling between 0 and 1 has been used for describing the SMD and NSMD pad configuration respectively. Model predictions show good correlation with experimental data.

3.9.7 BOARD FINISH

Three different board finishes including OSP, HASL and Ni-Au have been investigated to analyze the effect of board finish on thermo-mechanical reliability of FlexBGA packages. OSP surface finishes are found to give the best reliability followed by HASL. The reduction in reliability is not very significant for transition from OSP to HASL. However, the thermo-mechanical reliability of FlexBGA packages reduces significantly for boards with Ni-Au finish. The primary reason for differences in thermal fatigue life for different board finishes is due to the different inter-metallic system formations due for different board finishes. The different inter-metallic formations induce different failure modes thus impacting the thermal reliability of the component. The board finish is described in binary system using two variables boardfinish1 and boardfinish2. A 0-0 configuration denotes OSP finish and 1-0 and 0-1 denotes HASL and OSP configurations respectively. The effect of board finish on thermo-mechanical reliability is demonstrated by Figure 3..



Figure 3.9: Effect of solder mask definition on thermal fatigue reliability of Flex-BGA packages

Pad Configuration	Ball Count	PCB Thickness	DeltaT	Experiment	MLR	Sensitivity Factor For Pad Configuration
SMD	160	1.6	165	805	807	832.8
NSMD	132	1.6	165	1597	1636	

Table 3.12: Sensitivity of the package reliability to pad configuration and comparison of model predictions with actual failure data

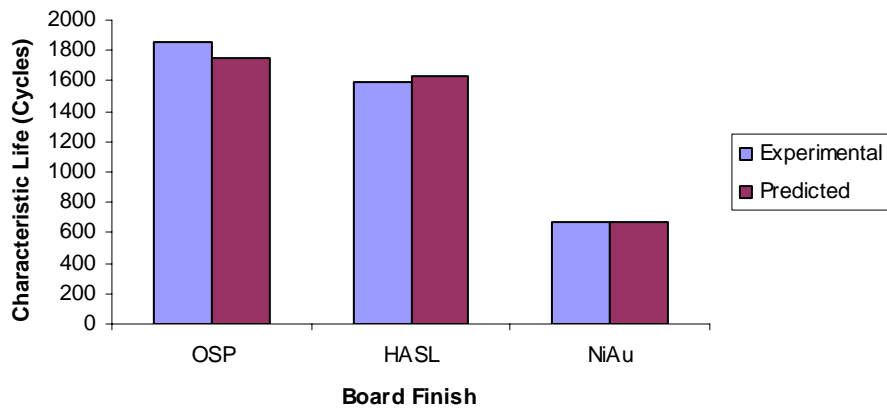


Figure 3.10: Effect of board finish on thermal fatigue reliability of Flex-BGA packages

Board Finish	Die To Body Ratio	Ball Count	DeltaT	Experiment	MLR	Sensitivity Factor For Board Finish
OSP	0.34	40	165	1855	1749	-656.7
HASL	0.54	132	165	1597	1636	
NiAu	0.54	132	165	673	673	

Table 3.13: Sensitivity of the package reliability to board finish and comparison of model predictions with actual failure data

3.9.8 DELTA T

The environment or testing condition the package is subjected to has a great influence on thermo-mechanical reliability Flex-BGA packages. The characteristic life of the package decreases with the increase in the temperature range of the ATC. This trend has been demonstrated for two different cycling conditions including 0 to 100°C and -40 to 125°C. Temperature cycle magnitude has a negative sensitivity factor, indicated by decrease in thermo-mechanical reliability with increase in temperature cycle magnitude. The predicted values for characteristic life calculated based multiple linear regression model match the experimental values from the ATC test very accurately.

3.10 DESIGN GUIDELINES

The statistical models presented in this section have been used for providing design guidelines for smart selection of a flip chip technologies. The sensitivities from the statistical models have been used to analyze the effect of various parameters on the solder joint reliability of the Flex-BGA packages

- Thermo-mechanical reliability of Flex-BGA packages decreases with increase in die to body ratio. This effect has been demonstrated for various board finishes and solder pad configuration.
- The solder joint reliability of Flex-BGA package increases with increase in ball count.
- Increase in ball diameter increases the solder joint reliability of Flex-BGA package.

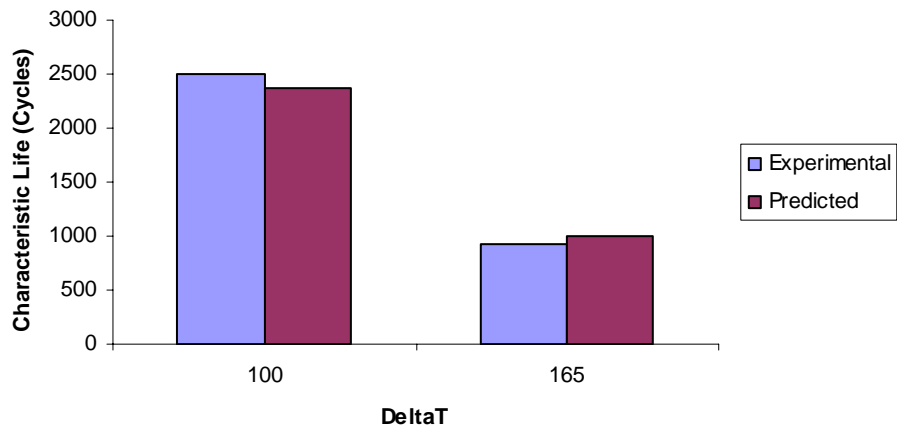


Figure 3.11: Effect of Delta T on thermal fatigue reliability of Flex-BGA packages

Delta T	Die To Body Ratio	Ball Count	Ball Diameter	Experiment	MLR	Sensitivity Factor For Delta T
100	0.53	132	0.45	2497	2374	-11.318
165	0.72	280	0.45	923	1009	

Table 3.14 : Sensitivity of the package reliability to Delta T and comparison of model predictions with actual failure data.

- PCB thickness has a negative sensitivity on solder joint reliability. Increasing the thickness of PCB decreases the thermo-mechanical reliability of Flex-BGA packages.
- Increasing the filler content of the encapsulant mold compound decreases the solder joint reliability of Flex-BGA packages.
- Solder joints with NSMD pad configuration have better reliability than solder joints with SMD pad configuration.
- HASL and OSP pad finishes are significantly more reliable than Ni-Au for FlexBGA packages, and OSP gives better thermo-mechanical reliability than HASL.
- Thermo-mechanical reliability of the solder joint in a Flex-BGA package is inversely proportional to the temperature differential through which the package under goes thermal cycling.

CHAPTER 4

STATISTICS BASED CLOSED FORM MODELS FOR FLIP CHIP PACKAGES

Increased utilization of flip chip packages in a wide variety of applications including portable consumer electronics like cellular phones [Sillanpaa et al. 2004], laptops [Pascariu et al. 2003], under-the-hood electronics [Jung et al. 1998], microwave applications [Bedinger 2000], system in package (SIP) [Van den Crommenacker, 2003], high-end workstations [Ray et al., 1997], and other high performance applications has driven the need for predictive methodologies for maintaining high levels of reliability and performing thermo-mechanical trade-offs. The reliability of flip chips has been found to depend on various factors including underfill material and process, moisture, flux, solder mask and solder mask opening design, chip passivation, chip and substrate thickness, gap between chip and substrate, and solder joint layout.[Borgensen, et al.] Solder joint fatigue due to difference in coefficients of thermal expansion of silicon chip and organic laminate substrate is a dominant failure mechanism [Lau, 1996].

In this section, a perturbation approach to prediction of reliability of flip-chip devices in harsh environments has been investigated. The proposed approach has been shown to achieve a much higher accuracy compared to traditional first-order models by perturbing known accelerated-test data-sets using models, using factors which quantify the sensitivity of reliability to various design, material, architecture and environmental parameters. The models are based on a combination of statistics, failure mechanics, and

finite element methods. The proposed approach has the potential of predicting both single and coupled factor effects on reliability, which are often ignored in closed form models.

Multiple linear regression models and principal components regression models have been used for relating characteristic life to various geometric aspects and material properties. Previous studies have developed multivariate regression models to study the influence of these parameters on thermal reliability [Lall et al 2005]. Previous analyses reported in the literature were confined to satisfying basic model assumptions however failed to cope with multi-collinearity problem. This section presents the results of an investigation on robust modeling methodologies for studying the effect of material and geometric parameters on the thermo-mechanical reliability of underfilled flip-chip devices on various substrates including organic laminate, and metal-backed flex.

4.1 FLIP CHIP PACKAGE ARCHITECTURE

Flip chip is a method of attaching the bumped chip on to a substrate. In flip chip packaging the die is inverted face down directly onto a package or a printed wired board, by means of solder bumps typically deposited on the integrated circuit or wafer and bonded to the package or PWB. A typical flip chip on board (FCOB) is shown in. Flip chip packages offer the advantages of high I/O, shortest electrical connection and hence improved electrical performance, low cost and high speed production. An underfill is used in flip chip packages for distributing the stresses in the solder thereby increasing the thermo-mechanical reliability of solder joints.

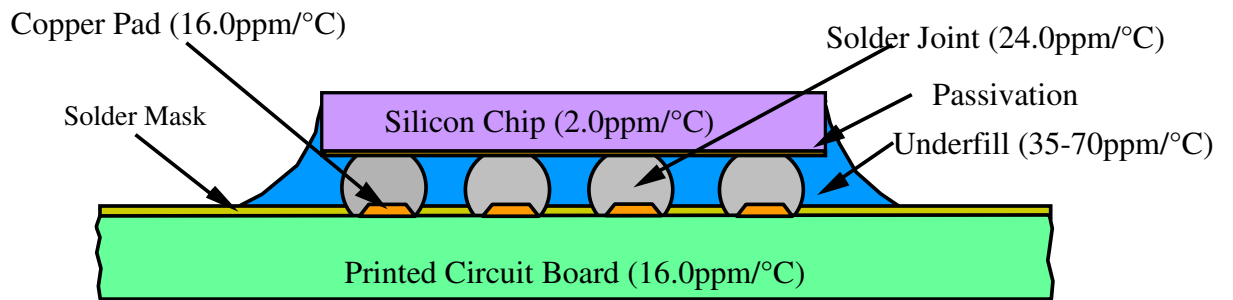


Figure 4.1: Cross Section of Flip Chip BGA Package

4.2 DATA SET

The dataset used for model building has been accumulated from an extensive flip-chip accelerated test reliability database based on the harsh environment testing by the researchers at the NSF Center for Advanced Vehicle Electronics (CAVE). This database has also been supplemented with the various datasets published in the literature. Each data point in the database is based on the characteristic life of a set of flip-chip devices of a given configuration tested under harsh thermal cycling or thermal shock conditions. The model parameters are based on failure mechanics of flip-chip assemblies subjected to thermo-mechanical stresses. The material properties and the geometric parameters investigated include die thickness, die size, ball count, ball pitch, bump metallurgy, underfill types (capillary-flow, reflow encapsulant), underfill glass transition temperature (T_g), solder alloy composition (SnAgCu, SnPbAg), solder joint height, bump size, and printed circuit board thickness. Range of data collected in each case is shown in Table 4.1. The database is fairly diverse in terms of materials and geometry parameters.

4.3 MODEL INPUT SELECTION

Predictor variables for model building have been selected by developing a super-set of variables that are known to influence the characteristic life of an area array package and then selecting the potentially important variables using stepwise regression and method of best subsets. Coefficient of multiple determination, adjusted R^2 , residual mean squares and induced bias has been used as criteria for variable selection. Coefficient of multiple determination (R^2), given by equation 1, measures the overall adequacy of the regression model and variables that create a significant increase in coefficient of multiple

Parameter	Data Range
Die Size	2.5 mm to 10 mm
Ball Count	24 to 184
Ball Pitch	0.2 mm to 0.457 mm
Ball Diameter	0.08 mm to 0.178 mm
Ball Height	0.06 mm to 0.13 mm
Solder Composition	Sn63Pb37, Sn96.5Ag3.5, 95.5Sn3.5Ag1.0Cu, Sn99.3Cu0.7, Sn95.8Ag3.5Cu0.7
PCB Thickness	0.5 mm to 1 mm
T _{High} , Accelerated Test	100°C, 125°C, 150°C
T _{Low} , Accelerated Test	-55°C, -40°C, 0°C

Table 4.1 Scope of accelerated test database

determination are retained in the model. As coefficient of multiple determination increases marginally for every newly added variable, adjusted R^2 , given by equation 2, has been used for studying the overall adequacy of the model and variables that create significant increase in adjusted R^2 are retained in the model.

$$R^2 = \frac{SS_{Residual}}{SS_{Total}} \quad \text{Eq 4.1}$$

$$R_{Adj}^2 = 1 - \left(\frac{n-1}{n-p} \right) (1 - R_p^2) \quad \text{Eq 4.2}$$

Residual mean square, given by Equation 3, is a measure of model errors. The residual mean square is calculated for all possible subset of variables and the subset that minimizes residual mean square is selected for model building. Mallows's C_p statistic, given by equation 4, determines the induced bias for a model with p variables and n data points. The C_p statistic is related to the mean square error of the fitted value and subset of variables with minimum C_p value also minimizes residual mean square. Potentially important variables are the ones that describe maximum information content in the data set with minimum variance and bias. Since there cannot be an optimum value for all the criteria, decision is based on satisfactory values. Stepwise regression and method of best subsets have been used for arriving at best set of predictor variables.

$$MS_{Res} = \frac{SS_{Res}}{n-p} \quad \text{Eq 4.3}$$

$$C_p = \frac{SS_{Res}}{\sigma^2} - n + 2p \quad \text{Eq 4.4}$$

Flip chip model variables have been selected by defining all the variables that are known to influence the characteristic life of a flip-chip device. Die length was identified as a potentially important and hence was selected as the first-variable. A regression equation was fit with characteristic life as response variable and die length as predictor variable and the criteria's for model selection were studied. Die length was found to explain large proportion of variation and the residual mean square and Cp values were quiet close model with all the variables. Diagonal length was selected as the next variable and a regression equation with die length and diagonal length as predictor variables was fit. Addition of diagonal length need not increase the coefficient of determination substantially as did die length and hence was dropped from the model. Underfill modulus was identified as the next potentially important variable and a regression equation with characteristic life as response variable and underfill modulus and die length as predictor variables was fit. Addition of underfill modulus yielded an increase in the coefficient of determination and reduction in residual mean square and hence was retained. Predictor variable were added in succession, regression equation was fit, criteria's of model selection were studied and decision for retention and drop of the variable was made. The best subset of flip chip predictor variables obtained include die length, underfill modulus, ball pitch, ball diameter, ball height, undercover area and Delta T. The results of stepwise regression are given by Table 4.2.

Step	1	2	3	4	5	6	7
Constant	2494.3	1783.9	2669.1	1088.2	910.2	3080.6	4438.8
DieLengthMM	-147	-115	-87	-87	-296	-543	-665
T-Statistic	-3.24	-2.59	-2.13	-2.30	-2.23	-3.59	-4.03
P-Value	0.002	0.013	0.039	0.026	0.031	0.001	0.000
UnderfillEGpa		56	136	158	144	128	110
T-Statistic		2.53	4.42	5.37	4.77	4.46	3.67
P-Value		0.015	0.000	0.000	0.000	0.000	0.001
BallPitchMM			-6555	-8877	-8351	-7227	-6925
T-Statistic			-3.41	-4.56	-4.31	-3.93	-3.83
P-Value			0.001	0.000	0.000	0.000	0.000
BallDiaMM				22923	29754	31895	32913
T-Statistic				2.94	3.41	3.93	4.13
P-Value				0.005	0.001	0.000	0.000
UndercoverAreaSqMM					19	43	53
T-Statistic					1.63	3.16	3.63
P-Value					0.110	0.003	0.001
BallHeightMM						-19650	-18387
T-Statistic						-2.83	-2.69
P-Value						0.007	0.010
DeltaT							-6.9
T-Statistic							-1.67
P-Value							0.102
R-Sq	18.28	28.27	43.00	52.37	55.16	62.33	64.74
R-Sq(Adj)	16.54	25.16	39.20	48.04	49.94	56.94	58.72
C-P	46.5	37.3	22.8	14.3	13.2	7.2	6.5

Table 4.2: Stepwise Regression of Flip-Chip Predictor Variables

4.4 MULTIPLE LINEAR REGRESSION

Multiple linear regression has been used for developing a linear relationship between characteristic life and best set of variables obtained from model input selection. The relationship is expressed as an equation that predicts a response variable from a function of predictor variables and parameters. The parameters are adjusted so that a measure of fit is optimized.

Multiple linear regression models were created using the potentially important variable's. Diagnosis of multicollinearity using Pearson's correlation coefficient, given by Table 4.3, revealed serious correlation between dielength and undercover area, suggesting suggesting that only one of the variables can be used in the multiple regression model. In the case of some models, removal of either predictor variables may result in significant drop in the coefficient of determination and in such cases, the original variables have been transformed using natural log, power and square root transformations and multiple linear regression has been carried out on the transformed variables. The prediction model based on natural log transformation, given by Table 4.4 displayed good model parameters with correct trends and hence has been chosen for prediction purposes.

The natural log transformed prediction equation is given by Equation 4.5

$$\begin{aligned} \ln \text{characteristic life} = & 66.924 + 34.088 \times \ln \text{Undarea} + 0.481 \times \ln \text{undE} - 0.292 \times \ln \text{UndCTE} \\ & - 0.665 \times \ln \text{solderE} + 1.805 \times \ln \text{SolderDia} - 4.813 \times \text{DeltaT} - 0.800 \times \ln \text{pitch} + 2.645 \times \ln \text{Ballht} \\ & - 68.216 \times \ln \text{diaglen} \end{aligned}$$

Eq 4.5

4.5 HYPOTHESIS TESTING

The overall adequacy of the regression model and significance of individual regression coefficients have been tested using hypothesis testing methods. ANOVA table given by Table 4.5 has been used for testing the overall adequacy of the model. The p-value in the ANOVA table indicates the statistical significance of the regression equation. A P value of less than 0.05 is a rejection of the null hypothesis signifying the presence of linear relationship between characteristic life and at least one of the geometric, material properties and environmental conditions.

Coefficient of determination, R^2 , which determine the percentage of variation of the response variable explained by the predictor variables, has also been used for assessing the overall adequacy of the prediction model. An R^2 value of 0.96 suggests the predictor variables describe almost 96% of variation in characteristic life proving the overall adequacy of the model. Since, R^2 increases for every additional predictor variable, adjusted R^2 , which is a modification of R^2 , that accounts of addition of new predictor variable has also been studied. An adjusted R^2 value of 95% of the prediction equation reconfirms the overall adequacy of the model.

T tests on individual regression coefficients have been performed for determining the importance of each predictor variable for retaining in the model. The p-value of a parameter in Table 4.4 indicates the statistical significance of that parameter and the parameter with p-value less than 0.05 is considered to be statistically significant and expected to have a significant effect on the reliability of the package, with confidence level of more than 95.0%. All the predictor variables in Table 4.4 are statistically significant with p-values in the neighborhood of 0 to 5%.

	DiLengthMM	UndAreaSqMM	BallPitchMM	BallDiaMM	BallheightMM	UnderfillEGpa	DeltaTDegC
DiLengthMM	1	0.94287	-0.06288	0.18536	0.20931	-0.27463	-0.12668
UndAreaSqMM	0.94287	1	-0.08799	-0.06426	0.40774	-0.21080	0.03898
BallPitchMM	-0.06288	-0.08799	1	0.22462	0.01424	0.77619	-0.27825
BallDiaMM	0.18536	-0.06426	0.22462	1	-0.36201	0.11882	-0.44602
BallheightMM	0.20931	0.40774	0.01424	-0.36201	1	0.02007	0.36292
UnderfillEGpa	-0.27463	-0.21080	0.77619	0.11882	0.02007	1	-0.24482
DeltaTDegC	-0.12668	0.03898	-0.27825	-0.44602	0.36292	-0.24482	1

Table 4.3 Pearson's correlation matrix of flip chip predictor variables

Predictors (ln a ₀ , f _k)	Coeff (b _k)	SE Coeff	T	P-Value
Constant (ln a ₀)	66.924	19.565	3.421	0.002
lnUndCovSqmm	34.088	10.841	3.144	0.004
lnUndEGpa	0.481	0.219	2.195	0.035
lnUndCTEppm	-0.292	0.102	-2.862	0.007
lnSolderEGpa	-0.665	0.283	-2.352	0.025
lnSolderDiaMM	1.805	0.867	2.082	0.045
lnDeltaTdegC	-4.813	2.342	-2.055	0.048
lnPitchMM	-0.800	0.366	-2.184	0.036
lnBallHgtMM	2.645	0.794	3.331	0.002
lnDiagLenMM	-68.216	21.645	-3.152	0.003

Table 4.4: Multiple linear regression model of Flip-Chip package using natural log transformed flip chip predictor variables

Source	D.F	SS	MS	F	P
Regression	9.00	39.6757	4.4084	80.93	0.000000
Residual Error	29.00	1.5798	0.0545		
Total	38.00	41.2555			

Table 4.5 : Analysis of variance Of log transformed flip chip prediction model.

4.6 MODEL ADEQUACY CHECKING

Model appropriateness for application has been checked using any one or combination of the several of the features of the model, such as linearity, normality, variance which may be violated. Model residuals which measure deviation between data and fit have been studied and plotted to check model appropriateness and violation of assumptions. Residual plots studied include, the normal probability plot, histogram plot of residuals, plot of residuals against fitted values, plot of residual against regressor and plot of residual in time sequence (Figure 4.2). Departures from normality and the resultant effect on t-statistic or f-statistic and confidence and prediction intervals have been studied using normal probability plots. A straight line variation indicates a cumulative normal distribution. Plots of residuals against fitted values and plots of residuals against the regressors have been used to check for constant-variance. Existence of residuals within the normal band indicates constant variance.

Multi-collinearity has been checked using Pearson's correlation matrix and variance inflation factor values. Although the natural log transformation corrected the wrong sign of coefficients in the regression equation, multi-collinearity problem did not cease to exist. This is evident from the large values in the Pearson's correlation matrix. However, since the natural log transformed model has a high coefficient of determination and conforms to model assumptions it can very well be used for prediction purposes. Advanced multivariate techniques have been discussed for coping with multi-collinearity problem.

Residual Model Diagnostics

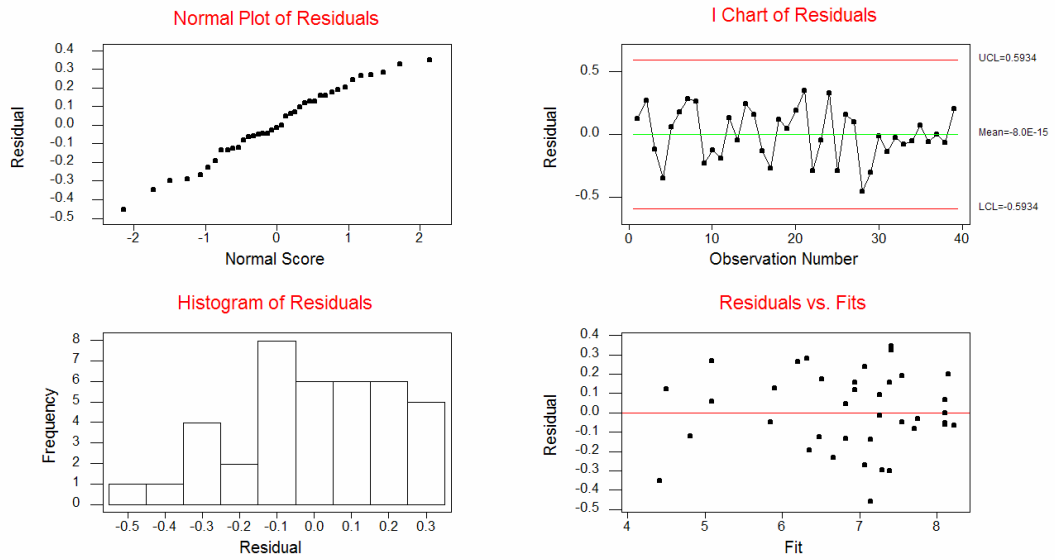


Figure 4.2: Residual plots of log transformed flip chip prediction model

	LnUndcover Area	Ln UnderfillE	Ln Underfill CTE	Ln SolderE	Ln Solder CTE	Ln DeltaT	Ln Pitch	Ln Ball Height	Ln Diagonal Length
LnUnder coverArea	1.00000	-0.14587	-0.18018	0.29163	-0.03948	-0.13070	-0.27052	0.00672	0.99892
Ln UnderfillE	-0.14587	1.00000	0.86323	0.13244	0.57261	0.81460	-0.41973	0.57967	-0.18489
Ln Underfill CTE	-0.18018	0.86323	1.00000	0.09936	0.65041	-0.87380	-0.22910	0.51306	-0.21992
Ln SolderE	0.29163	0.13244	0.09936	1.00000	-0.05906	0.06497	-0.23586	0.16766	0.28708
Ln Solder CTE	-0.03948	0.57261	0.65041	-0.05906	1.00000	0.40160	-0.43848	0.19506	-0.01841
Ln DeltaT	-0.13070	0.81460	0.87380	0.06497	-0.40160	1.00000	0.00583	0.60647	-0.17461
Ln Pitch	-0.27052	-0.41973	-0.22910	-0.23586	0.43848	0.00583	1.00000	-0.08005	-0.26502
Ln Ball Height	0.00672	0.57967	0.51306	0.16766	-0.19506	0.60647	-0.08005	1.00000	-0.01616
Ln Diagonal Length	0.99892	0.18489	-0.21992	0.28708	-0.01841	-0.17461	-0.26502	-0.01616	1.00000

Table 4.6: Pearson's correlation matrix of log transformed flip chip predictor variables

4.7 PRINCIPAL COMPONENTS REGRESSION

Multiple linear regression methods assume the predictor variables to be independent of each other. Linearly dependent variables result in multi-collinearity, instability and variability of the regression coefficients [Cook et al. 1977]. Principal components models have been used for dealing with multi-collinearity and producing stable and meaningful estimates for regression coefficients [Fritts et al 1971]. The principal components technique determines a linear transformation for transforming the set of X predictor variables into new set Z predictor variables known as the principal components. The set of new Z variables are uncorrelated with each other and together account for much of variation in X . The principal components correspond to the principal axes of the ellipsoid formed by scatter of simple points in the n dimensional space having X as a basis. The principal component transformation is thus a rotation from the original x coordinate system to the system defined by the principal axes of this ellipsoid [Massay 1965].

The principal component transformation ranks the new orthogonal principal components in the order of their importance. Scree plots, eigen values and proportion of total variance explained by each principal component are then used to eliminate the least important principal components. Multiple linear regression is then performed with the original response variable and reduced set of principal components and the parameters of regression are obtained using method of least squares. The principal components estimators are then transformed back to original predictor variables using the same linear transformation. Since the ordinary least square method has been used on principal

components, which are pairwise independent, the new set of predictor coefficients are more reliable.

The matrix of original correlated variables X, has been created from the flip chip dataset. A principal component analysis has been performed on this original predictor variable matrix X and its eigen values and corresponding eigen vectors have been extracted. The first four eigen vectors explained more than 85% of the original matrix and had eigen values greater than 1. A kink in the scree plot (Figure 4.3) supports the selection of first four eigen vectors. A transformation matrix, V has been created with first four eigen vectors.

$$X = \begin{bmatrix} 5.10 & 26.01 & 0.200 & 0.112 & 0.111 & 10.7 & 165 \\ 2.50 & 6.250 & 0.300 & 0.080 & 0.110 & 5.6 & 180 \\ 5.00 & 25.00 & 0.300 & 0.080 & 0.110 & 5.6 & 100 \\ 10.00 & 100.0 & 0.300 & 0.080 & 0.110 & 5.6 & 180 \\ - & - & - & - & - & - & - \\ - & - & - & - & - & - & - \\ 2.50 & 6.250 & 0.200 & 0.080 & 0.110 & 5.6 & 200 \end{bmatrix}$$

$$V = \begin{bmatrix} 0.460 & 0.484 & -0.190 & 0.022 \\ 0.512 & 0.434 & 0.021 & 0.075 \\ -0.387 & 0.475 & 0.299 & -0.089 \\ -0.233 & 0.302 & -0.345 & -0.802 \\ 0.300 & 0.116 & 0.621 & -0.190 \\ -0.423 & 0.332 & 0.415 & 0.228 \\ 0.230 & -0.371 & 0.444 & -0.504 \end{bmatrix}$$

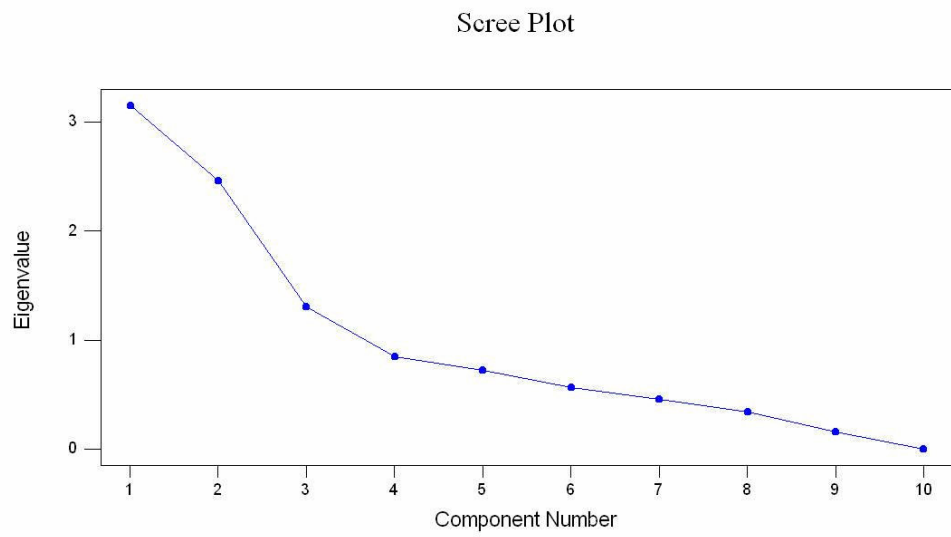


Figure 4.3: Scree plot for selecting the number of principal components

The original predictor variable matrix X has then been transformed into principal component scores Z using the transformation

$$Z = X \times V$$

Each score of principal component or Z is a linear combination of the original flip chip predictor variables and can be used as an independent variable for model building. The first principal component score, Z_1 is given by Equation 4.6

$$z_1 = 0.460 \times \text{Dielength} + 0.512 \times \text{Under cov erarea} - 0.387 \times \text{ballpitch} - 0.233 \times \text{BallDiameter} + 0.300 \times \text{Ballheight} - 0.423 \times \text{UNderfillE} + 0.230 \times \text{DeltaT} \quad \text{Eq 4.6}$$

A multiple linear regression analysis has been performed with characteristic life as response variable and the four principal components as predictor variables. The regression equation of the principal components is given by Table 4.7. An Alpha matrix with coefficients of principal components is then created.

$$\text{Alpha} = [797.6 \quad -1286.4 \quad 825.2 \quad 2055.5]$$

The coefficients of regression of the original variables are obtained by transforming the coefficients of regression of the principal components using the transformation,

$$\text{Beta} = V \times \text{Alpha}$$

$$\text{Beta} = [4389 \quad -367.3 \quad 21.6 \quad -855.9 \quad 2507.5 \quad 212 \quad 46.6 \quad -8.9]$$

where, beta is a matrix of regression coefficients of original variables. The prediction equation with original variables is given by Table 4.9. The prediction equation is given by Equation 4.7

$$63\% \text{Characteristic life} = -367.3 \times \text{Dielength} + 21.6 \times \text{Underarea} - 855.9 \times \text{Ballpitch} + 2507.5 \times \text{Balldiameter} + 212 \times \text{Ballheight} + 46.6 \times \text{UnderfillE} - 8.9 \times \text{DeltaT} \quad \text{Eq 4.7}$$

Predictor	Coeff (bk)	SECoeff	T value	P value
Constant	4389	1354	3.24	0.002
Z1	797.6	322.6	2.47	0.017
Z2	-1286.4	504.6	-2.55	0.014
Z3	825.2	292.5	2.82	0.007
Z4	2055.5	780.7	2.63	0.012

Table 4.7: Multiple linear regression model using principal components of flip chip predictor variables

Source	D.F	SS	MS	F	P
Regression	9.00	39.6757	4.4084	80.93	0.000000
Residual Error	29.00	1.5798	0.0545		
Total	38.00	41.2555			

Table 4.8: Analysis of variance of multiple linear regression model with principal components as variables

Predictors (a_0, f_k)	Coeff (b_k)	SE Coeff	T Statistic	P-Value
Constant	4389	1354	3.24	0.002
DeilengthMM	-367.3	48.313	7.60	0.000
UndercoverAreaSqMM	21.6	4.5798	4.72	0.000
BallPitchMM	-855.9	500.32	1.71	0.001
BallDiaMM	2507.5	946.80	2.64	0.000
Ball HeightMM	212	59.324	3.57	0.000
UnderfillEGpa	46.6	5.5540	8.30	0.000
DeltaDegC	-8.9	7.2452	1.22	0.0043

Table 4.9: Principal component regression model using original flip chip predictor variables

4.8 HYPOTHESIS TESTING

The overall adequacy of the model has been tested using ANOVA table given by Table 4.8. Small P value of the ANOVA table rejects the null hypothesis proving the overall adequacy of the model. Individual T tests on the coefficients of regression of principal components yielded very small P values indicating the statistical significance of all the four variables.

The individual T test values of principal components regression components are then used for conducting individual T test on the coefficients of regression of original variables. The test statistic proposed by Mansfield et al.[1997] and Gunst et al. [1980] for obtaining the significance of coefficients of regression of original variables is given by Equation 4.8

$$t = \frac{b_{j,pc}}{\left[MSE \times \left(\sum_{m=1}^l \lambda_m^{-1} v_{jm}^2 \right) \right]^{\frac{1}{2}}} \quad \text{Eq 4.8}$$

Where $b_{j,pc}$ is the coefficient of regression of the j^{th} principal component, MSE is the mean square error of the regression model with l principal components as its predictor variables, v_{jm} is the j^{th} element of the eigen vector v_m and λ_m is its corresponding eigen value. M takes the values from 1 to l , where l is the number of principal components in the model. The test statistic follows a students T distribution with $(n-k-1)$ degrees of freedom. The P values of individual T tests given by Table 4.9 are very small proving the statistical significance of individual regression coefficients of original predictor variables.

4.9 MODEL ADEQUACY CHECKING

The principal components regression model has been checked for underlying model assumptions such as normality, constant variance and independence. Residual plots have been used for studying the violations of model assumptions. The residual plots studied include normal probability plot, histogram plot of residuals, plot of residuals against fitted values, plot of residual against regressor and plot of residual in time sequence. Straight line variation of normal probability plot shows cumulative normal distribution. Presence of residuals in a horizontal band shows no violation of constant variance assumption. Since each principal component is a linear combination of original predictor variables, they become multivariate variables. Multivariate normality of each principal component has been checked using Chi-Square plots and Q-Q plot. Straight line variation of both the plots shows cumulative multivariate normal distribution.

Multicollinearity of the principal component variables has been studied using Pearson's correlation matrix and variance inflation values. Since the principal components are orthogonal to each other the multi-collinearity problem ceased to exist. Addition of fifth principal component however created serious multi-collinearity problems justifying the decision of retaining only first four variables.

4.10 MODEL CORRELATION WITH EXPERIMENTAL DATA

The predicted characteristic life of the statistical model has been compared with the actual characteristic life to assess the prediction ability of the statistical models. A single factor design of experiment study with prediction method as the factor and multiple linear regression, principal components regression and experimental results as

its three levels has been used for correlating the statistical model results with experimental results. Analysis of variance has been used for testing the equality of mean predicted characteristic life. The null hypothesis of the test is that the mean characteristic life of all the prediction methods is the same. The alternate hypothesis is there is at least one method with predicted characteristic life different from the others. High P values of ANOVA table [Table 4.10] shows a clear acceptance of the null hypothesis. Thus it can be concluded that there is no significant difference in the characteristic life predicted by the statistical models and experimental methods. T tests [Table 4.11] have been used for comparing the individual pairs of means. High P values of both the paired T tests shows that the predicted characteristic life of MLR and PCR methods is same as that of experimental values.

4.11 MODEL VALIDATION

The statistical modeling methodology presented in this section has been validated against the experimental accelerated test failure data. Statistical model predictions have been done by using multiple linear regression models and principal components regression models. Statistics and failure mechanics based sensitivity factors quantifying the effect of design, material, architecture, and environment parameters on thermal fatigue reliability have been used to compute life. The predictions from the statistical model have also been compared with the experimental data. The effect of the various design parameters on the thermal reliability of the package has been presented. The sensitivity study can be used in building confidence during trade-off studies by arriving at

Residual Model Diagnostics

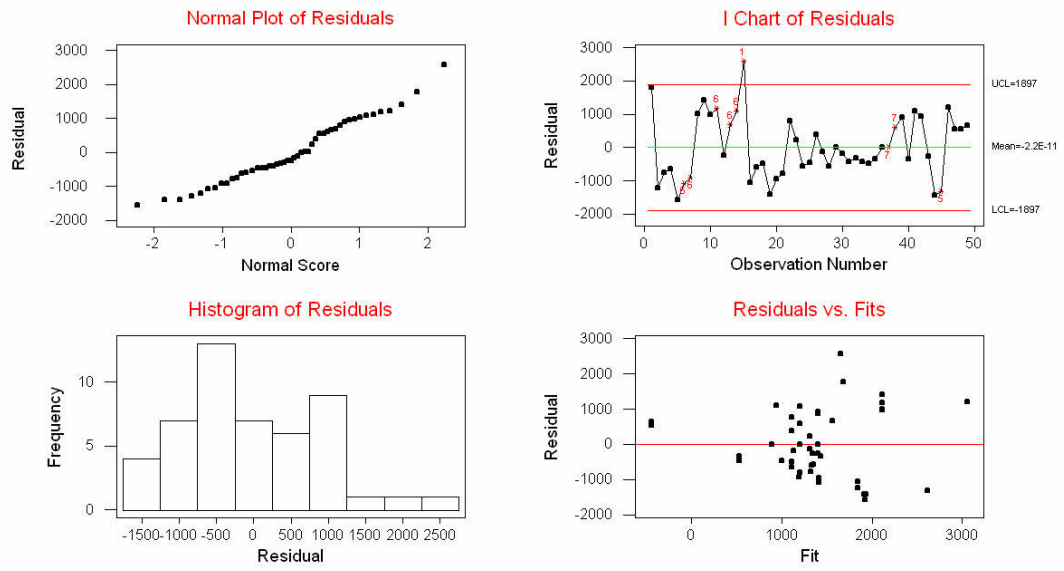


Figure 4.4 : Residual plot of principal components regression model

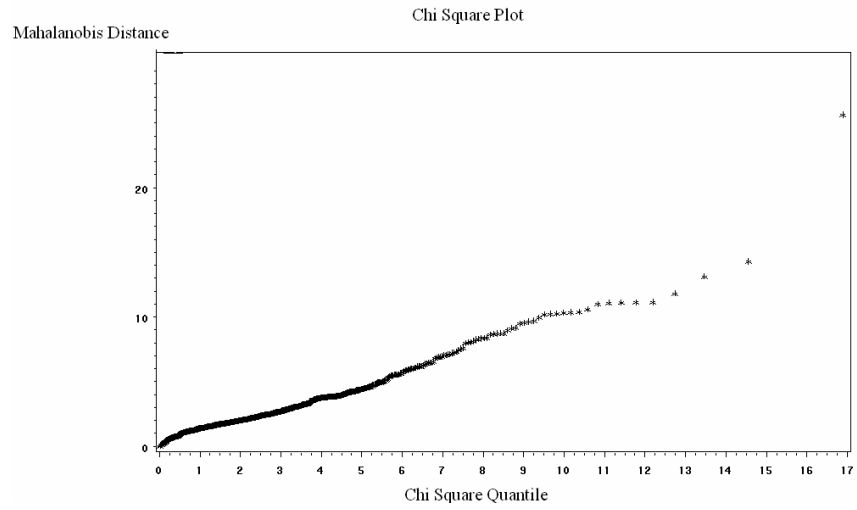


Figure 4.5 : Chi Square plot of principal components regression model

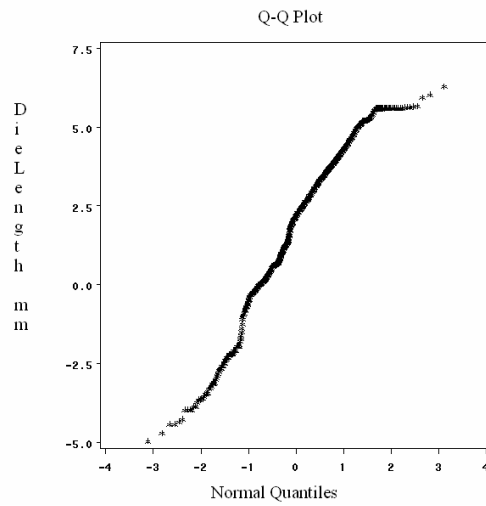


Figure 4.6: Q-Q plot of principal components regression model

Source	DF	SeqSS	Adj SS	Adj MS	F Statistic	P value
Prediction Method	2	121420582	121420582	60710291	1.10	0.336
Error	92	5055826106	5055826106	54954632		
Total	94	5177246688				

Table 4.10: Single Factor Analysis of Variance

Prediction Method	Diff Of Means	SE Of Difference	T Statistic	P value
MLR & Experimental	2721.4	1941	1.4019	0.4929
PCR & Experimental	354.9	1772	0.2003	1.0000

Table 4.11 : Pair-wise T Test

consistent results in terms of reliability impact of changes in material, configuration and geometry using different modeling approaches.

4.11.1 DIE LENGTH

The thermo-mechanical reliability of flip-chip devices generally decreases with increase in the die length. This effect has been demonstrated in flip-chip devices soldered to both FR4-substrate and BT-substrates. Multiple linear regression and principal components regression models have been used to evaluate sensitivity to die length. The cycles for 63.2% failure from the experimental data and multiple linear regression and principal components model's have been plotted against the die length of various devices. The predicted values from the prediction model follow the experimental values quite accurately and show the same trend (Figure 4.7). This trend is also consistent from the failure mechanics standpoint, as the solder joints with larger die length are subjected to much higher strains due to the increased distance from the neutral point, thus having lower reliability.

Encapsulated flip-chip packages with die length of 6.3mm and 10mm have been used for the comparison of the principal components regression and multiple linear regression model predictions with the actual test failure data. Both the packages had eutectic (Sn37Pb) solder joints of different ball diameter, pitch and pad definition and were subjected to different air-to-air thermal cycles (ATC) including thermal cycle of -40°C to 125°C , and -55°C to 125°C . Thus, the model is being tested for its ability to predict both single and coupled effects. A negative sensitivity has been computed for the effect of die length. A negative sensitivity factor indicates that the characteristic life of a

flip-chip decreases when the die length increases and all the other parameters remaining constant. The characteristic life of both the packages is plotted in Figure 4.7

4.11.2 SOLDER JOINT DIAMETER

The thermo-mechanical reliability of the flip-chip devices is also influenced by the solder joint or bump diameter. Flip-chip with bigger bump size usually gives higher reliability for the device. This trend is supported by the characteristic life plot for the flip-chip device for two different ball diameters. Flip-chip with larger bumps has lower stress concentration and longer crack propagation path in the solder interconnects, thus adding to the thermo-mechanical reliability of the device. The encapsulated flip-chip used for the validation had ball diameter of 0.08 mm and 0.112 mm respectively. A positive sensitivity factor indicates the characteristic life of flip chip increases with increase in bump size.

4.10.2 SOLDER JOINT HEIGHT

The effect of solder height on thermo-mechanical reliability of flip chip has been presented in Figure 4.9. The increase in the thermo-mechanical reliability of the device with increase in the ball height is demonstrated by both multiple linear and principal components regression models. This trend is supported by failure mechanics theory, as taller solder joints have longer crack propagation length. Encapsulated flip-chip packages with ball height of .08mm and .11mm, die size 10 and 5.1 respectively have been used for the comparison of the principal components regression and multiple linear regression model predictions with the actual test failure data. A positive sensitivity factor

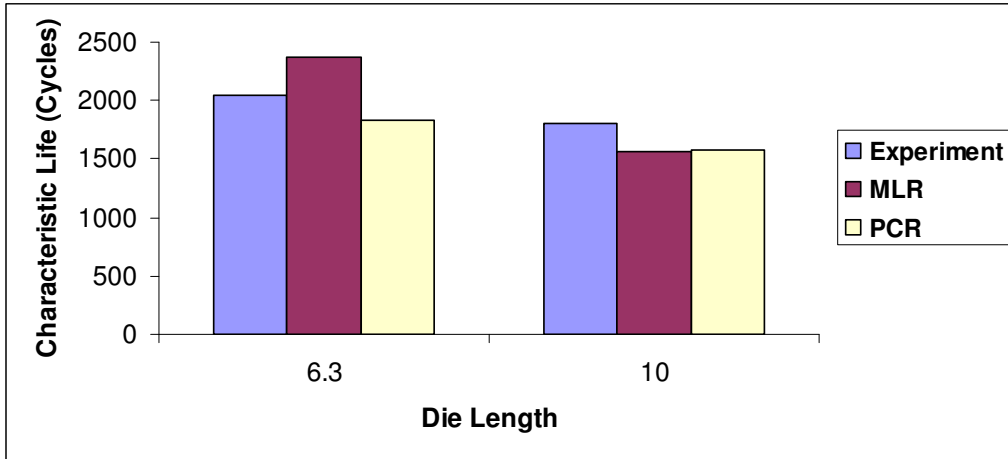


Figure 4.7: Effect of die length on thermal fatigue reliability of encapsulated flip-chip with Sn37Pb solder joints.

Die Length (mm)	Ball Pitch (mm)	Ball Dia (mm)	Experiment	MLR	PCR	Sensitivity Factor For Die length
6.3	0.457	0.178	2050	1829	2378	-367.3
14.14	0.2	0.08	1800	1575	1558	

Table 4.12: Sensitivity of the package reliability to the die length and comparison of model predictions with actual failure data.

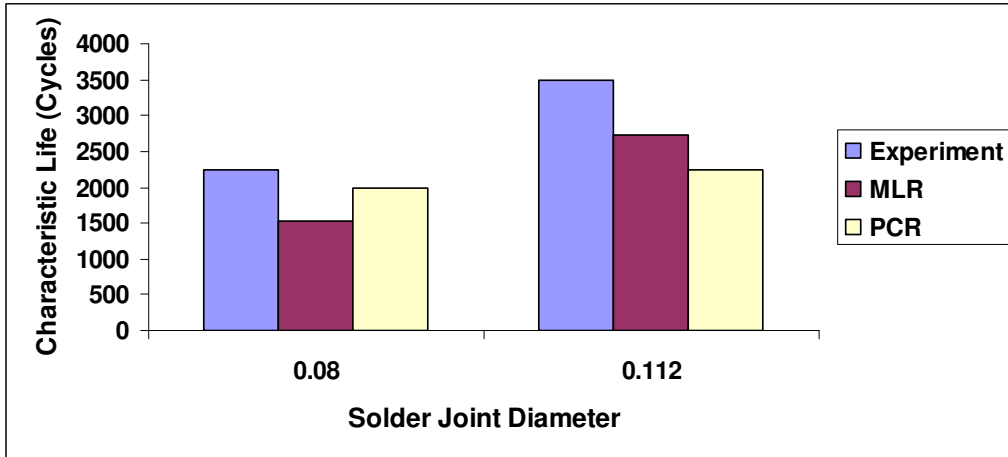


Figure 4.8 Effect of solder joint diameter on thermal fatigue reliability of flip-chip packages subjected to thermal cycling of -55°C to 125°C

Solder Joint Diameter (mm)	Diagonal Length (mm)	Ball Pitch (mm)	Ball Height (mm)	Ball Dia (mm)	Experiment	MLR	PCR	Sensitivity Factor For Solder Joint Diameter
0.08	8.50	0.2	0.094	0.08	2250	1985	1525	2507.5
0.112	7.21	0.2	0.112	0.111	3485	2240	2727	

Table 4.13: Sensitivity of the package reliability to the solder joint diameter and comparison of model predictions with actual failure data

indicates the characteristic life of flip chip increases with increase in bump height when all other parameters are remaining constant.

4.11.3 SOLDER MODULUS

The elastic modulus of the solder joint is found to have a great influence on the thermo-mechanical reliability of Flip chip packages. The thermo-mechanical reliability of the device decreases with increase in the solder joint modulus. This is supported by the failure mechanics theory that increase in elastic modulus leads to higher stress conditions resulting in higher hysteresis loops with more dissipated energy per cycle. Flip chip packages with leaded and lead free solder joints of elastic modulus 35 and 37.91 Gpa respectively [Figure 4.10] have been used for the comparison of the principal components regression and multiple linear regression model predictions with the actual test failure data. A negative sensitivity factor indicates the characteristic life of flip chip decreases with increase in solder modulus.

4.11.4 BALL PITCH

The effect of ball pitch on thermo-mechanical reliability has been shown in Figure 4.11. Encapsulated flip chip packages with ball pitch of 0.2 mm and 0.3 mm have been used for the comparison of the principal components regression and multiple linear regression model predictions with the actual test failure data. Ball pitch is inversely proportional to ball count for constant die size. A trend of increase in the reliability with the decrease in the ball pitch is predicted by the multiple linear regression and principal components regression models and supported by experimental data.

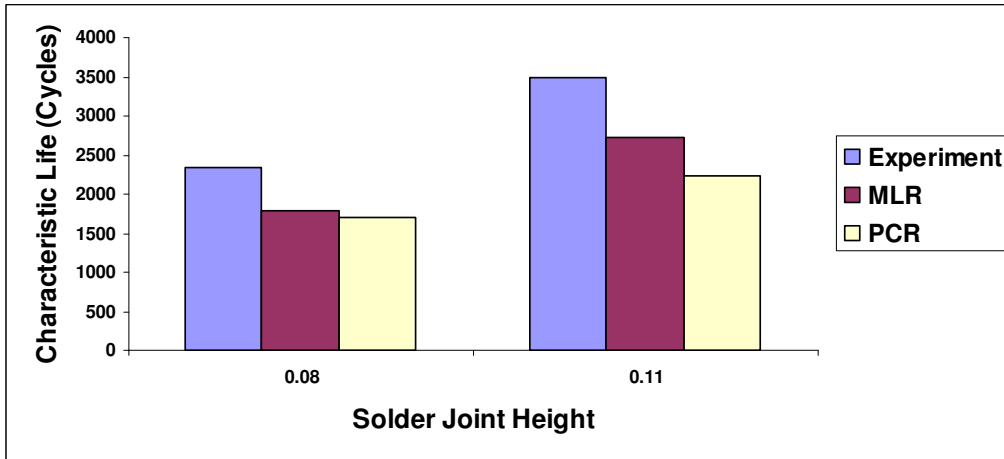


Figure 4.9: Effect of ball height on thermal fatigue reliability of flip-chip packages

Solder Joint Height (mm)	Ball Dia (mm)	Diagonal Length (mm)	Ball Pitch (mm)	Delta T	Experiment	MLR	PCR	Sensitivity Factor For Solder Joint Height
0.08	0.08	14.14	0.2	180	2350	1698	1796	212
0.11	0.112	7.21	0.2	165	3485	2240	2727	

Table 4.14: Sensitivity of the package reliability to the solder joint height and comparison of model predictions with actual failure data.

This is consistent with a negative coefficient for ball-pitch for the prediction models in Table 4.4. The trend is also supported by failure mechanics theory. The shear stress under thermo-mechanical loads is distributed over a larger number of solder interconnects, with the decrease in the ball pitch. The reduction in load reduces the stress in the individual joint and increases the life of the solder joint. The predicted effect of ball count is only applicable in the case where the failure mode is solder joint cracking. The trend might be different for other failure modes such as underfill-delamination or trace-cracking.

4.11.5 UNDERFILL MODULUS

Flip-chip devices with underfill show very high thermo-mechanical reliability as compared to the flip-chip devices without underfill. This trend has been shown to hold true for both eutectic (63Sn37Pb) and lead-free flip-chip devices mounted on both rigid-organic, e.g. BT and FR-4 substrates and metal-backed flex substrates. The main reason for this trend from thermo-mechanics standpoint is that the underfill material provides a mechanical support and shares the shear stresses generated in the solder joints due to the thermal mismatch between the chip and the board. Also, the presence of underfill redistributes the displacement fields within a joint thereby reducing the extreme local strains concentrations that occur in the joint. The elastic modulus of the underfill is found to have a great significance in determining the thermo-mechanical reliability of flip chip packages. Stiffer underfill's with higher elastic modulus are found to share greater shear loads reducing the inelastic strain sustained by the solder thus enhancing the solder life. Underfilled flip chip packages with elastic modulus 6.8 and 10 Gpa respectively have

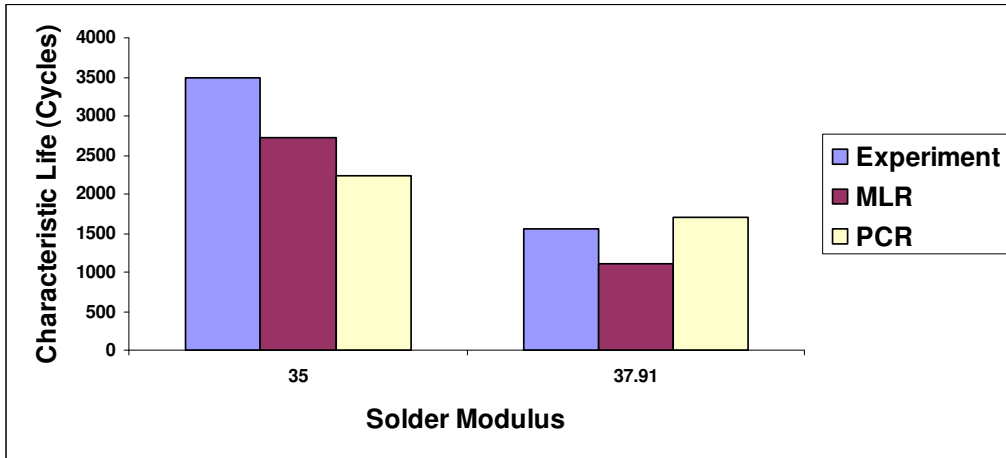


Figure 4.10: Effect of solder modulus on thermal fatigue reliability of flip-chip packages.

Solder Modulus (Gpa)	Ball Dia (mm)	Ball Height (mm)	Ball Pitch (mm)	Experiment	MLR	PCR	Sensitivity Factor For Solder Modulus
35	0.2	0.111	0.112	3485	2240	2727	-0.82
37.91	0.3	0.13	0.08	1550	1711	1098	

Table 4.15: Sensitivity of the package reliability to the solder modulus and comparison of model predictions with actual failure data.

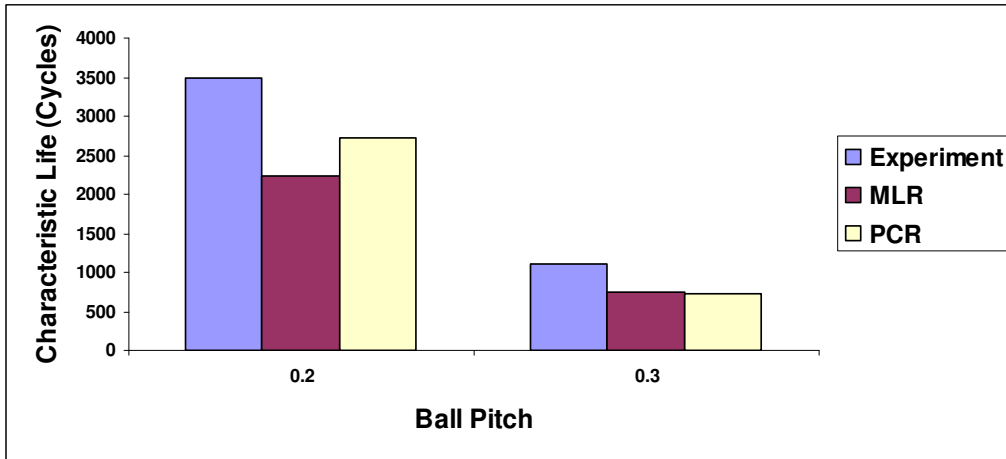


Figure 4.11: Effect of ball pitch on thermal fatigue reliability of flip-chip packages.

Ball Pitch (mm)	Experiment	MLR	PCR	Sensitivity Factor For Ball Pitch
35	3485	2240	2727	-855.9
37.91	1550	1711	1098	

Table 4.16: Sensitivity of the package reliability to ball pitch and comparison of model predictions with actual failure data.

been used for the comparison of the principal components regression and multiple linear regression model predictions with the actual test failure data [Figure 4.12]. A positive sensitivity factor indicates the characteristic life of flip chip increases with increase in underfill modulus when all other parameters are remaining constant. However this trend is reversed for the case where the failure mode is trace cracking, because the application of underfill leads to much higher stresses on the Cu traces and has a peeling effect.

4.11.6 DELTA T

The thermo-mechanical life of the flip-chip devices, similar to other package architectures, is a function of the environment or the testing condition to which it is subjected. Magnitude of the temperature range experienced during the accelerated test is an influential parameter. The characteristic life of the package decreases with the increase in the temperature range of the ATC [Figure 4.13]. Temperature cycle magnitude has a negative sensitivity factor, indicated by decrease in thermo-mechanical reliability with increase in temperature cycle magnitude. Data presented includes coupled effects of other parameter variations such as, die size, ball diameter, ball count and cycle time. The predicted values for characteristic life calculated based on the principal components and multiple linear regression model match the experimental values from the ATC test very accurately.

4.11.7 UNDERCOVER AREA

Flip chip devices with larger undercover area are found to exhibit better thermo-mechanical reliability. This is supported by failure mechanics theory as larger undercover areas provide scope of filling more underfill reducing the shear stress on the solder joints.

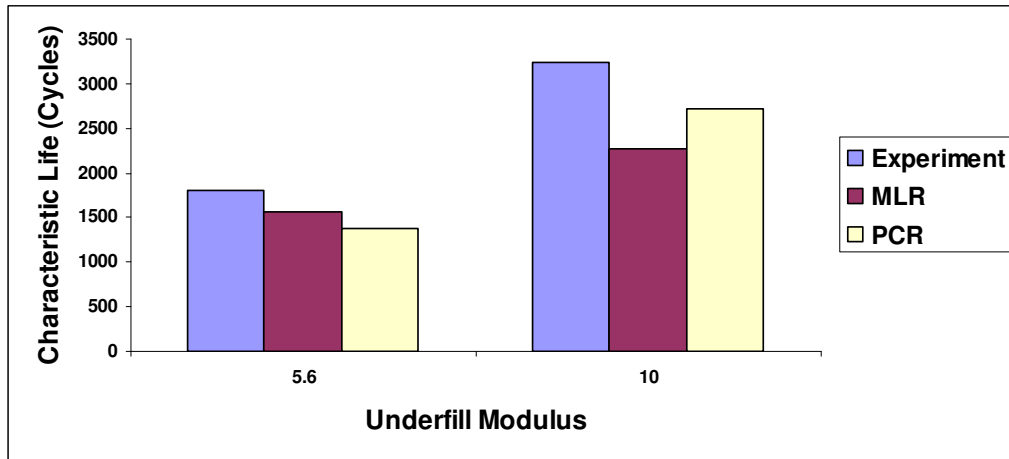


Figure 4.12: Effect of underfill modulus on thermal fatigue reliability of flip-chip packages.

Underfill Modulus (Gpa)	Diagonal Length (mm)	Ball Pitch (mm)	Ball Dia (mm)	Experiment	MLR	PCR	Sensitivity Factor For Underfill Modulus
5.6	14.14	0.2	0.08	1800	1369	1558	46.6
10	4.24	0.2	0.08	3243	2715	2273	

Table 4.17 : Sensitivity of the package reliability to underfill modulus and comparison of model predictions with actual failure data

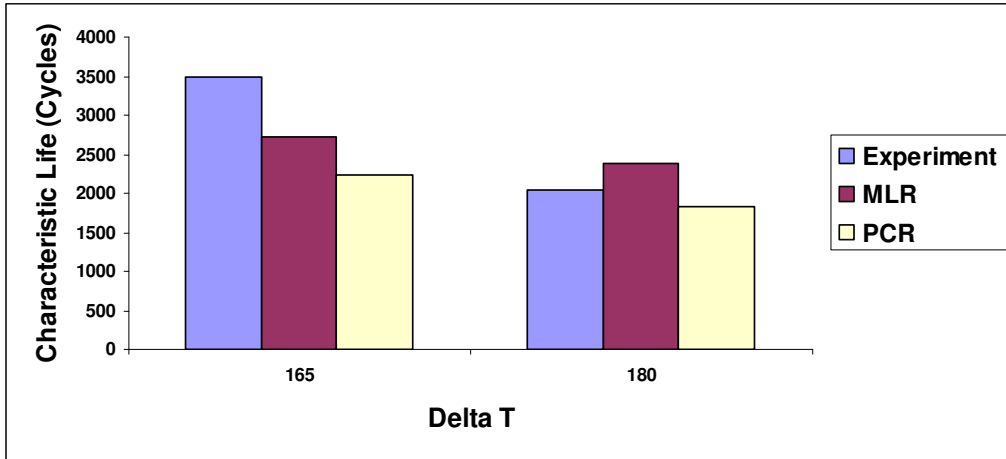


Figure 4.13: Effect of Delta T on thermal fatigue reliability of flip-chip packages.

Delta T	Ball Dia (mm)	Ball Pitch (mm)	Diagonal Length (mm)	Experiment	MLR	PCR	Sensitivity Factor For Delta T
165	0.112	0.2	7.21	3485	2240	2727	-8.9
180	0.178	0.45	8.90	2050	1829	2378	

Table 4.18 : Sensitivity of the package reliability to Delta T and comparison of model predictions with actual failure data

The effect has been shown in Figure 4.14 for encapsulated flip chip packages with under cover area of 35.84 sqmm and 39.69 sqmm for the comparison of the principal components regression and multiple linear regression model predictions with the actual test failure data. A positive sensitivity factor indicates the characteristic life of flip chip increases with increase in undercover area.

4.12 DESIGN GUIDELINES

The statistical models presented in this section have been used for providing design guidelines for smart selection of a flip chip technologies. The sensitivities from the statistical models have been used to analyze the effect of various parameters on the solder joint reliability of the flip chip packages.

- The solder joint reliability of Flip-Chip packages decreases with increase in the die length. This effect has been demonstrated for both leaded and lead free solder joints.
- Thermo-mechanical reliability of solder joints increases with increase in solder ball diameter of Flip chip packages.
- Increase in the solder ball height increases the solder joint reliability of Flip chip packages.
- Ball pitch is found to have a negative sensitivity on solder joint reliability. The reliability of solder joint decreases with increase in the ball pitch.
- Leaded solder joints with smaller elastic modulus are found to be more reliable than lead free solder joints with higher elastic modulus.

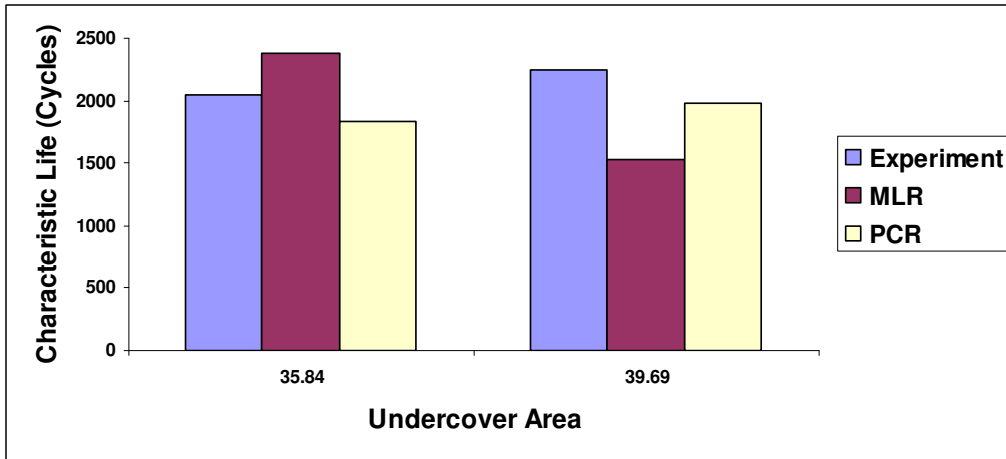


Figure 4.14 : Effect of under cover area on thermal fatigue reliability of flip-chip packages.

Undercover Area (Sqmm)	Ball Dia (mm)	Ball Pitch (mm)	Ball Height (mm)	Experiment	MLR	PCR	Sensitivity Factor For Undercover Area
35.84	0.178	0.457	0.112	2050	1829	2378	21.6
39.69	0.086	0.203	0.094	2250	1985	1525	

Table 4.19: Sensitivity of the package reliability to undercover area and comparison of model predictions with actual failure data

- Stiffer underfills with higher elastic modulus are found to improve the solder joints reliability of flip chip packages.
- Thermo-mechanical reliability of the solder joint in a Flip Chip package is inversely proportional to the temperature differential through which the package under goes thermal cycling.
- Increasing the area of undercover is found to increase the thermo-mechanical reliability of Flip chip packages.

CHAPTER 5

STATISTICS BASED CLOSED FORM MODELS FOR CBGA PACKAGES

Ceramic ball grid array (CBGA) packages are high density, high performance surface mount (SMT) packages. The broadening of application space of ceramic packages to be included in the high volume market of personal computer microprocessors [Master 1998], telecommunication products [Lau et al 2004], workstations and avionic products has necessitated the need for understanding the package design and assembly influence on reliability. In this section, decision support models for prediction of thermo-mechanical reliability of ceramic ball grid array and ceramic column grid array packages have been presented. Multiple linear regression modeling methodologies has been used for the model building.

The models presented in this section, aid in understanding effect of design and material parameters towards thermo-mechanical reliability and provide decision guidance for smart selection of component packaging technologies and perturbing product designs for minimal risk insertion of new packaging technologies. In addition, parameter interaction effects, which are often ignored in closed form modeling, have been incorporated in this work. Convergence of statistical models with experimental data has been demonstrated using a single factor design of experiment study.

5.1 CBGA PACKAGE ARCHITECTURE

Ceramic ball grid array (CBGA) packages [Figure 5.1] are an extension of controlled collapsed chip connection (C4) and use a co-fired alumina ceramic substrate [Lau 1995]. The multilayered ceramic substrates are chosen for their superior electrical performance such as option for multiple power and ground planes and the ability to choose the signal, power and ground locations within the column array locations. Also, the low difference coefficients of thermal expansions of ceramic (6.7 ppm/C) and silicon (2.7ppm/C) increases the component level reliability [Burnette 2000], making ceramic substrates a good choice for flip chip applications.

5.2 DATA SET

The dataset used for model building has been accumulated from an extensive CBGA accelerated test reliability database based on the harsh environment testing by the researchers at the NSF Center for Advanced Vehicle Electronics (CAVE). This database has also been supplemented with the various datasets published in the literature. Each data point in the database is based on the characteristic life of a set of CBGA devices of a given configuration tested under harsh thermal cycling or thermal shock conditions. The model parameters are based on failure mechanics of CBGA assemblies subjected to thermo-mechanical stresses. The material properties and the geometric parameters investigated include die size, substrate CTE, substrate thickness, ball count, ball pitch, solder alloy composition (SnAgCu, SnPbAg), solder joint height, underfill modulus, underfill CTE, bump size, and printed circuit board thickness. The range of data collected in each case is given by Table 5.1.

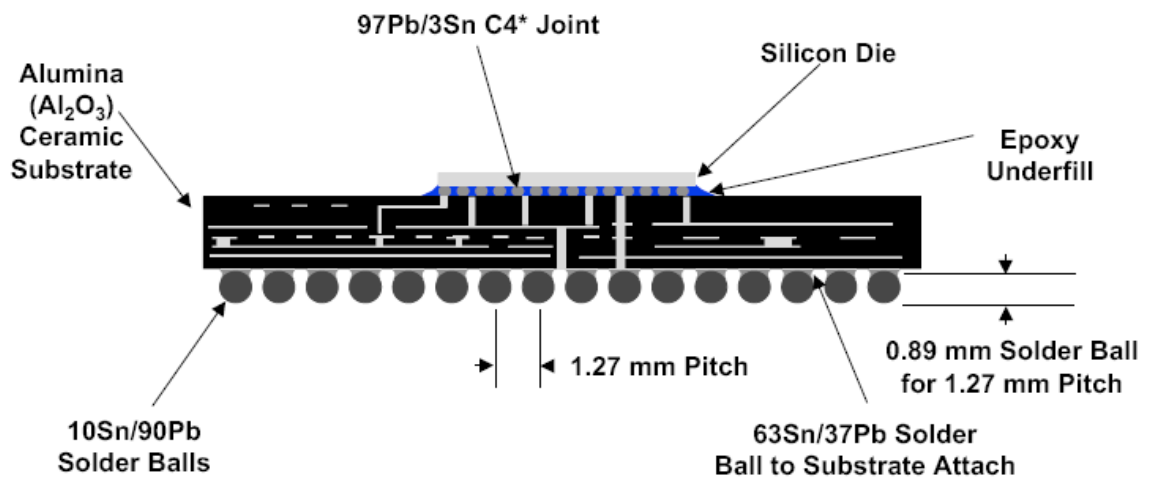


Figure 5.1: Motorola CBGA Cross-Section View

Parameter	CBGA
Die Size	4mm to 42mm
Number of I/O	64 to 1657
Ball Pitch	1mm to 1.27mm
Ball Diameter	0.508mm to 0.195mm
Solder Composition	Sn63Pb37, 95.5Sn3.5Ag1.0Cu
Ceramic CTE	6.8PPM/°C, 12.3PPM/°C
Underfill Modulus	2.6Gpa to 8.5Gpa, No Underfill
Underfill CTE	26PPM/°C to 75PPM/°C, No underfill
Ceramic Thickness	0.635MM to 2.9MM
PCB Thickness	1.27mm to 2.8mm
Thigh in ATC	90°C, 100°C, 125°C
Tlow in ATC	-55°C, -40°C, -15°C, 0°C

Table 5.1: Scope of accelerated test database

5.3 MODEL INPUT SELECTION

A superset of predictor variables including all the variables that are known to influence the characteristic life has been created. This set included all the geometric properties, material properties and thermal cycling conditions including die length, diagonal length, package area, under cover area, die thickness, ball count, bump diameter, bump height, solder modulus, solder CTE, underfill modulus, underfill CTE, PCB type, PCB thickness, pad diameter, pad type, substrate CTE, substrate thickness and thermal cycling conditions. Model input selection involves selecting a subset of variables that are just enough for model building. The criteria for variable selection are based on maximization of coefficient of determination and Adj R^2 and minimization of residual mean squares and induced bias. The potentially important variables selected are the ones that describe maximum information content in the data set with minimum variance and bias.

Substrate CTE was found to be the most influential factor and a regression equation with characteristic life as response and substrate CTE alone as predictor variable was built. Underfill modulus was identified as the next most influential observation and a regression equation with underfill modulus and substrate CTE as predictor variables and characteristic life as response variable was fit. Inclusion of underfill modulus increased the coefficient of determination (R^2) and reduced the residual errors and hence was retained in the model. Substrate thickness, solder CTE, DeltaT respectively were found to be the next most influential variables and were added in steps and the criteria's for model selection were studied. The variables satisfied the selection criteria and hence were retained. Ball pitch and die length were identified as important variables, however the

inclusion of these variables did not increase the coefficient of determination significantly and hence were dropped. Predictor variables from the super set were added in subsequent steps and their effect on variable selection criteria was studied for decision making on variable addition. The best subset of input variables include substrate CTE, underfill modulus, Solder CTE, substrate thickness, Delta T, PCB thickness, underfill CTE, ball diameter, ball count and diagonal length.

5.4 MULTIPLE LINEAR REGRESSION MODELS

Prediction equations for solder joint reliability prediction of CBGA packages have been built with characteristic life as response variable and best subset variables as predictor variables. All of the model variables have been modeled in continuous form. Categorical variables such as solder type, underfill type and ceramic type have been input as continuous variables by taking into consideration the elastic modulus and coefficient of thermal expansion of the corresponding material. In case of no underfill, a zero is input for both Young's modulus and CTE. Multiple linear regression models are built using MINITABTM statistical software. The model is given by Table 5.2. The model [Equation 5.1] indicates an increase in reliability with increase in underfill elastic modulus, ball count and ball diameter. The model also indicates a reduction in reliability with increase in temperature cycle magnitude, chip diagonal-length, substrate thickness, underfill coefficient of thermal expansion, solder elastic modulus and PCB thickness.

$$63\% \text{CharacteristicLife} = -1694.9 - 71.06 \times \text{DiagonalLength} - 582.87 \times \text{SubstrateThickness} + 1.6131 \times \text{Ballcount} + 478.96 \times \text{CeramicCTE} + 125.86 \times \text{SolderCTE} + 2594.6 \times \text{Balldia} + 547.33 \times \text{UnderfillE} - 19.697 \times \text{UnderfillCTE} - 245.4 \times \text{PWBThickness} - 16.458 \times \text{DeltaT}$$

Eq 5.1

5.5 HYPOTHESIS TESTING

The overall adequacy of the prediction model has been tested using ANOVA table given by Table 5.3 . Small P value in the table signifies the overall adequacy of the model rejecting the null hypothesis. This means that there is at least one predictor variable that is contributing significantly towards prediction of characteristic life of the package. Coefficient of determination, R^2 , which determine the percentage of variation of the response variable explained by the predictor variables, has also been used for assessing the overall adequacy of the prediction model. A coefficient of determination value of 92% for the model suggests that the predictor variables together account for 92% of variation in characteristic life. Since coefficient of determination is dependent on number of predictor variable the Adj R^2 parameter has also been studied. An Adj R^2 of 91% reconfirms the overall adequacy of the model. Thus the model is adequate for prediction purposes.

T tests on individual regression coefficients have been performed for determining the statistical significance of each predictor variable for retaining in the model. The p-value of a parameter in Table 5.2 indicates the statistical significance of that parameter and the parameter with p-value less than 0.05 is considered to be statistically significant and expected to have a significant effect on the reliability of the package, with confidence level of more than 95.0%. All the predictor variables in Table 5.2 are statistically significant with p-values in the neighborhood of 0 to 5%.

Predictor	Coefficient	SE Coeff	T Statistic	P Value
Constant	-1694.9	766.6	-2.21	0.030
Diag-Length	-71.06	18.00	-3.95	0.000
Substrate Thk	-582.87	64.32	-9.06	0.000
Ball Count	1.6131	0.4294	3.76	0.000
Ceramic CTE	478.96	27.20	17.61	0.000
Solder CTE	125.86	20.09	6.26	0.000
Ball Dia	2594.6	784.7	3.31	0.001
Underfill E	547.33	65.26	8.39	0.000
Underfill CTE	-19.697	7.780	-2.53	0.013
PWB Thk	-245.4	116.6	-2.11	0.038
Delta T	-16.458	2.243	-7.35	0.000

Table 5.2 : Multiple linear regression model of CBGA package.

Source	D.F	SS	MS	F	P
Regression	10	199337887	19933789	89.08	0.00
Residual Error	84	18797042	223774		
Total	94	218134929			

Table 5.3: Analysis of variance of CBGA multiple linear regression model.

5.6 MODEL ADEQUACY CHECKING

Residuals which are realized or observed values of the model errors indicate any violations from model assumptions. Residual plots have been used for studying the conformance of model with underlying assumptions including linearity, normality, constant variance and independence. Residual plots (Figure 5.2) studied include, the normal probability plot, histogram plot of residuals, plot of residuals against fitted values, plot of residual against regressor and plot of residual in time sequence. Departures from normality and the resultant effect on t-statistic or f-statistic and confidence and prediction intervals have been studied using normal probability plots. A straight line variation of normal probability plot (Figure 5.2) indicates a cumulative normal distribution. The histogram plot of residuals has also been used to study non-normality. Plots of residuals against fitted values and plots of residuals against the regressors have been used to check for constant-variance. Existence of residuals within the normal band indicates constant variance of regression model. Violation of assumptions may have been indicated by inward and outward funneling. The plot of residual in time sequence is used to study correlation between model errors at different time periods. Patterns in the plot of residuals in time sequence have been studied to determine if the errors are auto-correlated. Absence of any visible pattern indicates no violation of independence assumptions. Pearson's correlation matrix (Table 5.4) has been studied for checking the linear dependence of predictor variables. Absence of large values in correlation matrix confirms the absence of any multi-collinearity problems.

Residual Model Diagnostics

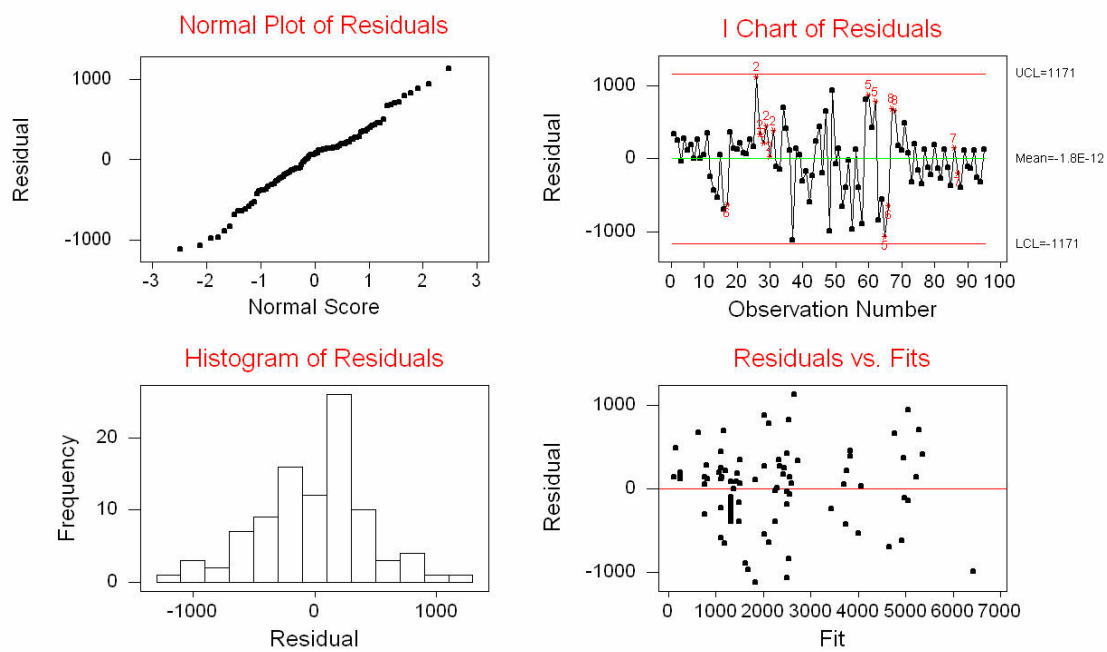


Figure 5.2: Residual plot of CBGA multiple linear regression model.

	Die Length	Substrate Thickness	Ball Count	Ceramic CTE	Solder CTE	Ball Dia	Und Mod	Und CTE	PWB Thk	DeltaT
Die Length	1	0.155	0.868	0.054	-0.537	0.618	-0.21	-0.21	0.14	-0.02
Substrate Thickness	0.155	1	0.254	0.145	0.325	0.214	-0.10	-0.10	0.05	-0.08
Ball Count	0.868	0.254	1	0.054	-0.405	0.324	-0.20	-0.20	0.11	-0.10
Ceramic CTE	0.054	0.145	0.054	1	0.298	0.075	-0.08	-0.08	0.35	-0.20
Solder CTE	-0.537	0.325	0.400	0.298	1	0.308	0.12	0.12	0.08	-0.20
Ball Diam	0.618	0.214	0.324	0.075	-0.308	1	-0.03	-0.03	0.13	0.13
Und Mod	-0.218	-0.109	0.206	-0.088	0.129	0.032	1	0.77	-0.11	-0.08
Und CTE	-0.217	-0.108	0.205	-0.087	0.129	0.032	0.77	1	-0.11	-0.08
PWB Thk	0.142	0.056	0.114	0.351	0.085	0.133	-0.11	-0.11	1	-0.15
DeltaT	-0.025	-0.080	0.104	-0.204	-0.203	0.137	-0.08	-0.08	-0.15	1

Table 5.4: Pearson's correlation matrix of CBGA predictor variables

5.7 MODEL CORRELATION WITH EXPERIMENTAL DATA

Characteristic life predicted by the multiple linear regression models have been correlated with experimental values using a single factor design of experiment study for assessing the prediction ability of the statistical models. Prediction method with multiple linear regression and experimental method has been used as the factor and predicted characteristic life corresponding to each method is used as the response variable. Analysis of variance has been used for testing the equality of mean predicted life. The null hypothesis of the test is that the mean characteristic life of all the prediction methods is the same. The alternate hypothesis is there is at least one method with predicted characteristic life different from the others.

The analysis was conducted using commercially available statistical software MINITAB™. The equality of means has been studied using the generalized linear model function. The characteristic life which is used as response variable contains values of predicted characteristic life obtained from both statistical and experimental method. The prediction method which is used a model variable, uses a binary variable to describe the type of method. A value of zero is assigned for experimental method and a value of 1 is assigned for statistical method.

High P values of ANOVA table [Table 5.5] shows a clear acceptance of the null hypothesis. Thus it can be concluded that there is no significant difference in the characteristic life predicted by the statistical models and experimental methods. Since the factor has only two levels the ANOVA table in itself becomes a paired T test eliminating the need for a separate T test.

Source	DF	SeqSS	Adj SS	Adj MS	F Statistic	P value
Prediction Method	1	57231	57231	57231	0.02	0.877
Error	188	444844550	444844550	2366194		
Total	189	444901781				

Table 5.5: Single factor analysis of variance

5.8 MODEL VALIDATION

The effect of various design parameters on the thermal reliability of package have been presented in this section. Multiple linear regression based sensitivity factors, quantifying the effect of design, material, architecture and environmental parameters on thermal fatigue reliability, have been used to compute life. The sensitivity study can be used in building confidence during trade-off studies by arriving at consistent results in terms of reliability impact of changes in material, configuration and geometry using different modeling approaches. The predictions from the statistical model have also been compared with the experimental data

5.8.1 DIAGONAL LENGTH

The Thermo-mechanical reliability of flip chip packages reduces with increase in diagonal length. This effect has been demonstrated on CBGA packages with both low CTE and High CTE ceramic substrates. Multiple linear regression models have been used for evaluating the sensitivity of solder joint reliability to diagonal length. The cycles for 63.2% failure from the experimental data and multiple linear regression models have been plotted against the diagonal lengths of various devices. . The predicted values from the prediction model follow the experimental values quite accurately and show the same trend (Figure 5.2). This trend is also consistent from the failure mechanics standpoint, as the solder joints with larger diagonal length are subjected to much higher strains due to the increased distance from the neutral point, thus having lower reliability.

Ceramic ball grid array packages with diagonal length 29.69mm, 35.35mm and 45.96mm have been used for the comparison of multiple linear regression model

predictions with the actual test failure data. Both the packages had different ball diameter, pitch and pad definition and were subjected to different air-to-air thermal cycles (ATC) of 0°C to 100°C. Thus, the model is being tested for its ability to predict both single and coupled effects. A negative sensitivity has been computed for the effect of diagonal length. A negative sensitivity factor indicates that the characteristic life of a CBGA package decreases when the diagonal length increases and all the other parameters remaining constant. The characteristic life of the three packages plotted in the Figure 5.3.

5.8.2 SUBSTRATE THICKNESS

Thickness of substrate material has a great influence on thermo-mechanical reliability of ceramic packages. Ceramic ball grid array packages with thinner substrates have higher cycles to failure than thicker substrates. This trend is consistent from failure mechanics point of view as increased substrate thickness leads to higher assembly stiffness, which leads to increases stress levels in the interconnect.. This effect has been demonstrated for ceramic substrates of 0.8 mm, 1mm and 2.65mm substrate thickness [Figure 5.2]. A negative sensitivity factor indicates the characteristic life of CBGA packages decreases with increase in substrate thickness. Sensitivity has been calculated using multiple linear regression modeling for substrate thickness in the range of 0.635mm to 3.7mm for CBGA packages including 0.635mm, 0.8mm, 1mm, 1.65mm, 2.4mm, 2.9mm and 3.7mm thick substrates. Model predictions show good correlation with experimental data.

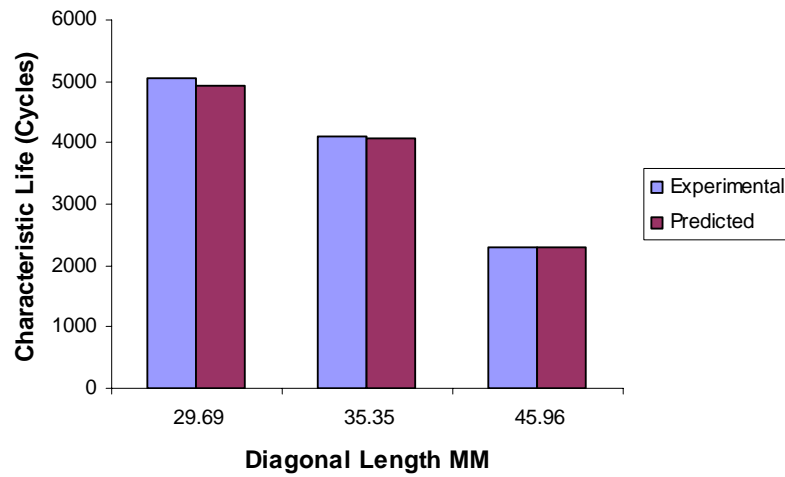


Figure 5.3 :Effect of diagonal length on thermal fatigue reliability of CBGA packages

Diagonal Length (mm)	Ball Count	Ball Diameter	PCB Thickness	Experiment	MLR	Sensitivity Factor For Diagonal length
29.69	552	0.8	2.8	5060	4921	-71.06
35.35	361	0.89	1.57	4091	4063	
45.96	932	0.8	2.8	2302	2293	

Table 5.6 : Sensitivity of the package reliability to diagonal length and comparison of

model predictions with actual failure data

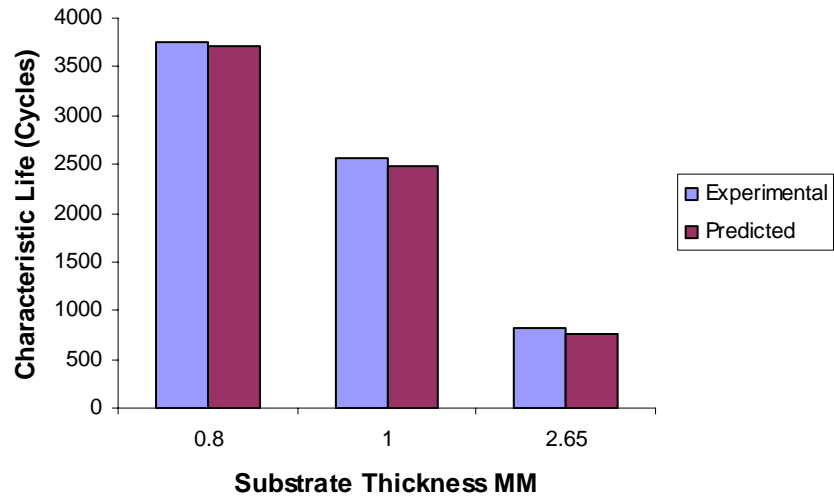


Figure 5.4: Effect of substrate thickness on thermal fatigue reliability of CBGA packages

Substrate Thickness (mm)	Ball Count	Ball Diameter (mm)	Diagonal Length (mm)	Experiment	MLR	Sensitivity Factor For Substrate Thickness
0.8	937	0.81	45.96	3754	3703	-582.87
1	256	0.81	29.69	2561	2490	
2.65	256	0.81	29.69	819	767	

Table 5.7 : Sensitivity of the package reliability to substrate thickness and comparison of model predictions with actual failure data

5.8.3 BALL COUNT

The effect of ball count on thermo-mechanical reliability has been shown in Figure 5.5. A trend of increase in the reliability with the increase in the ball count is visible, which is also supported by the failure mechanics theory. With the increase in the ball count the shear stress generated in the solder joints due to the thermal mismatch gets distributed, thus reducing the stress in the individual joint and increasing the life of the solder joint. Since this failure mechanics is only applicable in the case where the failure mode is solder joint cracking, so the trend might be different for other failure modes such as underfill delamination or copper trace cracking. CBGA packages with ball counts 256, 552 and 625 have been used to validate the effect of ball count on the thermo-mechanical reliability predicted by the model. The characteristic life predicted by the model lies in close proximity to the actual characteristic life from the experimental thermal cycling test. The sensitivity factor indicates an increase in cycles to failure of CBGA package by 2 cycles for every additional solder ball.

5.8.4 CERAMIC CTE

The CTE of the ceramic is found to have a direct relationship with thermo-mechanical reliability of CBGA packages. The thermo-mechanical reliability of CBGA packages increases with increase in CTE of the ceramic substrate which is inline with the failure mechanics theory. Increasing the CTE of the ceramic substrate decreases the difference in coefficients of thermal expansion between the substrate and the board there

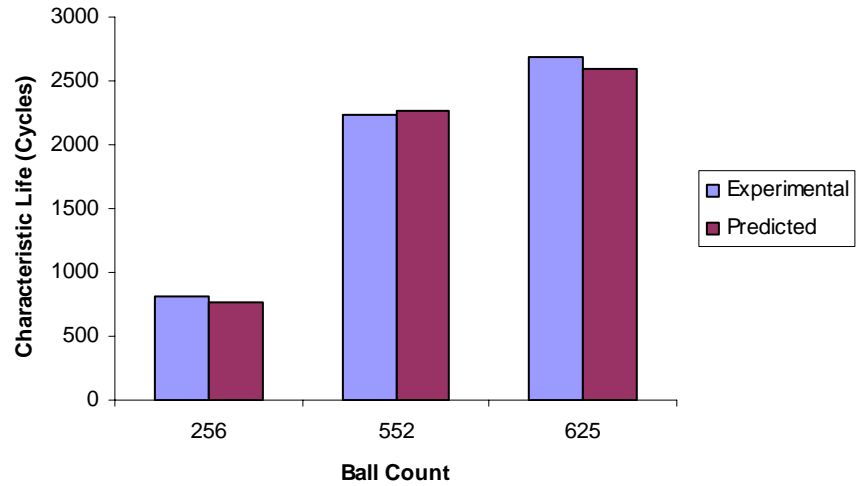


Figure 5.5: Effect of ball count on thermal fatigue reliability of CBGA packages

Ball Count	Diagonal Length (mm)	Ball Dia (mm)	Substrate Thickness (mm)	Experiment	MLR	Sensitivity Factor For Ball Count
256	29.69	0.81	2.9	819	761	1.6131
552	35.35	0.81	1.65	2240	2258	
625	45.91	0.81	0.8	2654	2595	

Table 5.8 : Sensitivity of the package reliability to ball count and comparison of model

predictions with actual failure data

by reducing stresses induced due thermal mismatch. Since this failure mechanics is only applicable in the case where the failure mode is solder joint cracking, so the trend might be different for other failure modes such as underfill delamination or copper trace cracking. Ceramic substrates with CTE of 6.8 PPM/⁰C and 12.3 PPM/⁰C have been used to validate the effect of ceramic on the thermo-mechanical reliability predicted by the model. A positive sensitivity factor indicates the characteristic life of CBGA packages increases with increase in substrate CTE. Model predictions show good correlation with experimental data.

5.8.5 SOLDER CTE

The solder joints of CBGA packages have a high lead solder ball with eutectic or lead free solder fillets. The thermo-mechanical reliability of solder joints is found to depend on the Coefficient of thermal expansion of the solder fillet. Solder joints with higher CTE fillets are more flexible leading to reduced stress conditions thereby reducing the amount of dissipated energy per cycle. Ceramic ball grid array packages with solder joint CTE of 17.6 PPM/⁰C and 25.5 PPM/⁰C have been used for demonstrating the effect of solder CTE on thermo-mechanical reliability [Figure 5.7]. Sensitivity of thermo-mechanical reliability on solder joint CTE have been determined using multiple linear regression method. The sensitivity factor indicates that for every unit increase of solder joint CTE keeping all other parameters constant the characteristic life of the CBGA package increases by 125 cycles. A positive sensitivity indicates the characteristic life of CBGA packages increases with increase in solder CTE. Model prediction shows good correlation with experimental data.

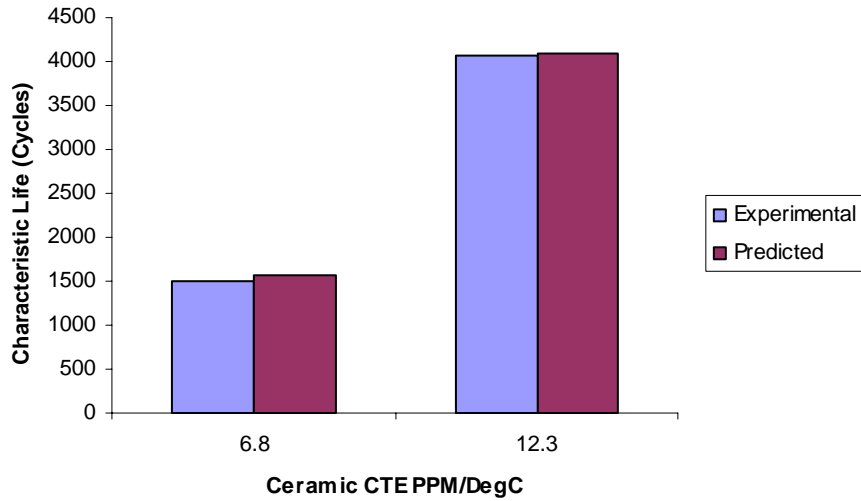


Figure 5.6: Effect of ceramic CTE on thermal fatigue reliability of CBGA packages

Ceramic CTE (PPM/ ⁰ C)	Substrate Thickness (mm)	Ball Dia (mm)	Ball Count (mm)	Experiment	MLR	Sensitivity Factor For Ceramic CTE
6.8	2.9	0.81	552	1503	1567	478.96
12.3	2.9	0.89	361	4063	4091	

Table 5.9 : Sensitivity of the package reliability to ceramic CTE and comparison of model predictions with actual failure data

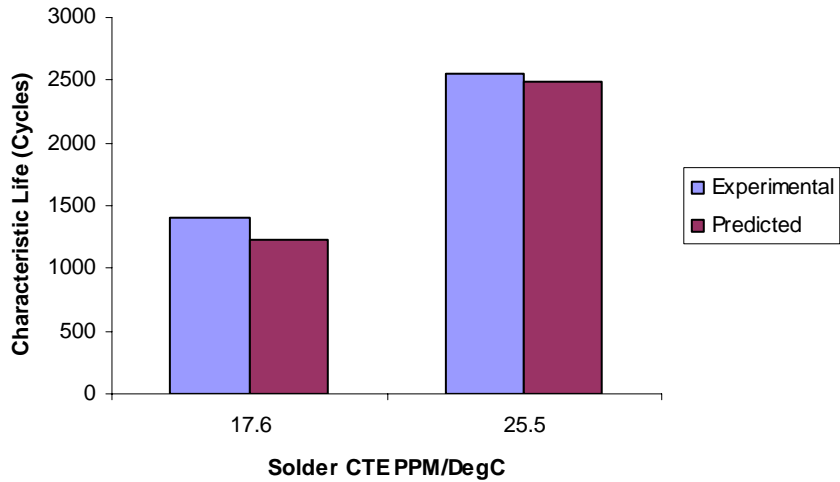


Figure 5.7: Effect of solder CTE on thermal fatigue reliability of CBGA packages

Solder CTE (PPM/ ^o C)	Ball Dia (mm)	Ball Count	Substrate Thickness (mm)	Experiment	MLR	Sensitivity Factor For Solder CTE
17.6	0.89	625	0.8	1408	1235	125.86
25.5	0.89	361	1.2	2561	2490	

Table 5.10 : Sensitivity of the package reliability to Solder CTE and comparison of model predictions with actual failure data

5.8.6 SOLDER JOINT DIAMETER

The thermo-mechanical reliability of the CBGA devices is also influenced by the solder joint or bump diameter. CBGA packages with bigger bump size usually give higher reliability for the device. This trend is supported by the characteristic life plot for the CBGA device for three different ball diameters. CBGA packages with larger bumps have lower stress concentration and longer crack propagation path in the solder interconnects, thus adding to the thermo-mechanical reliability of the device. This trend has been demonstrated for CBGA packages with solder joint diameter of 0.5mm, 0.81mm and 0.89mm. A positive sensitivity factor indicates the characteristic life of CBGA packages increases with increase in bump size and all other parameters are remaining constant. Model predictions show good correlation with experimental data.

5.8.7 UNDERFILL MODULUS

The elastic modulus of underfill material is found to have a positive sensitivity on thermo-mechanical reliability of CBGA packages. The trend has been demonstrated for n CBGA packages with no underfills and underfilled CBGA packages with underfill elastic modulus of 2.6 Gpa and 5.6 Gpa. The main reason for this trend from thermo-mechanics standpoint is that the underfill material provides a mechanical support and shares the shear stresses generated in the solder joints due to the thermal mismatch between the chip and the board. Also, the presence of underfill redistributes the displacement fields within a joint thereby reducing the extreme local strains concentrations that occur in the joint. Increasing the elastic modulus of the underfills makes it stiffer and hence share's greater

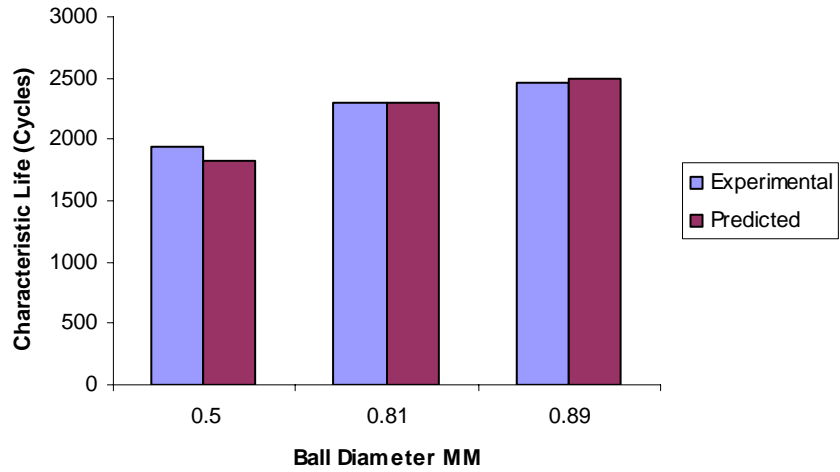


Figure 5.8: Effect of ball diameter on thermal fatigue reliability of CBGA packages

Ball Diameter (mm)	Ball Count (mm)	Substrate CTE	Substrate Thickness (mm)	Experiment	MLR	Sensitivity Factor For Ball Diameter
0.5	381	6.8	2.9	1944	1831	2594.6
0.81	625	6.8	0.8	2293	2302	
0.89	361	6.8	1.2	2462	2493	

Table 5.11 : Sensitivity of the package reliability to ball diameter and comparison of model predictions with actual failure data

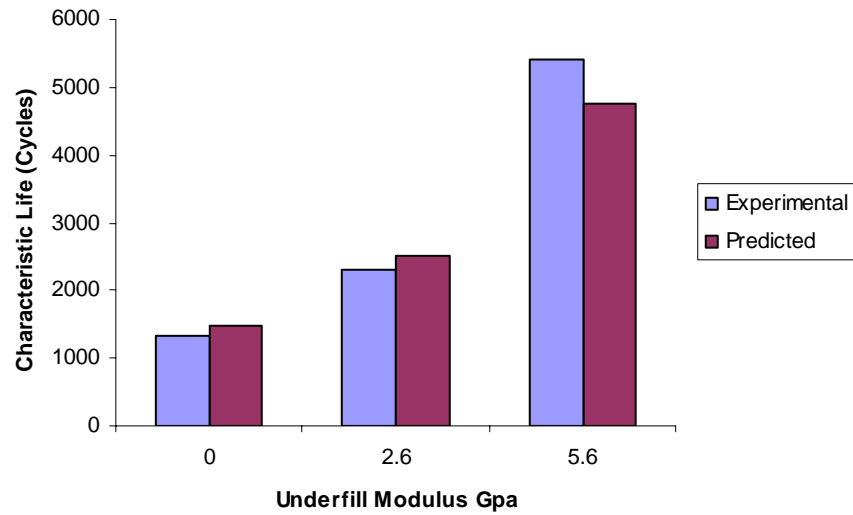


Figure 5.9: Effect of underfill modulus on thermal fatigue reliability of CBGA packages

Underfill Modulus (Gpa)	Ball Count	Ball Diameter (mm)	Substrate Thickness (mm)	Experiment	MLR	Sensitivity Factor For Underfill Modulus
0	256	0.89	1.0	1320	1487	547.33
2.6	256	0.81	1.0	2320	2507	
5.6	256	0.81	1.0	5420	4759	

Table 5.12 : Sensitivity of the package reliability to underfill modulus and comparison of model predictions with actual failure data

part of shear loads caused by thermal mismatches reducing the inelastic strain sustained by the solder thereby improving the thermo-mechanical reliability of solder joints.

5.8.8 UNDERFILL CTE

Coefficient of thermal expansion of the underfill material has an inverse relationship on thermo-mechanical reliability of solder joint. The thermo-mechanical reliability of CBGA packages decreases with increase in CTE of the underfill material, which is inline with the failure mechanics theory. With increase in underfill CTE, the underfill modulus decreases and the underfill becomes more flexible. This reduces the shear load on the underfill thereby increasing the shear load on the solder joint causing reduction in thermo-mechanical reliability of the joint. This trend has been demonstrated for underfilled CBGA packages [Figure 5.9] with underfill CTE of 44PPM/⁰C and 75 PPM/⁰C. A positive sensitivity factor indicates the characteristic life of CBGA packages increases with increase in bump size and all other parameters are remaining constant. Model predictions show good correlation with experimental data.

5.8.9 PCB THICKNESS

Thermo-mechanical reliability of CBGA packages decreases with increase in PCB thickness. This trend has been demonstrated for CBGA packages with PCB thickness of 1.57 mm, 1.8mm and 2.8 mm. This trend is consistent from failure mechanics point of view as increased PCB thickness leads to higher assembly stiffness, which leads to increases stress levels in the interconnect. Sensitivity of thermo-mechanical reliability on PCB thickness has been determined using multiple linear regression method. The sensitivity factor indicates that for every unit increase of PCB

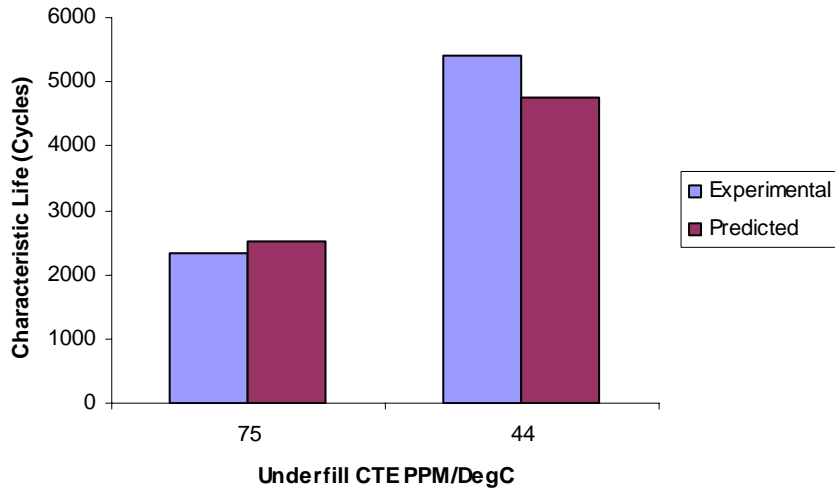


Figure 5.10: Effect of underfill CTE on thermal fatigue reliability of CBGA packages

Underfill CTE (PPM/ ^o C)	Ball Count	Ball Dia (mm)	Substrate Thickness (mm)	Experiment	MLR	Sensitivity Factor For Underfill CTE
75	256	0.81	1.0	2320	2597	-19.697
44	256	0.81	1.0	5420	4759	

Table 5.13: Sensitivity of the package reliability to underfill CTE and comparison of model predictions with actual failure data

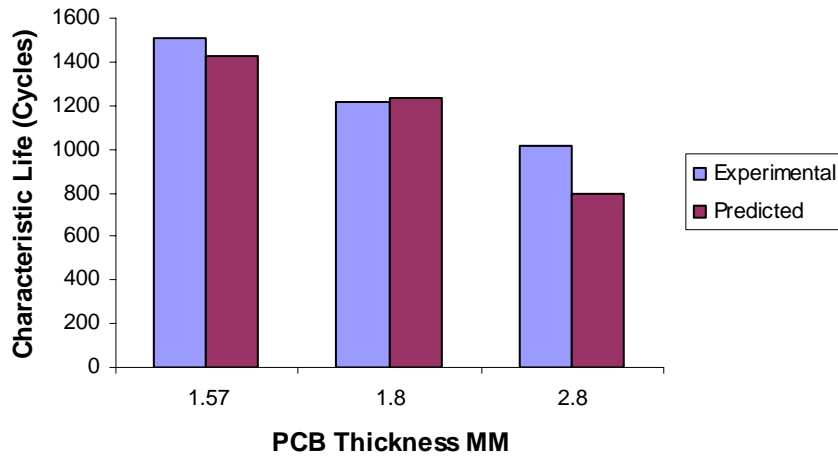


Figure 5.11: Effect of PCB thickness on thermal fatigue reliability of CBGA packages

PCB Thickness (mm)	Substrate Thickness (mm)	Ball Count	Ball Dia (mm)	Experiment	MLR	Sensitivity Factor For PCB Thickness
1.57	2.9	361	0.89	1511	1429	-245.4
1.8	0.8	625	0.89	1212	1234	
2.8	2.9	625	0.89	1013	800	

Table 5.14 : Sensitivity of the package reliability to PCB thickness and comparison of model predictions with actual failure data

thickness keeping all other parameters constant the characteristic life of the CBGA package decreases by 245 cycles. Model predictions show good correlation with experimental data.

5.8.10 DELTA T

The environment or testing condition the package is subjected to has a great influence on thermo-mechanical reliability CBGA packages. The characteristic life of the package decreases with the increase in the temperature range of the ATC. This trend has been demonstrated for two different cycling conditions including 0 to 100°C and -40 to 125°C. Temperature cycle magnitude has a negative sensitivity factor, indicated by decrease in thermo-mechanical reliability with increase in temperature cycle magnitude. Data presented includes coupled effects of other parameter variations such as, die size, ball diameter, ball count and cycle time. The predicted values for characteristic life calculated based multiple linear regression model match the experimental values from the ATC test very accurately.

5.9 DESIGN GUIDELINES

The statistical models presented in this section have been used for providing design guidelines for smart selection of CBGA technologies. The sensitivities from the statistical models have been used to analyze the effect of various parameters on the solder joint reliability of the flip chip packages.

- Solder joint reliability of CBGA packages decreases with increase in diagonal length. This effect has been demonstrated on both high CTE and low CTE ceramic substrates.

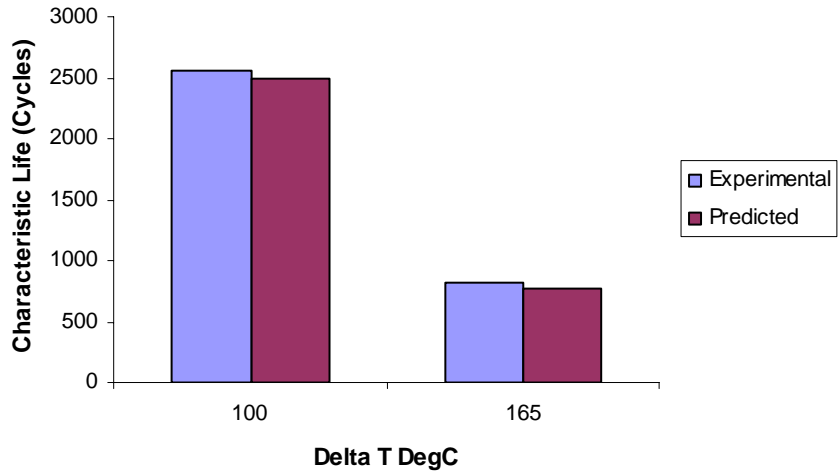


Figure 5.12: Effect of Delta T on thermal fatigue reliability of CBGA packages

Delta T	Ball Count	Ball Dia (mm)	Substrate Thickness (mm)	Experiment	MLR	Sensitivity Factor For DeltaT
100	256	0.81	1.0	2561	2490	-16.458
165	361	0.89	2.9	819	767	

Table 5.15: Sensitivity of the package reliability to Delta T and comparison of model

predictions with actual failure data

- Thermo-mechanical reliability of CBGA packages increases with increase in substrate thickness.
- Ball count has a positive sensitivity on solder joint fatigue life. Increasing the ball count increases the thermo-mechanical reliability of CBGA packages.
- Increasing the CTE of the ceramic substrate increases the solder joint reliability of CBGA packages.
- Increasing the CTE of the solder joint fillet increases the solder joint reliability of CBGA packages.
- Thermo-mechanical reliability of CBGA packages increases with increase in solder joint diameter.
- Solder joint reliability increases with increase in elastic modulus of the underfill and decrease in CTE of the underfill.
- Thicker printed circuit boards are less reliable than thinner printed circuit boards.
- Thermo-mechanical reliability of the solder joint in a CBGA package is inversely proportional to the temperature differential through which the package under goes thermal cycling.

CHAPTER 6

STATISTICS BASED CLOSED FORM MODELS FOR CCGA PACKAGES

Ceramic column grid array (CCGA) packages are an extension of ceramic ball grid array packages and use a column instead of a high melt ball to create higher standoff, more flexible interconnection, and to achieve significant increase in reliability. [Figure 6.1, Figure 6.2].The broadening of application space of ceramic packages to be included in the high volume market of personnel computer microprocessors [Master 1998], telecommunication products [Lau et al 2004], workstations and avionic products has necessitated the need for understanding the package design and assembly influence on reliability. In this section, a reliability assessment numerical model that could take into account the geometric details of a CCGA package, the material properties of the widely used material and the operating conditions has been developed help in understanding the influence of design and material parameters on thermo-mechanical reliability of CCGA packages.

Multiple linear regression has been used for model building. Parameter interaction effects, which are often ignored in closed form modeling, have been incorporated in this work. In addition, categorical variables such as solder volume have been incorporated in this model. Convergence of statistical models with experimental data has been demonstrated using a single factor design of experiment study.

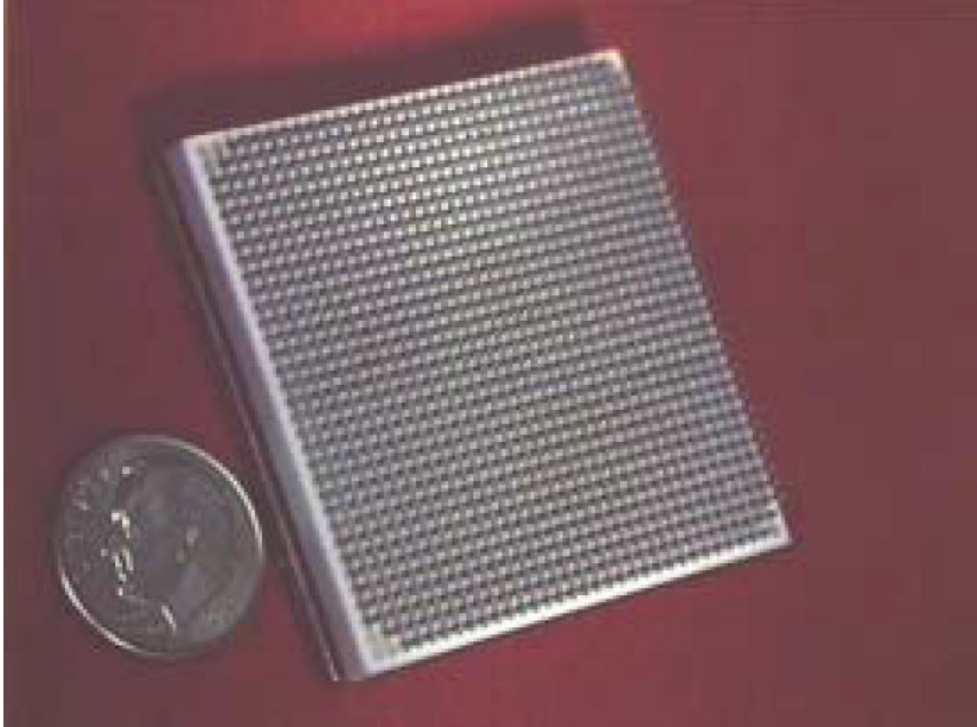


Figure 6.1: Layered View of IBM CCGA Package

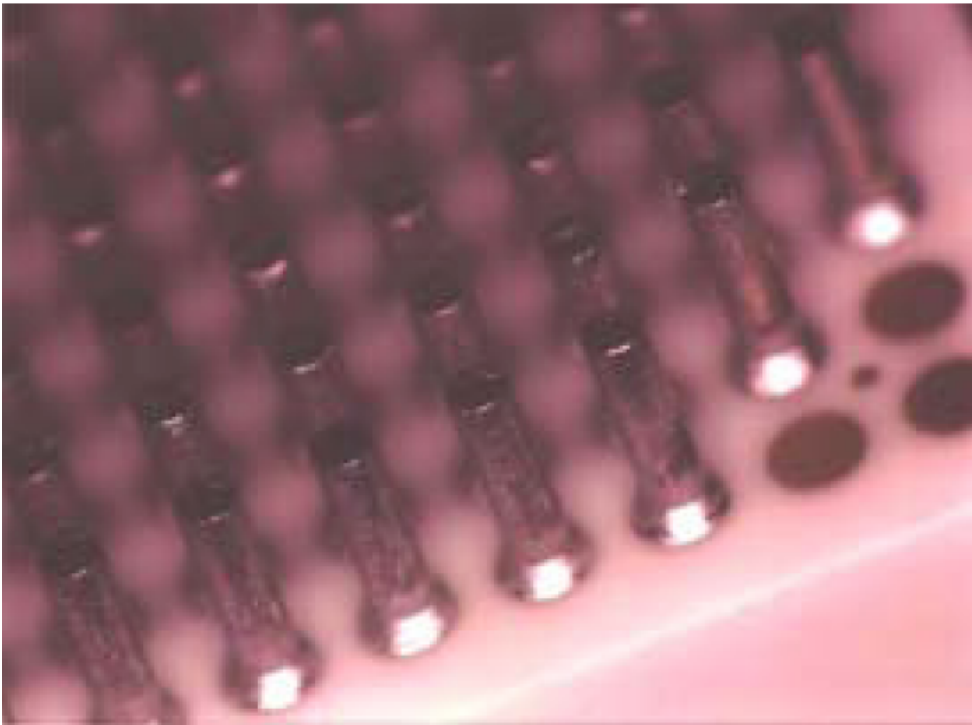


Figure 6.2: Column Grid Arrays of IBM CCGA Package

6.1 DATA SET

The dataset used for model building has been accumulated from an extensive CCGA accelerated test reliability database based on the harsh environment testing by the researchers at the NSF Center for Advanced Vehicle Electronics (CAVE). This database has also been supplemented with the various datasets published in the literature. Each data point in the database is based on the characteristic life of a set of CCGA devices of a given configuration tested under harsh thermal cycling or thermal shock conditions. The model parameters are based on failure mechanics of CCGA assemblies subjected to thermo-mechanical stresses.

The material properties and the geometric parameters investigated include substrate length, substrate area, substrate thickness, die length, ball count, ball pitch, solder type, solder ball height, solder ball volume, PCB surface finish, PCB thickness, PCB pad diameter ΔT , ramp rate, and dwell time. The range of data collected in each case is given by Table 6.1 .

6.2 MODEL INPUT SELECTION

All the predictor variables that are known to influence the characteristic life of CCGA package have been selected from the data set. The best subset of variables for model building has been selected based on the criteria of maximization of coefficient of determination and adjusted R^2 at the cost of minimum variance and bias. Ball height was found to be the most influential factor and a regression equation with characteristic life as response and ball height alone as predictor variable was built. Substrate area was

Parameter	CCGA
Die Size	32mm to 42.5mm
Number of I/O	1024 to 1806
Ball Pitch	1mm to 1.27mm
Ball Height	0.89mm to 2.2mm
Solder Composition	Sn63Pb37, 95.5Sn3.5Ag1.0Cu,
Solder Volume	Low, Nominal, High
Substrate Thickness	0.8mm to 3.75mm
PCB thickness	1.5mm to 2.8mm
T _{high} in ATC	100°C, 110°C, 125°C
T _{low} in ATC	-55°C, 0°C

Table 6.1: Accelerated test database

identified as the next most influential observation and a regression equation with substrate area and ball height as predictor variables and characteristic life as response variable was fit. Inclusion of substrate area increased the coefficient of determination (R^2) and reduced the residual errors and hence was retained in the model. Substrate thickness, solder volume, DeltaT respectively were found to be the next most influential variables and were added in steps and the criteria's for model selection were studied. The variables satisfied the selection criteria and hence were retained. Ball pitch, ball diameter and die length were identified as important variables, however the inclusion of these variables did not increase the coefficient of determination significantly and hence were dropped. Predictor variables from the super set were added in subsequent steps and their effect on variable selection criteria was studied for decision making on variable addition. The process was repeated by changing the first selected variable and subsequently adding and dropping variables forming new subset of predictor variables. The subset that best optimized the variable selection criteria was used for model building. The best subset of input variables includes ball height, substrate thickness, substrate area, solder volume and delta T.

6.3 MULTIPLE LINEAR REGRESSION

Multiple linear regression has been used for developing a relation between characteristic life of CCGA package with its geometric details, material properties and operating conditions. The best subset of variables obtained from stepwise methods has been used as predictor variables and 63% characteristic life has been used as the response variable. All predictor variables except solder volume have been input in continuous

form. Solder volume with two levels, nominal and high has been input in binary form using a binary variable, soldervolume. A zero state represents a case of nominal solder volume and one state represents high solder volume. When soldervolume is input zero, the term is knocked out of the equation and the prediction equation modifies itself for nominal solder volume. When a one is input for soldervolume, the effect of high solder volume is added to the equation. Since transition from nominal solder volume to low solder volume does not create a significant increase in the characteristic life it has not been included in the model building. MINITAB™ statistical software has been used for model building. The multiple linear regression models are given by Table 6.2. The prediction equation is given by Equation 6.1

$$63\%CharacteristicLife = 6271.8 - 1.247 \times SubstrateArea - 352.79 \times SubstrateThickness + 2790.6 \times BallHeight - 814.9 \times SolderVolume - 49.439 \times DeltaT$$

Eq 6.1

6.4 HYPOTHESIS TESTING

Analysis of variance has been used for testing the overall adequacy of the model. Small P value in the ANOVA table given by Table 6.3 shows the overall adequacy of the model signifying, the presence of at least one variable that is contributing significantly towards life prediction. Coefficient of determination, R^2 , which determine the percentage of variation of the response variable explained by the predictor variables, has also been used for assessing the overall adequacy of the prediction model. A coefficient of determination value of 89% for the model suggests that the predictor variables together account for 89% of variation in characteristic life. Since coefficient of determination is

Predictors (In a_0, f_k)	Coeff (b_k)	SE Coeff	T	P-Value
Constant	6271.8	808.3	7.76	0.000
SubAreaSqMM	-1.2479	0.3454	-3.61	0.001
SubThkMM	-352.79	95.80	-3.68	0.001
BallHtMM	2790.6	301.7	9.25	0.000
SolderVolume	-814.9	285.7	-2.85	0.007
DeltaT	-49.439	3.558	-13.89	0.000

Table 6.2: Multiple linear regression model for characteristic life prediction of CCGA package.

Source	D.F	SS	MS	F	P
Regression	6	131084172	21847362	55.05	0.000
Residual Error	42	16666954	396832		
Total	48				

Table 6.3: Analysis of variance of CCGA multiple linear regression model.

dependent on number of predictor variable the Adj R^2 parameter has also been studied. An Adj R^2 of 88% reconfirms the overall adequacy of the model. Thus the model is adequate for prediction purposes.

T tests on individual regression coefficients have been performed for determining the statistical significance of each predictor variable for retaining in the model. The p-value of a parameter in Table 6.2 indicates the statistical significance of that parameter and the parameter with p-value less than 0.05 is considered to be statistically significant and expected to have a significant effect on the reliability of the package, with confidence level of more than 95.0%. All the predictor variables in Table 6.2 are statistically significant with p-values in the neighborhood of 0 to 5%.

6.5 MODEL ADEQUACY CHECKING

Model appropriateness for application has been checked using any one or combination of the several of the features of the model, such as linearity, normality, variance which may be violated. Model residuals which measure deviation between data and fit have been studied and plotted to check model appropriateness and violation of assumptions. Residual plots studied include, the normal probability plot, histogram plot of residuals, plot of residuals against fitted values, plot of residual against regressor and plot of residual in time sequence (Figure 6.3). Departures from normality and the resultant effect on t-statistic or f-statistic and confidence and prediction intervals have been studied using normal probability plots. A straight line variation indicates a cumulative normal distribution. Plots of residuals against fitted values and plots of residuals against the regressors have been used to check for constant-variance. Existence

Residual Model Diagnostics

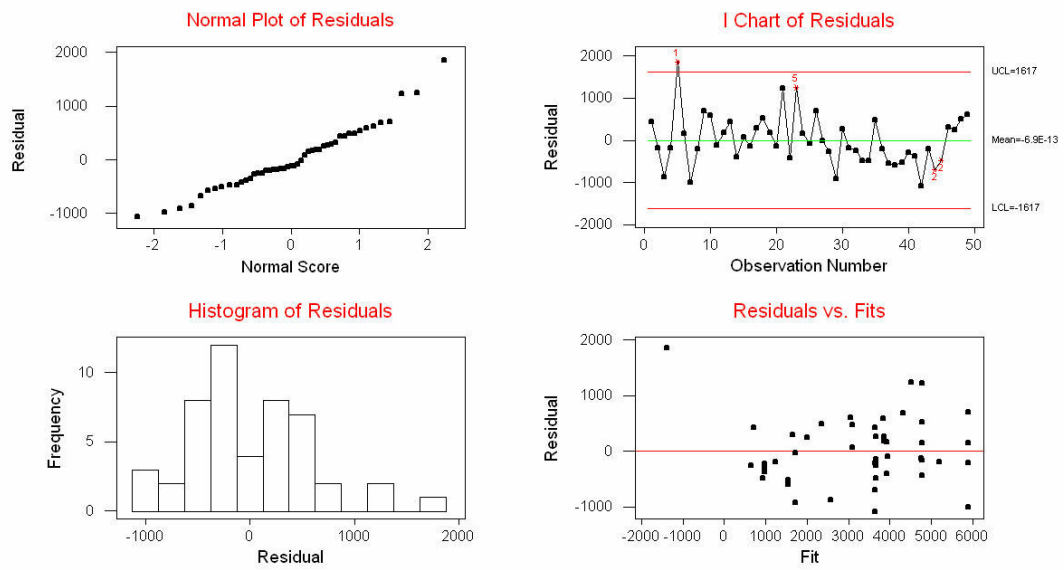


Figure 6.3: Residual plots of CCGA multiple linear regression model.

	Substrate Area	Substrate Thickness	Ball Height	Solder Volume	DeltaT
Substrate Area	1	0.33156	0.37405	-0.30384	-0.01379
Substrate Thickness	0.33156	1	-0.20341	0.04287	-0.11346
Ball Height	0.37405	-0.20341	1	-0.31305	0.08106
Solder Volume	-0.30384	0.04287	-0.31305	1	-0.19267
DeltaT	-0.01379	-0.11346	0.08106	-0.19267	1

Table 6.4: Pearson's correlation matrix of CCGA predictor variables

of residuals within the normal band indicates constant variance. Multi-collinearity has been checked using Pearson's correlation matrix (Table 6.4) and variance inflation factor values. Absence of any large values in the Pearson's correlation matrix shows absence of any multi-collinearity problems.

6.6 MODEL CORRELATION WITH EXPERIMENTAL DATA

The predicted characteristic life of the statistical model have been compared with the actual characteristic life using a single factor design of experiment study to assess the prediction ability of the statistical models. 63% characteristic life has been used as response variable and prediction method, used for obtaining the characteristic life, with, experimental method and statistical method as its two levels, has been used as the factor of study. The objective of the study is to analyze if the characteristic life predicted by both the methods for any given test case is the same under 95% confidence level.

Analysis of variance has been used for testing the equality of mean predicted life. The null hypothesis of the test is that the mean characteristic life prediction by all the methods is the same. The alternate hypothesis is that, there is at least one method with predicted characteristic life different from the others. The analysis was conducted using commercially available statistical software MINITABTM. The equality of means has been studied using the generalized linear model function. The characteristic life, which is used as response variable contains values of predicted characteristic life obtained from both statistical and experimental method. The prediction method which is used a model variable, uses a binary variable to describe the type of method. A value of zero is assigned for experimental method and a value of 1 is assigned for statistical method.

Source	DF	SeqSS	Adj SS	Adj MS	F Statistic	P value
Prediction Method	2	2420582	2420582	710291	1.10	1.000
Error	96	278835298	278835298	2904534		
Total	97	278835298				

Table 6.5: Single factor analysis of variance

High P values of ANOVA table [Table 6.5] shows a clear acceptance of the null hypothesis. Thus it can be concluded that there is no significant difference in the characteristic life predicted by the statistical models and experimental methods. Since the factor has only two levels the ANOVA table in itself becomes a paired T test eliminating the need for a separate T test.

6.7 MODEL VALIDATION

The statistical modeling methodology presented in this section has been validated against the experimental accelerated test failure data. Statistical model predictions have been done by using multiple linear regression models. Statistics based sensitivity factors quantifying the effect of design, material, architecture, and environment parameters on thermal fatigue reliability have been used to compute life. The sensitivity study can be used in building confidence during trade-off studies by arriving at consistent results in terms of reliability impact of changes in material, configuration and geometry using different modeling approaches. The effect of various design parameters on the thermal reliability of package have been presented in this section. The predictions from statistical model have also been compared with the experimental statistical data.

6.7.1 SUBSTRATE AREA

The thermo-mechanical reliability of ceramic column grid array packages decreases with increase in substrate area. Multiple linear regression models have been used for evaluating the sensitivity of thermo-mechanical reliability to substrate area. The cycles for 63.2% failure from the experimental data and multiple linear regression models have been plotted against the die length of various devices. The predicted values from

the prediction model follow the experimental values quite accurately and show the same trend (Figure 6.4). This trend is also consistent from the failure mechanics standpoint, as the solder joints with larger substrate area are subjected to much higher strains due to the increased distance from the neutral point, thus having lower reliability.

Encapsulated CCGA packages with substrate area of 1024 Sqmm, 1764 Sqmm and 1806Sqmm have been used for comparing the multiple linear regression model predictions with the actual test failure data (Figure 6.4). All the three packages had high lead solder joints of different ball pitch and substrate thickness and were subjected to different air-to-air thermal cycles (ATC) including thermal cycle of -55°C to 125°C , and 0°C to 100°C . Thus, the model is being tested for its ability to predict both single and coupled effects. A negative sensitivity has been computed for the effect of substrate area. A negative sensitivity factor indicates that the characteristic life of a CCGA package decreases when the die length increases and all the other parameters remaining constant.

6.7.2 SUBSTARTE THICKNESS

Substrate thickness has a great influence on the thermo-mechanical reliability of CCGA packages. Increasing the thickness of the ceramic substrate decreases the thermo-mechanical reliability of solder joints. This trend is also consistent from the failure mechanics standpoint, as thicker substrates tend to be rigid increasing the overall assembly stiffness thereby inducing great stresses on the solder joints. Ceramic column grid array packages with substrate thickness of 0.8 mm, 2.9 mm and 3.75 mm have been used for demonstrating this effect [Figure 6.5]. Sensitivity of thermo-mechanical reliability on substrate thickness has been determined using multiple linear regression.

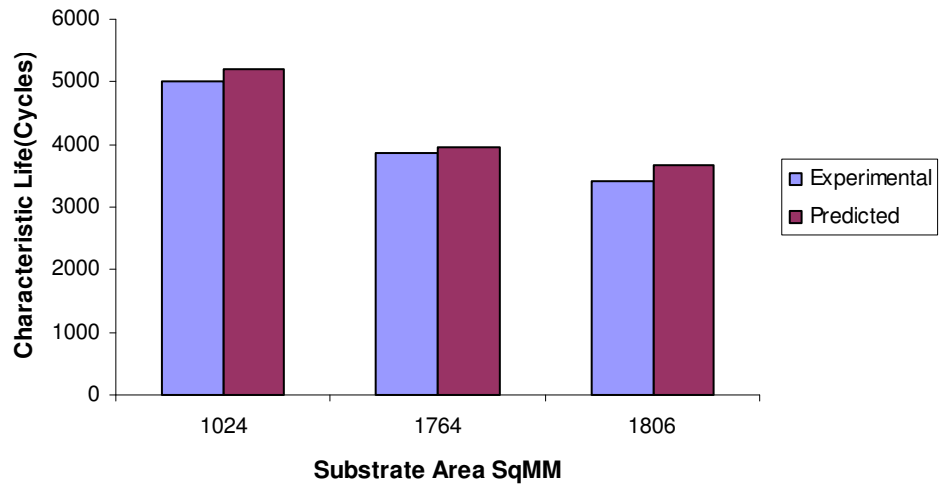


Figure 6.4: Effect of substrate area on thermal fatigue reliability of CCGA packages

Substrate Area (mm)	Substrate Thickness (mm)	Ball Height (mm)	Solder Volume	Experiment	MLR	Sensitivity Factor For Substrate Area
1024	2.9	2.21	Nominal	5010	5194	-1.2479
1764	1.4	2.21	Nominal	3874	3957	
1806	3.75	2.21	Nominal	3417	3761	

Table 6.6: Sensitivity of the package reliability to Delta T and comparison of model predictions with actual failure data

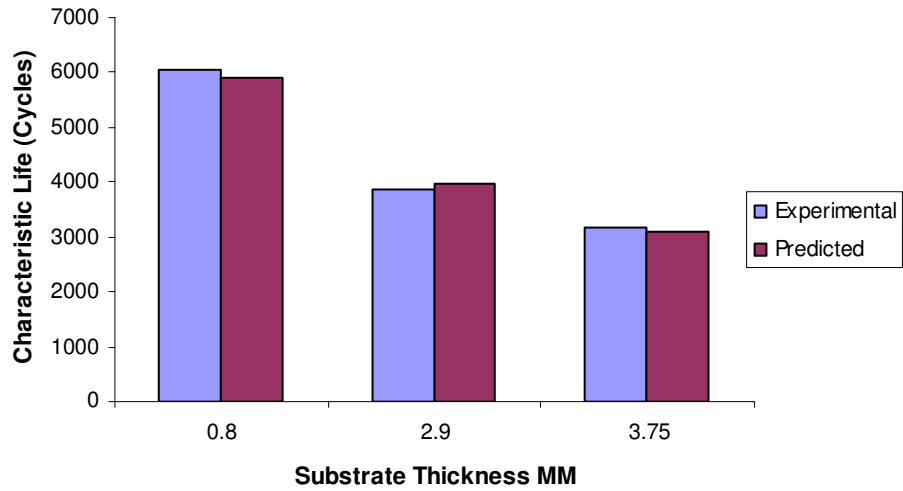


Figure 6.5 Effect of substrate thickness on thermal fatigue reliability of CCGA packages

Substrate Thickness (mm)	Substrate Area (Sqmm)	Ball Height	DeltaT	Experiment	MLR	Sensitivity Factor For Substrate Thickness
0.8	1056.25	2.21	100	6056	5894	-352.79
2.9	1764	2.21	100	3874	3957	
3.75	1806	2.21	100	3185	3103	

Table 6.7: Sensitivity of the package reliability to die length and comparison of model predictions with actual failure data

method. The sensitivity factor indicates that for every unit increase of substrate thickness keeping all other parameters constant the characteristic life of the CCGA package decreases by 352 cycles. The characteristic life predicted by the model lies in close proximity to the actual characteristic life from the experimental thermal cycling test.

6.7.3 BALL HEIGHT

The height of the solder joint has direct influence on the thermo-mechanical reliability of CCGA packages. The thermo-mechanical reliability increases with increase in the solder joint height. This is supported by failure mechanics theory as, taller solder joints have longer crack propagation length leading giving more time for the joint to fail. This trend has been demonstrated for CCGA packages with ball heights of 0.89 mm, 1.27 mm and 2.21 mm [Figure 6.6]. Sensitivity of thermo-mechanical reliability on substrate thickness has been determined using multiple linear regression method. The sensitivity factor indicates that for every unit increase of solder ball height keeping all other parameters constant the characteristic life of the CCGA package increases by 2790 cycles. Model predictions show good correlation with experimental data.

6.7.4 SOLDER VOLUME

The effect of solder joint volume on thermo-mechanical reliability has been shown [Figure 6.7]. The decrease in the thermo-mechanical reliability of the device with increase in the solder volume is demonstrated by both multiple linear regression model and experimental data. This trend is supported by failure mechanics theory as increasing the solder volume make the solder joint very stiff leading to higher stress conditions resulting in higher hysteresis loops with more dissipated energy per cycle. Ceramic ball

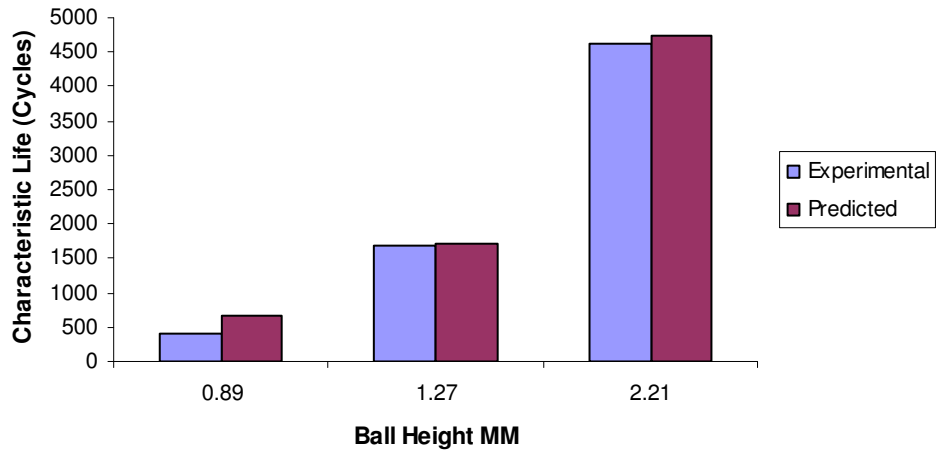


Figure 6.6: Effect of ball height on thermal fatigue reliability of CCGA packages

Ball Height (mm)	Substrate Area (Sqmm)	Substrate Thickness (mm)	Solder Volume	Experiment	MLR	Sensitivity Factor For Ball Height
0.89	1056.25	2.9	Nominal	400	655	2790.6
1.27	1056.25	2.9	Nominal	1700	1715	
2.21	1764	1.4	Nominal	4629	4747	

Table 6.8: Sensitivity of the package reliability to ball height and comparison of model predictions with actual failure data

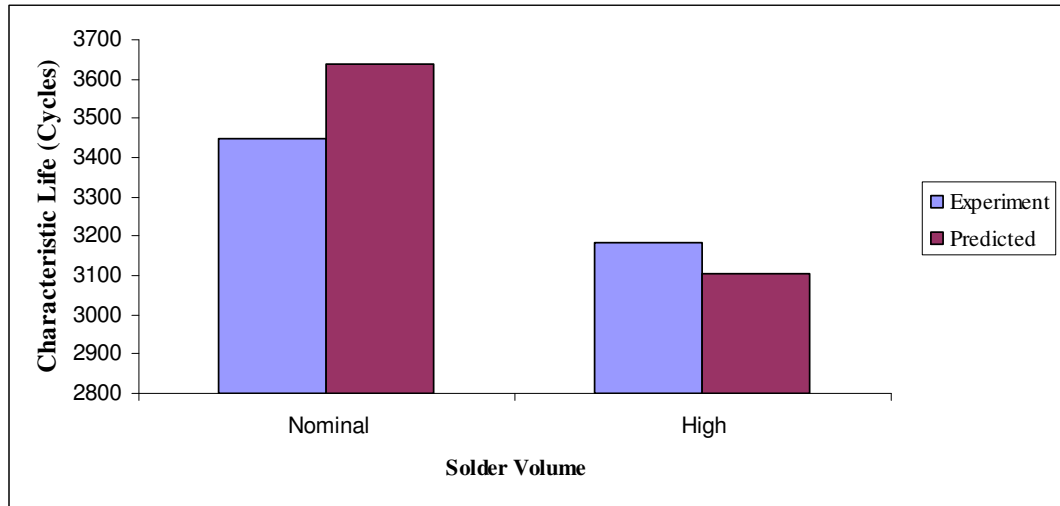


Figure 6.7: Effect of solder volume on thermal fatigue reliability of CCGA packages

Solder Volume	Substrate Area (Sqmm)	Substrate Thickness (mm)	Ball Height (mm)	Experiment	MLR	Sensitivity Factor For Solder Volume
Nominal	1806	3.75	2.11	3447	3639	-814.9
High	1806	3.75	2.11	3185	3103	
Low	1806	3.75	2.11	3540	3671	

Table 6.9: Sensitivity of the package reliability to solder volume and comparison of model predictions with actual failure data

grid array packages with nominal, low and high solder volumes have been for comparing multiple linear regression model predictions with the actual test failure data. A negative sensitivity factor indicates the characteristic life of CCGA package decreases with increase in solder volume. Model predictions show good correlation with experimental data.

6.7.5 DELTA T

The thermo-mechanical life of the CCGA devices, similar to other package architectures, is a function of the environment or the testing condition to which it is subjected. Magnitude of the temperature range experienced during the accelerated test is an influential parameter. The characteristic life of the package decreases with the increase in the temperature range of the ATC [Figure 6.8] . Temperature cycle magnitude has a negative sensitivity factor, indicated by decrease in thermo-mechanical reliability with increase in temperature cycle magnitude. Data presented includes coupled effects of other parameter variations such as, die size, ball diameter, ball count and cycle time. Sensitivity of thermo-mechanical reliability on DeltaT has been determined using multiple linear regression method. The sensitivity factor indicates that for every unit increase of DeltaT keeping all other parameters constant the characteristic life of the CCGA package decreases by 49 cycles. The predicted values for characteristic life calculated based on multiple linear regression model matches the experimental values from the ATC test very accurately.

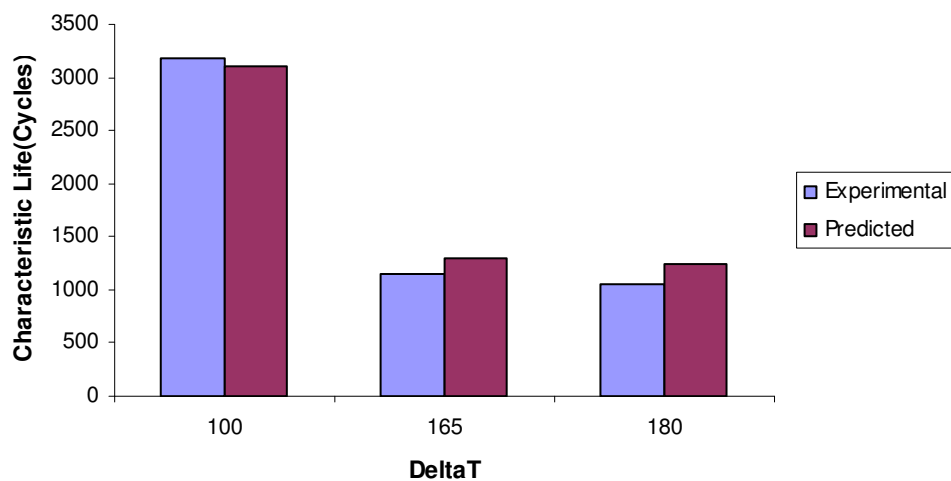


Figure 6.8: Effect of DeltaT on thermal fatigue reliability of CCGA packages

DeltaT	Substrate Area (mm)	Substrate Thickness (mm)	Ball Height (mm)	Experiment	MLR	Sensitivity Factor For DeltaT
100	1806	3.75	2.11	3185	3103	-49.439
165	1806	3.75	2.11	1139	1304	
180	1024	2.9	2.21	1060	1239	

Table 6.10: Sensitivity of the package reliability to Delta T and comparison of model predictions with actual failure data

6.8 DESIGN GUIDELINES

The statistical models presented in this section have been used for providing design guidelines for smart selection of CBGA technologies. The sensitivities from the statistical models have been used to analyze the effect of various parameters on the solder joint reliability of the flip chip packages.

- Solder joint reliability of CCGA packages decreases with increase in substrate area.
- CCGA packages with thinner ceramic substrate's yield higher reliability than CCGA packages with thicker ceramic substrates.
- Thermo-mechanical reliability of CCGA packages decreases with increase in solder volume.
- Solder joint height has a positive sensitivity on solder joint reliability. Increasing the height of the solder joint increases the solder joint reliability of CCGA packages.
- Thermo-mechanical reliability of the solder joint in a CCGA package is inversely proportional to the temperature differential through which the package under goes thermal cycling

CHAPTER 7

POWER LAW DEPENDENCY OF PREDICTOR VARIABLES

Power law relationship of predictor variables with 63 % characteristic life have been developed for various area array packages including flip chip BGA, Flex BGA, CBGA and CCGA packages. These power law relationships form the basis of reliability models in determining the appropriate family of transformations for linearizing the predictor variables for building robust multiple linear regression models that describe the data more efficiently . The power law relationship also help determining the appropriate transformation of predictor variables for coping with multi-collinearity, non normality and hetro-skedasticity. The power law dependence of predictor variables have been obtained using Box-Tidwell power law modelling and compared with traditional failure mechanics values.

7.1 BOX TIDWELL POWER LAW MODELLING

Box-Tidwell power law model attempts to model the power law dependence between predictor variable and a response variable. The relationship is expressed as an equation that predicts a response variable from a function of predictor variables and parameters. The parameter is adjusted so that residual sum of squares is minimized. The prediction equation is of the form given by Equation 7.1

$$t_{63.2\%} = a_0 \prod_{k=1}^n (f_k)^{\lambda_k} \quad \text{Eq 7.1}$$

Where, parameter $t_{63.2\%}$ on the left hand side of the equation represents the characteristic life of three-parameter Weibull distribution for the flip-chip package when subjected to accelerated thermo-mechanical stresses. The parameters on the right hand side of the equation are the predictor variables or the various parameters that influence the reliability of the package and the parameter λ_k is the power law value obtained from box Tidwell method.

The Box-Tidwell method has been used to identify a transformation from the family of power transformations on predictor variables. Box, et. al. [1962] described an analytical procedure for determining the form of the transformation on regressor variables, so that the relation between the response and the transformed regressor variables can be determined. Assume that the response variable t , is related to a power of the regressor,

$$E(t) = f(\xi, \beta_0, \beta_1) = \beta_0 + \beta_1 \xi \quad \text{Eq 7.2}$$

Where,

$$\xi = \begin{cases} x^\alpha, & \alpha \neq 0 \\ \ln x, & \alpha = 0 \end{cases} \quad \text{Eq 7.3}$$

and β_0, β_1, α are unknown parameters. Suppose that α_0 is the initial guess of the constant α . Usually the first guess is $\alpha_0 = 1$, so that $\xi_0 = x^{\alpha_0} = x$, or that no transformation at all is applied in the first iteration. Expanding about the initial uses in Taylor series,

$$E(t) = f(\xi, \beta_0, \beta_1) + (\alpha - \alpha_0) \left(\frac{df(\xi, \beta_0, \beta_1)}{d\alpha} \right)_{\substack{\xi=\xi_0 \\ \alpha=\alpha_0}} + \frac{(\alpha - \alpha_0)^2}{2!} \left(\frac{d^2f(\xi, \beta_0, \beta_1)}{d^2\alpha} \right)_{\substack{\xi=\xi_0 \\ \alpha=\alpha_0}} + \frac{(\alpha - \alpha_0)^3}{3!} \left(\frac{d^3f(\xi, \beta_0, \beta_1)}{d^3\alpha} \right)_{\substack{\xi=\xi_0 \\ \alpha=\alpha_0}} + \dots + \frac{(\alpha - \alpha_0)^n}{n!} \left(\frac{d^nf(\xi, \beta_0, \beta_1)}{d^n\alpha} \right)_{\substack{\xi=\xi_0 \\ \alpha=\alpha_0}} \quad \text{Eq 7.4}$$

and ignoring terms of higher than first order gives,

$$\begin{aligned}
 E(t) &= f(\xi, \beta_0, \beta_1) + (\alpha - \alpha_0) \left(\frac{df(\xi, \beta_0, \beta)}{d\alpha} \right)_{\substack{\xi=\xi_0 \\ \alpha=\alpha_0}} \\
 &= \beta_0 + \beta_1 x + (\alpha - 1) \left(\frac{df(\xi, \beta_0, \beta)}{d\alpha} \right)_{\substack{\xi=\xi_0 \\ \alpha=\alpha_0}} \quad \text{Eq 7.5}
 \end{aligned}$$

Now if the terms in braces in Equation (B) were known, it could be treated as an additional regressor variable, and it would be possible to estimate the parameters β_0 , β_1 , and α by method of least squares. This way the value necessary to linearize the regressor variable can be determined.

This procedure has been carried out for all the four devices for each of its predictor variable and the results are tabulated and compared with power law dependence values obtained from failure mechanics method. The power law dependence values obtained from Box-Tidwell method are found be very close to the power law dependence values obtained from failure mechanics models.

7.2 POWER LAW DEPENDENCY OF FLIP CHIP PREDICTOR VARIABLES

The power law dependency of predictor variables of flip chip package have been obtained using Box-Tidwell power law modeling. The predictor variables obtained from model input selection method has been used for power law dependency studies. The predictor and response variables are transformed using a natural log transformation and a regression analysis using the transformed variables has been conducted in order to obtain the initial guess value of alpha for each predictor variable. The predictor variables are

then power transformed using their corresponding alpha value's obtained from initial guess and the residual sum of squares is obtained which is then fitted into Equation 7.5. Equation 7.5 represents a multiple linear regression model and the parameters of the equation including α and β have been obtained using method of least squares. The predictor variables are again power transformed using the newly obtained alpha value and the residual sum of squares is extracted. The residual sum of squares is again fitted into Equation 7.5 and the next alpha value is obtained using method of least squares. This iteration is continued until the residual sum of squares is minimized. The procedure for power law modeling has been coded in commercial statistical software SASTM.

Power law dependency of flip chip predictor variables is given by **Table 7.1**. The table gives an alpha value of 2.08 for solder ball diameter which matches very closely with failure mechanics value of 2.3. Also, alpha values of -2.55 for Delta T and 3.7 for ball height match closely with failure mechanics values of 2.3 and 2.7 respectively. Apart from magnitude the sensitivity trends of power law dependency values are found to conform to experimental data and statistical models. Trends of positive sensitivity for under cover area, solder ball diameter, underfill modulus and ball height and negative sensitivity for die length, solder modulus, underfill CTE are very much inline with experimental data and statistical model predictions. The power law dependency values can be used for developing generalized linear model with appropriate distributions corresponding to the power law dependency values of each predictor variables. Also, the power law dependence values can be used for adding correcting terms for addition for extra variables in the traditional failure mechanics model for more accurate reliability prediction of flip chip packages

Parameter	Box-Tidwell	$N \left(\alpha_{rel} \Delta T \left(\frac{V}{\pi^2 h^{1+\beta}} \right)^{\frac{1}{\beta}} \right)^n = C$ [Norris Landzberg 1998]	$N (\Delta \varepsilon_p)^n = C$ [Coffin-Manson 1954]	$N_f = K_T \left(T_u \Pi r_f^2 \frac{h^{1+\beta}}{AV} \right)^{\frac{m}{\beta}} \left(\frac{1}{\delta} \right)^m$ [Goldmann 1969]
Die Length	-69.31			
Undercover Area	34.625			
Solder Modulus	-0.827			
Underfill CTE	-0.202			
Solder Ball Dia	2.0827	4	2.3	5.44
Ball Pitch	-2.9369			
Delta T	-2.55	-2	-2.3	-2
Ball Height	3.741	2.7	2.3	2
Underfill Modulus	0.5009			

Table 7.1: Power law dependency of flip chip predictor variables

7.3 POWER LAW DEPENDENCE OF CBGA PREDICTOR VARIABLES

The power law dependency of CBGA predictor variables with characteristic life is given by Table 7.2. The variables for power law dependency have been selected from model input selection. The power law relations have been obtained using Box-Tidwell power law modeling in a manner similar to that of flip chip variables. The initial alpha value for each variable has been obtained using a regression analysis on natural log transformed data and the residual sum of squares have extracted. The residual sum of squares is then substitutes in Equation 7.5 and the next alpha value is obtained. The iteration has been continued until the residual sum of squares has been minimized.

The Box Tidwell method yields an alpha value of -2.147 which matches closely with failure mechanics values of -2 and -2.3. The power dependency value of -1.209 for diagonal length is also very close with failure mechanics value of -2. Also, the power law dependence values of underfill CTE, underfill modulus and solder modulus match closely for CBGA and Flip chip BGA. This gives scope for adding correction factors for the inclusion of material properties in the traditional failure mechanics models which are based more on geometric aspects of the package. The sensitivity trends of power law values are found to be inline with sensitivity trends of statistical model and experimental data. A trend of positive sensitivity for ball count, ball diameter, underfill modulus and ceramic CTE and negative sensitivity for Delta T, PCB thickness, underfill CTE, solder modulus, substate thickness and diagonal length is in good conformance with sensitivity trend of experimental data and statistical prediction model. Power law dependence values show good correlation with failure mechanics values.

7.4 POWER LAW DEPENDENCE OF CCGA PREDICTOR VARIABLES

The power law dependence value of CCGA predictor variable has been obtained using Box-Tidwell power law modeling. The power law dependence of predictor variables are given by Table 7.3. The power law dependence value of 2.4 for ball height is found to match closely with failure mechanics values of 2.3. The power law dependency values of -2.8 and -0.14 are found to match closely with failure mechanics value of -2.3 and -.152 respectively. A trend of positive sensitivity for ball height and solder diameter and negative sensitivity for substrate area, substrate thickness, solder volume and delta T is inline with sensitivity trends of experimental data and statistical prediction models.

7.5 POWER LAW DEPENDENCE OF Flex-BGA PREDICTOR VARIABLES

The power law dependency of Flex BGA predictor variables with characteristic life is given by Table 7.4. The power law dependence values have been obtained in a manner similar to that of Flip chip, CBGA and CCGA packages. The sensitivity trends of power law values are found to be inline with sensitivity trends of statistical model and experimental data. A trend of positive sensitivity for ball count, ball diameter and encapsulant mold compound filler content and negative sensitivity for die to body ratio, PCB thickness, delta T and board finish is well in conformance with sensitivity trend of experimental data and statistical prediction models. The power law dependency values of ball diameter and Delta T are roughly in the range of failure mechanics values however not very close. However, values in correct sensitivity and rough range indicates

convergence with failure mechanics can be achieved by expanding the data set and increasing the number of iterations.

Parameter	Box-Tidwell	$N \left(\alpha_{rel} \nabla T \left(\frac{V}{\pi^2 h^{1+\beta}} \right)^{\frac{1}{\beta}} \right)^n = C$ [Norris Landzberg 1998]	$N(\Delta \varepsilon_p)^n = C$ [Coffin-Manson 1954]	$N_f = K_T \left(T_u \Pi r_f^2 \frac{h^{1+\beta}}{AV} \right)^{\frac{m}{\beta}} \left(\frac{1}{\delta} \right)^m$ [Goldmann 1969]
Ball Count	0.2501			
Delta T	-2.147	-2	-2.3	-2
PCB Thickness	-0.255			
Ball Diameter	0.667	4	2.3	5.44
Underfill CTE	-0.3172			
Underfill Modulus	0.6498			
Solder CTE	-0.571			
Ceramic CTE	0.93			
Substrate Thickness	-0.41			
Diagonal Length	-1.029	-2.3	-2	-2

Table 7.2: Power law dependency of CBGA predictor variables

Parameter	Box-Tidwell	$N \left(\alpha_{rel} \sqrt{T} \left(\frac{V}{\pi^2 h^{1+\beta}} \right)^{\frac{1}{\beta}} \right)^n = C$ [Norris Landzberg 1998]	$N(\Delta \epsilon_p)^n = C$ [Coffin-Manson 1954]	$N_f = K_T \left(T_u \Pi r_f^2 \frac{h^{1+\beta}}{AV} \right)^{\frac{m}{\beta}} \left(\frac{1}{\delta} \right)^m$ [Goldmann 1969]
Substrate Area	-0.61			
Substrate Thk	-0.22			
Ball Height	2.4096	2.7	2.3	2
Delta T	-2.862	-2	-2.3	-2
Solder Volume	-0.1485	-0.152		-0.175
Solder Dia	0.3027	4	2.3	5.44

Table 7.3: Power law dependency of CCGA predictor variables

Parameter	Box-Tidwell	$N \left(\alpha_{rel} \sqrt{T} \left(\frac{V}{\pi^2 h^{1+\beta}} \right)^{\frac{1}{\beta}} \right)^n = C$ [Norris Landzberg 1998]	$N(\Delta \varepsilon_p)^n = C$ [Coffin-Manson 1954]	$N_f = K_T \left(T_u \Pi r_f^2 \frac{h^{1+\beta}}{AV} \right)^{\frac{m}{\beta}} \left(\frac{1}{\delta} \right)^m$ [Goldmann 1969]
Die To Body Ratio	-1.739			
Ball Count	0.4162			
Ball Diameter	0.9485	4	2.3	5.44
PCB Thickness	-0.5322			
Delta T	-0.9454	-2	-2.3	-2
EMC Filler ID	0.1913			
Board Finish ID	-0.0779			

Table 7.4: Power law dependency of Flex-BGA predictor variables

CHAPTER 8

SUMMARY AND CONCLUSION

A perturbation modeling methodology based on multiple linear regression, principal components regression and power law modeling has been presented in this paper. The method provides an extremely cost effective and time effective solution for doing trade-offs and the thermo-mechanical reliability assessment of various BGA packages including Flex-BGA, CBGA, CCGA and Flip-chip BGA subjected to extreme environments. This methodology also allows the user to understand the relative impact of the various geometric parameters, material properties and thermal environment on the thermo-mechanical reliability of the different configurations of BGA packages with leaded as well as lead-free solder joints.

The model predictions from both statistics and failure mechanics based models have been validated with the actual ATC test failure data. The convergence between experimental results and the model predictions with higher order of accuracy than achieved by any first order closed form models has been demonstrated, which develops the confidence for the application of the models for comparing the reliability of the different BGA packages for various parametric variations. The current approach allows the user to analyze independent as well as coupled effects of the various parameters on the package reliability under harsh environment. It is recommended to use these models

for analyzing the relative influence of the parametric variations on the thermo-mechanical reliability of the package instead of using them for absolute life calculations.

Power law relationship of predictor variables with 63 % characteristic life have been developed for various area array packages including flip chip BGA, Flex BGA, CBGA and CCGA packages. These power law relationships form the basis of reliability models in determining the appropriate family of transformations for linearizing the predictor variables for building robust multiple linear regression models that describe the data more efficiently. The power law values show good conformance with failure mechanics values for most of the variables. Convergence of power law values can best be achieved by expanding the existing data set. Advanced power law models can then be developed by transforming each predictor variable with its appropriate power law transformation and then conducting a linear regression analysis. Such power law transformed linear regression models can describe the data more efficiently and resulting in better prediction models. Also, the power law lamda values can be used for adding correction factors to existing first order failure mechanics models and building power law based models.

Parameter interactions, their effect on reliability and model optimization can be considered for an extension of this work. Parameter interaction effects can be studied using factor plots and factorial study. If interaction between two variables is found to be significant, an interaction term as a product of the original variables can be added to existing model the effect of interaction can be studied. Polynomial regression models can be used for model building as multiple linear regression can fail due to multi-collinearity of original and interaction variable. Response surface methodologies can be used for

visualizing the sensitivity of parameter to reliability and optimization of parameter for maximizing the reliability.

BIBLIOGRAPHY

- Anand, L., "Constitutive Equations for Hot-Working of Metals", *International Journal of Plasticity*, Vol. 1, pp. 213-231, 1985.
- Amagai, M., Watanabe, M. Omiya, M. Kishimoto, K and Shibuya, T., "Mechanical Characterization of Sn-Ag Based Lead-Free Solders", *Transactions on Microelectronics Reliability*, Vol. 42, pp. 951-966, 2002.
- Amagai, M., Nakao, M., "Ball Grid Array (BGA) Packages with the Copper Core Solder Balls" Proceedings of *Electronic Components and Technology Conference*, Seattle, WA, pp. 692-701, May 25-28, 1998.
- Banks, D. R., Burnette, T. E. Gerke, R.D. Mammo, E. Mattay, S., "Reliability Comparison of Two Metallurgies for Ceramic Ball Grid Array", *IEEE Transactions on Components, Packaging and Manufacturing Technology, Part B*, Vol. 18, No. 1, February 1995.
- Barker, D. B., Mager, B. M. And Osterman, M. D., "Analytic Characterization of Area Array Interconnect Shear Force Bahavios", *Proceedings of ASME International Mechanical Engineering Congress and Exposition*, New Orleans, LA, pp. 1-8, November 17-22, 2002.
- Bedinger, J. M., "Microwave Flip Chip and BGA Technology", *IEEE MTT-S International Microwave Symposium Digest*, v 2, pp 713-716, 2000.
- Box, G. E. P., Cox, D, R., "An analysis of transformations revisited, rebutted", *Journal of American Statistical Association*, vol. 77, no. 377, pp. 209-210, March 1982.
- Box, G. E. P., Tidwell, P. W., "Transformation of the independent variables" *Technometrics*, vol. 4, no. 4, pp.531-550, Nov.1962.
- Braun, T., Becker, K.F. Sommer, J.P. Löher, T. Schottenloher, K. Kohl, R. Pufall, R. Bader, V. Koch, M. Aschenbrenner, R.Reichl, H., "High Temperature Potential of Flip Chip Assemblies for Automotive Applications" *Proceedings of the 55th Electronic Components and Technology Conference*, Orlando, Florida, pp. 376-383, May 31-June 3, 2005.

- Brooks, S. P., N. Friel, R. King, Classical Model Selection via Simulated Annealing, *Journal of the Royal Statistical Society*, Vol. 65, No. 2, pp. 503, May 2003.
- Brown, S. B., Kim, K. H. and Anand, L., “An Internal Variable Constitutive Model for Hot Working of Metals”, *International Journal of Plasticity*, Vol. 5, pp. 95-130, 1989.
- Burnettel, T., Johnson, Z. Koschmieder, T. and Oyler, W., “Underfilled BGAs for Ceramic BGA Packages and Board-Level Reliability”, *Proceedings of the 50th Electronic and Components Technology Conference*, Las Vegas, NV, pp. 1221-1226, May 23-26, 2000.
- Busso, E. P., and Kitano, M., “A Visco-Plastic Constitutive Model for 60/40 Tin-Lead Solder Used in IC Package Joints,” *ASME Journal of Engineering Material Technology*, Vol. 114, pp. 331-337, 1992.
- Cheng, Z., “Lifetime of Solder Joint and Delamination in Flip Chip Assemblies”, *Proceedings of 2004 International Conference on the Business of Electronic Product Reliability and Liability*, Shanghai, China, pp. 174- 186, April 27-30, 2005.
- Clech, Jean-Paul, “Solder Reliability Solutions: A PC based design-for-reliability tool”, *Proceedings of Surface Mount International Conference*, San Jose, CA, pp. 136-151, Sept. 8-12, 1996.
- Clech, Jean-Paul, “Tools to Assess the Attachment Reliability of Modern Soldered Assemblies”, *Proceedings of NEPCON West '96*, Anaheim, CA, pp.35-45, February 23-27, 1997
- Clech, Jean-Paul, “Flip-Chip/CSP Assembly Reliability and Solder Volume Effects”, *Proceedings of Surface Mount International Conference*, San Jose, CA, pp. 315-324, August 23-27, 1998.
- Coffin, L. F., “A Study of the Effects of Cyclic Thermal Stresses on a Ductile Metal”, *Transactions of ASME*, Vol. 76, pp. 931-950, 1954.
- Corbin, J.S., “Finite element analysis for Solder Ball Connect (SBC) structural design Optimization”, *IBM Journal of Research Development*, Vol. 37, No. 5 pp. 585-596, 1991.
- Darveaux, R., and Banerji, K., “Fatigue Analysis Of Flip Chip Assemblies Using Thermal Stress Simulations and Coffin-Manson Relation” *Proceedings of 41st Electronic Components and technology Conference*, pp. 797-805, 1991.
- Darveaux, R., “How to use Finite Element Analysis to Predict Solder Joint Fatigue Life”, *Proceedings of the VIII International Congress on Experimental Mechanics*, Nashville, Tennessee, June 10-13, pp. 41-42, 1996.

- Darveaux, R., and Banerji, K., "Constitutive Relations for Tin-Based Solder Joints," *IEEE Transactions on Components, Hybrids and Manufacturing Technology*, Vol. 15, No. 6, pp. 1013-1024, 1992.
- Darveaux, R., Banerji, K., Mawer, A., and Dody, G., "Reliability of Plastic Ball Grid Array Assembly", *Ball Grid Array Technology*, J. Lau, ed., McGraw-Hill, Inc. New York, pp. 379-442, 1995.
- Darveaux, R., "Effect of Simulation Methodology on Solder Joint Crack Growth Correlation," *Proceedings of the 50th Electronic Components and Technology Conference*, Las Vegas, Nevada, pp.1048-1058, May 21-24, 2000.
- Darveaux, R., and Banerji, K., "Constitutive Relations for Tin-Based Solder Joints," *IEEE Transactions on Components, Hybrids and Manufacturing Technology*, Vol. 15, No. 6, pp. 1013-1024, 1992.
- Dougherty, D., Fusaro, J. and Culbertson, D., " Reliability Model For Micro Miniature Electronic Packages" *Proceedings of International Symposium On Microelectronics*, Singapore, pp. 604-611, 23-26 June 1997.
- Duan, Z., He, J., Ning, Y. and Dong, Z., "Strain Energy Partitioning Approach and Its Application to Low-Cycle Fatigue Life Prediction for Some Heat-Resistant Alloys," *Low-Cycle Fatigue*, ASTM STP 942, H. D. Solomon, G. R. Halford, L. R. Kaisand, and B. N. Leis, Eds., ASME, Philadelphia, pp.1133-1143, 1988.
- Dwinnell, W., Modeling Methodology, *PCAI Magazine*, Vol. 12, No. 1, pp. 23-26, Jan. 1998.
- Engelmaier, W., "Fatigue life of leadless chip carrier solder joints during power cycling," *IEEE Transactions on Components, Hybrids, Manufacturing Technology*, Vol. 6, pp. 52-57, September, 1983.
- Engelmaier, W., "Functional Cycles and Surface Mounting Attachment Reliability", *ISHM Technical Monograph Series*, pp. 87-114, 1984.
- Engelmaier, W., "The Use Environments of Electronic Assemblies and Their Impact on Surface Mount Solder Attachment Reliability" *IEEE Transactions on Components, Hybrids, and Manufacturing Technology*, Vol. 13, No. 4, pp. 903-908, December 1990.
- Farooq, M., Gold, L. Martin, G. Goldsmith, C. Bergeron, C., "Thermo-Mechanical Fatigue Reliability of Pb-Free Ceramic Ball Grid Arrays: Experimental Data and Lifetime Prediction Modeling", *Proceedings of the 52nd Electronic Components and Technology Conference*, New Orleans, LA, pp. 827-833, May 27-30, 2003.
- Fusaro, J. M., and Darveaux, R., "Reliability of Copper Base-plate High Current Power Modules", *Int. Journal Of Microcircuits Electronic Packaging*, Vol. 20, No. 2, pp. 81-88, 1997.

- Garofalo, F., *Fundamentals of Creep and Creep-Rupture in Metals*, The Macmillan Company, New York, NY, 1965.
- Gerke, R.D., Kromann, G.B., "Solder Joint Reliability of High I/O Ceramic-Ball-Grid Arrays and Ceramic Quad-Flat-Packs in Computer Environments: The PowerPC 603TM and PowerPC 604TM Microprocessors", *IEEE Transactions on Components and Packaging Technology*, Vol. 22, No. 4, December 1999.
- Goetz, M., Zahn, B.A., "Solder Joint Failure Analysis Using FEM Techniques of a Silicon Based System-In-Package", *Proceedings of the 25th IEEE/CPMT International Electronics Manufacturing Symposium*, pp. 70-75 October 2000.
- Goldmann, L.S., "Geometric Optimization of Controlled Collapse Interconnections", *IBM Journal of Research Development*, Vol. 13, pp. 251-265, 1969.
- Gonzalez, M., Vandeveld, M. Vanfleteren, J. and Manassis, D., "Thermo-Mechanical FEM Analysis of Lead Free and Lead Containing Solder for Flip Chip Applications" *Proceedings of 15th European Microelectronics and Packaging Conference*, Brugge, Belgium, pp. 440-445, June 12-15, 2005.
- Hong, B.Z., Yuan, T.D., "Integrated Flow-Thermo-mechanical and Reliability Analysis of a Densely Packed C4/CBGA Assembly" *Proceedings of 1998 Inter Society Conference on Thermal Phenomena*, Seattle, WA, pp. 220-228, May 27-30, 1998.
- Hong, B.Z., "Thermal Fatigue Analysis of a CBGA Package with Lead-free Solder Fillets", *Proceedings of 1998 Inter Society Conference on Thermal Phenomena*, Seattle, WA, pp. 205-211, May 27-30, 1998
- Hou, Z., Tian, G. Hatcher, C. Johnson, R.W., "Lead-Free Solder Flip Chip-on-Laminate Assembly and Reliability", *IEEE Transactions on Components and Packaging Technology*, Vol. 24, No. 4, pp. 282-292, October 2001.
- Ingalls, E.M., Cole, M. Jozwiak, J. Milkovich, C. Stack, J., "Improvement in Reliability with CCGA Column Density Increase to Imm Pitch", *Proceedings of the 48th Electronic and Components Technology Conference*, Seattle, WA, pp. 1298-1304, May 25-28, 1998.
- Interrante, M., Coffin, J. Cole, M. Sousa, I.D. Farooq, M. Goldmann, L., "Lead Free Package Interconnections for Ceramic Grid Arrays", *Proceedings of IEEE/CPMT/SEMI 28th International Electronics Manufacturing Technology Symposium*, San Jose, CA, pp. 1-8, July 16-18, 2003.

- Iyer, S., Nagarur, N. Damodaran, P., “Model Based Approaches For Selecting Reliable Underfill Flux Combinations for Flip- Chip Packages”, Proceedings Of 2005 Surface Mount Technology Association (SMTA 05), Rosemont, IL, Sep. 25-29 2005, pp. 488-493.
- Jagarkal, S.G., M. M.Hossain, D. Agouafer, “Design Optimization and Reliability of PWB Level Electronic Package” Proceedings of 2004 Inter Society Conference on Thermal Phenomena, Las Vegas, NV, p.p. 368-376, June 1-4,2004.
- Johnson, Z., “Implementation of and Extension to Darveaux’s Approach to Finite Element Simulation of BGA Solder Joint Reliability”, Proceedings Of 49th *Electronic Components and Technology Conference*”, pp. 1190-1195, June 1999
- Ju, S.H., Kuskowski, S. Sandor, B. and Plesha, M.E., “Creep- Fatigue Damage Analysis of Solder Joints”, *Proceedings of Fatigue of Electronic Materials, ASTM STP 1153, American Society for Testing and Materials*, Philadelphia, PA, pp. 1-21, 1994.
- Jung, E. Heinricht, K. Kloeser, J. Aschenbrenner, R. Reichl, H., Alternative Solders for Flip Chip Applications in the Automotive Environment, IEMT-Europe, Berlin, Germany, pp.82-91, 1998.
- Kang, S.K., Lauro, P. Shish, D.Y., “Evaluation of Thermal Fatigue Life and Failure Mechanisms of Sn-Ag-Cu Solder Joints with Reduced Ag Contents”, *Proceedings of 54th Electronic Components & Technology Conference*, Las Vegas, NV, pp. 661-667, June 1-4, 2004.
- Karnezos, M., M. Goetz, F. Dong, A. Ciaschi and N. Chidambaram, “Flex Tape Ball Grid Array”, *Proceedings of the 46th Electronic and Components Technology Conference*, Orlando, FL, pp. 1271-1276, May 28-31, 1996.
- King, J. R., D. A. Jackson, Variable selection in large environmental data sets using principal component analysis, *Environmetrics Magazine*, Vol 10, No. 1, pp. 66-77, Feb. 1999
- Kitchenham, B., E. Mendes, Further comparison of cross-company and within- company effort estimation models for web Applications, 10th International Symposium on Software Metrics, Chicago, IL, USA, pp. 348-357, Sep 14-16, 2004
- Kutner, M.H., Nachtsheim, C.J., Neter, J., *Applied Linear Regression Models*, McGraw-Hill, New York, 2000.

- Knecht, S., and L. Fox, "Integrated matrix creep: application to accelerated testing and lifetime prediction", *Chapter 16, Solder Joint Reliability: Theory and Applications*, ed. J. H. Lau, Van Nostrand Reinhold, pp. 508-544, 1991.
- Lai, Y.S., T.H Wang, C.C.Wang, C.L.Yeh, "Optimal Design in Enhancing Board-level Thermomechanical and Drop Reliability of Package-on-Package Stacking Assembly", *Proceedings of 2005 Electronics Packaging Technology Conference*, Singapore, p.p. 335-341, December 7-9 2005.
- Lall, P., N. Islam, J. Suhling and R. Darveaux, "Model for BGA and CSP Reliability in Automotive Underhood Applications", *Proceedings of 53rd Electronic Components and Technology Conference*, New Orleans, LA, pp.189 –196, May 27-30, 2003.
- Lall, P.; Islam, M. N. , Singh, N.; Suhling, J.C.; Darveaux, R., "Model for BGA and CSP Reliability in Automotive Underhood Applications", *IEEE Transactions on Components and Packaging Technologies*, Vol. 27, No. 3, p 585-593, September 2004.
- Lau, J. H. and Dauksher, W., "Reliability of an 1657CCGA (Ceramic Column Grid Array) Package with Lead-Free Solder Paste on Lead-Free PCBs (Printed Circuit Boards)", *Proceedings of the 54th Electronic and Components Technology Conference*, Las Vegas, NV, pp. 718-725, June 1-4, 2004.
- Lau, J. H., *Ball Grid Array Technology*, McGraw-Hill, New York, 1995.
- Lau, J. H., Shangguan, D., Lau, D. C. Y., Kung, T. T. W. and Lee, S. W. R., "Thermal-Fatigue Life Prediction Equation for Wafer-Level Chip Scale Package (WLCSP) Lead-Free Solder Joints on Lead-Free Printed Circuit Board (PCB)", *Proceedings of 54th Electronic Components & Technology Conference*, IEEE, Las Vegas, NV, pp. 1563-1569, June 1-4, 2004.
- Manson, S.S. and Hirschberg, M.H., *Fatigue: An Interdisciplinary Approach*, Syracuse University Press, Syracuse, NY, pp. 133, 1964.
- Master, R. N., and T. P. Dolbear, "Ceramic Ball Grid Array for AMD K6 Microprocessor Application", *Proceedings of the 48th Electronic and Components Technology Conference*, Seattle, WA, pp. 702-706, May 25-28, 1998

- Master, R. N., Cole, M.S. Martin, G.B., “Ceramic Column Grid Array for Flip Chip Application”, *Proceedings of the Electronic and Components Technology Conference*, pp. 925-929, May 1995.
- Malthouse, E. C., Performance Based Variable Selection for Scoring Models, *Journal Of Interactive Marketing*, Vol. 16, No. 4, pp. 37-50, Oct. 2002.
- McCray, A. T., J. McNames, D. Abercromble, Stepwise Regression for Identifying Sources of Variation in a Semiconductor Manufacturing Process, *Advanced Semiconductor Manufacturing Conference*, Boston, MA, USA, pp. 448-452, May 4-6, 2004.
- Meiri, R., J. Zahavi , And the Winner is Stepwise Regression, Tel Aviv University, Urban Science Application.
- Mendes, E., N. Mosley, Further Investigation into the use of CBR and Stepwise Regression to Predict Development Effort for Web Hypermedia Applications, *International Symposium on Empirical Software Engineering*, Nara, Japan, pp. 69-78, Oct 3-4, 2002.
- Meng, H.H., Eng, O.K., Hua, W.E., beng, L.T., “Application of Moire Interferometry in Electronics Packaging”, *IEEE Proceedings of Electronic Packaging and Technology Conference*, pp. 277-282, October 8-10, 1997.
- Montgomery, D.C., Peck, E.A., Vining, G.G., “Introduction to Linear Regression Analysis”, Wiley, New York, 2000.
- Muncy, J. V. and Baldwin, D. F., “A Component Level Predictive Reliability Modeling Methodology”, *Proceedings of 2004 SMTA International Conference*, Chicago, IL, pp. 482-490, September 26-30, 2004.
- Muncy, J. V., Lazarakis, T. and Baldwin, D. F., “Predictive Failure Model of Flip Chip on Board Component Level Assemblies”, *Proceedings of 53rd Electronic Components & Technology Conference*, IEEE, New Orleans, LA, May 27-30, 2003.
- Muncy, J. V., Predictive Failure Model For Flip Chip On Board Component Level Assemblies, *Ph. D. Dissertation*, Georgia Institute of Technology, Atlanta, GA, January, 2004
- Norris, K.C., Landzberg, A.H, “Reliability of Controlled Collapse Interconnections”, *IBM Journal of Research Development*, Vol. 13, pp. 266-271, 1969.

- Ostergren, W., and Krempl, E., "A Uniaxial Damage Accumulation Law for Time-Varying Loading Including Creep-Fatigue Interaction," *Transactions of ASME, Journal of Pressure Vessel Technology*, Vol. 101, pp. 118-124, 1979.
- Pang, H. L. J., Kowk, Y.T. and SeeToh, C. W., "Temperature Cycling Fatigue Analysis of Fine Pitch Solder Joints", *Proceedings of the Pacific Rim/ASME International Intersociety Electronic and Photonic Packaging Conference, INTERPack '97*, Vol. 2, pp. 1495-1500, 1997.
- Pang, J. H. L., Prakash, K. H. And Low, T. H., "Isothermal and Thermal Cycling Aging on IMC Growth Rate in Pb-Free and Pb-Based Solder Interfaces", *Proceedings of 2004 Inter Society Conference on Thermal Phenomena*, Las Vegas, NV, pp. 109-115, June 1-4, 2004.
- Pang, J. H. L., Chong, D. Y. R., "Flip Chip on Board Solder Joint Reliability Analysis Using 2-D and 3-D FEA Models", *IEEE Transactions On Advanced Packaging*, Vol. 24, No. 4, pp. 499-506, November 2001.
- Pang, J. H. L., Xiong, B. S. and Che, F. X., "Modeling Stress Strain Curves for Lead-Free 95.5Sn-3.8Ag-0.7Cu Solder", *Proceedings of 5th International Conference on Thermal and Mechanical Simulation and Experiments in Microelectronics and Microsystems*, pp. 449-453, 2004.
- Pang, J. H. L., Xiong, B. S. and Low, T. H., "Creep and Fatigue Characterization of Lead Free 95.5Sn-3.8Ag-0.7Cu Solder", *Proceedings of 2004 Inter Society Conference on Thermal Phenomena*, Las Vegas, NV, pp. 1333-1337, June 1-4, 2004
- Pascariu G., Cronin P, Crowley D, "Next-generation Electronics Packaging Using Flip Chip Technology", *Advanced Packaging*, Nov.2003.
- Peng, C.T., Liu, C.M. Lin, J.C. Cheng, H.C., "Reliability Analysis and Design for the Fine-Pitch Flip Chip BGA Packaging", *IEEE Transactions on Components and Packaging Technology*, Vol. 27, No. 4, pp. 684-693, December 2004.
- Pendse, R., Afshari, B. Butel, N. Leibovitz, J. "New CBGA Package with Improved 2nd Level Reliability" *Proceedings of the 50th Electronic Components and Technology Conference*, Las Vegas, Nevada, pp.1189-1197, May 21-24, 2000.
- Perkins, A., and Sitaraman, S. K., "Predictive Fatigue Life Equations for CBGA Electronic Packages Based on Design Parameters", *Proceedings of 2004 Inter Society Conference on Thermal Phenomena*, Las Vegas, NV, pp. 253-258, June 1-4, 2004.
- Perkins, A., and Sitaraman, S.K., "Thermo-Mechanical Failure Comparison and Evaluation of CCGA and CBGA Electronic Packages" *Proceedings of the 52nd Electronic Components and Technology Conference*, New Orleans, LA, pp. 422-430, May 27-30, 2003.

- Pitarresi, J.M., Sethuraman, S. and Nandagopal, B., “Reliability Modelling Of Chip Scale Packages”, Proceedings of 25th IEEE/CPMT International Electronics Manufacturing Technology Symposium, pp. 60-69, October 2000.
- Qian, Z., and Liu, S., “A Unified Viscoplastic Constitutive Model for Tin-Lead Solder Joints,” *Advances in Electronic Packaging*, ASME EEP-Vol.192, pp. 1599–1604, 1997.
- Ray, S.K., Quinones, H., Iruvanti, S., Atwood, E., Walls, L., “Ceramic Column Grid Array (CCGA) Module for a High Performance Workstation Application”, Proceedings - Electronic Components and Technology Conference, pp 319-324, 1997.
- Riebling, J., “Finite Element Modelling Of Ball Grid Array Components”, Masters Thesis, Binghamton University, Binghamton, NY, 1996.
- Shi, X. Q., Pang, H. L. J., Zhou, W. and Wang, Z. P., “A Modified Energy-Based Low Cycle Fatigue Model for Eutectic Solder Alloy”, *Journal of Scripta Material*, Vol. 41, No. 3, pp. 289-296, 1999.
- Shi, X. Q., Pang, H. L. J., Zhou, W. and Wang, Z. P., “Low Cycle Fatigue Analysis of Temperature and Frequency Effects in Eutectic Solder Alloy”, *International Journal of Fatigue*, pp. 217-228, 2000
- Sillanpaa, M., Okura, J.H., “Flip chip on board: assessment of reliability in cellular phone application”, *IEEE-CPMT* Vol.27, Issue:3, pp. 461 – 467, Sept.2004.
- Singh, N.C., “Thermo-Mechanical Reliability Models for Life Prediction Of Area Array Packages”, Masters Dissertation, Auburn University, Auburn, AL, May 2006.
- Skipor, A. F., et al., “On the Constitutive Response of 63/37 Sn/Pb Eutectic Solder,” *ASME Journal of Engineering Material Technology*, 118, pp. 1–11, 1996.
- Solomon, H.D., “Fatigue of 60/40 Solder”, *IEEE Transactions on Components, Hybrids, and Manufacturing Technology*, Vol. No. 4, pp. 423-432, December 1986.
- Stoyanov, S., C. Bailey, M. Cross, “Optimisation Modelling for Flip-Chip Solder Joint Reliability”, *Journal of Soldering & Surface Mount Technology*, Vol. 14, No 1, p.p. 49-58, 2002.
- Suhir, E., “Microelectronics and Photonics-the Future”, *Proceedings of 22nd International Conference On Microelectronics (MIEL 2000)*, Vol 1, NIS, SERBIA, pp. 3-17, 14- 17 MAY, 2000.

- Swanson, N. R., H. White, A Model Selection Approach to Real-Time Macroeconomic Forecasting Using Linear Models and Artificial Neural Networks, International Symposium on Forecasters, Stockholm, Sweden, pp. 232-246, Mar. 1994.
- Syed, A. R., “Thermal Fatigue Reliability Enhancement of Plastic Ball Grid Array (PBGA) Packages”, *Proceedings of the 46th Electronic Components and Technology Conference*, Orlando, FL, pp. 1211-1216 May 28-31, 1996.
- Syed, A. R., “Thermal Fatigue Reliability Enhancement of Plastic Ball Grid Array (PBGA) Packages”, *Proceedings of the 46th Electronic Components and Technology Conference*, Orlando, FL, pp. 1211-1216, May 28-31, 1996.
- Syed, A., “Factors Affecting Creep-Fatigue Interaction in Eutectic Sn/Pb Solder Joints”, *Proceedings of the Pacific Rim/ASME International Intersociety Electronic and Photonic Packaging Conference, INTERPack '97*, Vol. 2, pp. 1535-1542, 1997.
- Syed, A., “Predicting Solder Joint Reliability for Thermal, Power and Bend Cycle within 25% Accuracy”, *Proceedings of 51st Electronic Components & Technology Conference*, IEEE, Orlando, FL, pp. 255-263, May 29-June 1, 2001.
- Syed, A., “Accumulated Creep Strain and Energy Density Based Thermal Fatigue Life Prediction Models for SnAgCu Solder Joints”, *Proceedings of 54th Electronic Components & Technology Conference*, Las Vegas, NV, pp. 737-746, June 1-4, 2004.
- Teo, P.S., Huang, Y.W. Tung, C.H. Marks, M.R. Lim, T.B. “Investigation of Under Bump Metallization Systems for Flip-Chip Assemblies”, *Proceedings of the 50th Electronic Components and Technology Conference*, Las Vegas, Nevada, pp.33-39, May 21-24, 2000.
- Teng, S.Y., Brillhart, M., “Reliability Assessment of a High CTE CBGA for high Availability Systems”, *Proceedings of 52nd Electronic and Components Technology Conference*, San Diego, CA, pp. 611-616, May 28-31, 2002.
- Tummala, R. R., Rymaszewski, E. J. and Klopfenstein, A. G., *Microelectronics Packaging Handbook Technology Drivers Part 1*, Chapman and Hall, New York, 1997.
- Tunga, K.R., “Experimental and Theoretical Assessment of PBGA Reliability in Conjunction With Field Use Conditions”, *Masters Dissertation*, Georgia Institute of Technology, Atlanta, GA, April, 2004.
- Van den Crommenacker, J., “The System-in-Package Approach”, *IEEE Communications Engineer*, Vol 1, No. 3, pp. 24-25, June/July, 2003.
- Vandavelde, B., Christiaens F., Beyne, Eric., Roggen, J., Peeters, J., Allaert, K., Vandepitte, D. and Bergmans, J., “Thermomechanical Models for Leadless Solder

- Interconnections in Flip Chip Assemblies”, *IEEE Transactions on Components, Packaging and Manufacturing Technology*, Part A, Vol.21, No. 1, pp.177-185, March 1998.
- Vandavelde, B., Gonzalez, M., Beyne, E., Zhang, G. Q. and Caers, J., “Optimal Choice of the FEM Damage Volumes for Estimation of the Solder Joint Reliability for Electronic Package Assemblies”, *Proceedings of 53rd Electronic Components and Technology Conference*, New Orleans, LA, pp.189 –196, May 27-30, 2003.
- Vandavelde, B, Beyne, E., Zhang, K. G. Q., Caers, J. F. J. M., Vandepitte, D. and Baelmans, M., “Solder Parameter Sensitivity for CSP Life-Time Prediction Using Simulation-Based Optimization Method”, *IEEE Transactions on Electronic Packaging Manufacturing*, Vol. 25, No. 4, pp. 318-325, October 2002.
- Vayman, S., “Energy Based Methodology for The fatigue Life Prediction Of Solder Materials”, *IEEE Transactions on Components, Hybrids, and Manufacturing Technology*, Vol. 16, No. 3, pp. 317-322, 1993.
- Wang, G.Z., Cheng, Z.N. Becker, K. Wilde. J., “Applying Anand Model to Represent the Viscoplastic Deformation Behavior of Solder Alloys”, *ASME Journal Of Electronic Packaging*, Vol. 123, pp. 247-253, September 2003
- Wang, L., Kang, S.K. Li, H., “Evaluation of Reworkable Underfills for Area Array Packaging Encapsulation”, *International Symposium on Advanced Packaging Materials*, Braseltopn, GA, pp. 29-36, March -11-14, 2001
- Warner, M., Parry, J., Bailey, C. and Lu, H., “Solder Life Prediction in a Thermal Analysis Software Environment”, *Proceedings of 2004 Inter Society Conference on Thermal Phenomena*, Las Vegas, NV, pp. 391-396, June 1-4, 2004
- Yi, S., Luo, G. Chian, K.S., “A Viscoplastic Constitutive Model for 63Sn37Pb Eutectic Solders”, *ASME Journal Of Electronic Packaging*, Vol. 24, pp. 90 -96, June 2002.
- Zahn, B.A., “Comprehensive Solder Fatigue and Thermal Characterization of a Silicon Based Multi-Chip Module Package Utilizing Finite Element Analysis Methodologies”, *Proceedings of the 9th International Ansys Conference and Exhibition*, pp. 274 -284, August 2000.
- Zhang, C., Lin, J.K. Li, L., “Thermal Fatigue Properties of Lead-free Solders on Cu and NiP”, *Proceedings of 51st Electronic Components & Technology Conference*, IEEE, Orlando, FL, pp. 464-470, May 29-June 1, 2001.
- Zhu, J., Zou, D. Liu, S., “High Temperature Deformation of Area Array Packages by Moire Interferometry/FEM Hybrid Method”, *Proceedings of Electronic Components and Technology Conference*, pp. 444-452, May 18-21, 1997.

APPENDIX

List of Symbols

α	Coefficient of thermal expansion
δ	Displacement of chip relative to substrate
α_{rel}	Relative thermal coefficient of chip to substrate
β	Exponent from plastic shear stress-shear strain relationship
ΔT	Temperature cycle range
BGA	Ball grid array
Ballcount	Number of I/O on area array device.
BoardFinishID	Binary variable for board finish.
CBGA	Ceramic Ball Grid Array
CCGA	Ceramic Column Grid Array
CeramicCTEppm	Coefficient of thermal expansion of ceramic substrate in parts per million per degree centigrade
Coeff	Regression Coefficient
C-P	Mallows statistic for bias estimation
DeltaTDegC	Temperature cycle range
DF	Degrees of freedom

DiagLenMM	Chip diagonal length in millimeter
DielenMM	Chip-length in millimeter
DieToBody	Ratio of Die Size to Body size
EMCFillerID	Binary variable for encapsulant mold compound filler content
f	(mean square of residual error) / (mean square of regression error)
Flex-BGA	Flex Ball Grid Array
H	height of the solder in millimeter
l	Distance from chip neutral point to interconnection in millimeter
m	Coffin Manson coefficient
MS	Mean Square Error
MaskDefID	Binary variable for solder mask definition
NSMD	Non-solder mask defined
PBGA	Plastic Ball Grid Array
P Value	Singificance value of null hypothesis
PCB	Printed circuit board
PCBThkMM	Thickness of printed circuit board in millimeter
PitchMM	Area array device I/O in millimeter
R	radius of the cross section under consideration
R-sq	Multiple coefficient of determination
R-sq(adj)	R-sq adjusted for degrees of freedom
S	Standard deviation
SE Coeff	Standard Error coefficient.

SMD	Solder Mask Defined.
SolderDiaMM	Diameter of solder joint in millimeter
SolderEGpa	Solder joint elastic modulus in giga pascal
SolderVolume	Volume of the solder joint
SS	Error Sum of Squares
SubThkMM	Thickness of substrate in millimeter
t-stat	t-statistic of the coefficient
UndCovSqMM	Underfilled area in Square Millimeter
UndCTEppm	Coefficient of thermal expansion of underfill in parts per million per degree centigrade
UnderfillE	Elastic modulus of underfill in giga pascal
V	volume of the solder
63.2%	Characteristic life
a_0	Regression constant
b_k	Regression coefficient
k_d	Diagonal flexural stiffness of unconstrained non soldered corner most solder joint